

RUBBER AND TIRE FRICTION

by

H. W. KUMMER

Research Assistant

W. E. MEYER

Professor of Mechanical Engineering

AUTOMOTIVE SAFETY PROJECT

Department of Mechanical Engineering

THE PENNSYLVANIA STATE UNIVERSITY  
College of Engineering and Architecture  
University Park, Pennsylvania

December 1960 [With minor corrections 1967]

AD-660 927

#### ABSTRACT

The mechanism of rubber friction is discussed, and an attempt is made to relate the friction characteristics of a rubber block to those of a slipping and sliding pneumatic tire. Several new or modified explanations of the behavior of tires on dry and wet surfaces are proposed.

The effects of pressure or normal load, sliding velocity, temperature, and contaminating and lubricating films on the adhesion and hysteresis components are separately investigated for the rubber block and the rolling, slipping, and sliding tire.

Attention is given to such topics as the existence or non-existence of a static coefficient, the transient behavior of adhesive friction at nonsteady sliding velocities, the rise of the sliding coefficient with sliding velocity, comparison of the coefficients obtained from a sliding and a slipping tire, the meaning of slip, and the dependence of the critical coefficient on slip and vehicle velocity. Also explored are the mechanism of water removal between tire and road surface under wet driving conditions, and the effects of tire geometry, pressure distribution in the footprint, vehicle speed, and water film thickness on the obtainable coefficient.

Experimental methods for measuring rubber and tire friction are reviewed. The Penn State brake test trailer is described.

## PREFACE

Highway traffic safety has become a matter of acute concern in the United States and throughout the civilized world. The growing problem of accident prevention cannot be left to the highway engineer and the psychologist alone; the vehicle itself must be made more foolproof. Recognizing this, the Department of Mechanical Engineering of The Pennsylvania State University has established a research program to approach highway accident prevention through better understanding of the driver-vehicle-road complex and improvement of mechanical controls. The initial activities of this project are directed toward finding improved means to stop a vehicle that is in motion.

Brakes as such, though they could be better, are not a critical factor in most cases. Rather, it is the operator's misuse of his vehicle's braking capacity on slippery roads that breeds danger or prevents him from extricating himself from a dangerous situation. When excessive application of brake pressure locks some or all of the wheels, skidding or spinning will occur, and jackknifing in the case of articulated vehicles. Obviously, then, prevention of wheel lock by automatic means would greatly enhance the safety of present-day driving, and will be an absolute necessity if vehicle movement is ever subject to some form of remote control.

Antilock systems are in use on aircraft, but there they serve mainly to prevent tire blowout. Transferred to road vehicles, these systems do eliminate the loss of directional control, but they increase stopping distances. To eliminate this disadvantage or reduce it to a tolerable minimum, brake control systems are needed that have optimum capability for dealing with all situations that may arise in road traffic. The design of such equipment must proceed from a full understanding of the frictional interaction of tire and road.

Prior knowledge of the frictional behavior of pneumatic tires, particularly on wet road surfaces, shows several serious gaps, some of which the authors have attempted to fill. This monograph reports the results of our research, but it also reviews the literature on the subject and offers several new interpretations of existing information. It should therefore be useful to researchers and engineers concerned not only with stopping problems but also with the design of tires and road surfaces.

Several graduate students in the Department of Mechanical Engineering have contributed to the overall picture through thesis research. Their work is acknowledged at appropriate locations in the text. The assistance of Miss Dorothy Anderson, technical editor for the College of Engineering and Architecture, has been extremely valuable. Above all, the research project which produced this monograph owes its existence entirely to financial support by The Pennsylvania State University.

H. W. KUMMER  
W. E. MEYER

University Park, Pennsylvania  
December 22, 1960

# CONTENTS

	Page
List of Figures . . . . .	ix
Nomenclature . . . . .	xiii
 I. FRICTIONAL BEHAVIOR OF RUBBER SLIDERS . . . . .	1
The Classic Laws of Friction . . . . .	2
Theories of Friction . . . . .	3
Mechanism of Rubber Friction . . . . .	3
Friction Caused by Adhesion . . . . .	4
Friction Caused by Hysteresis . . . . .	4
Friction Caused by Cohesion . . . . .	4
Factors Influencing Friction . . . . .	6
Factors in Friction Caused by Adhesion . . . . .	8
Normal Load . . . . .	8
Sliding Velocity . . . . .	11
Temperature . . . . .	23
Contamination and Lubrication . . . . .	24
Factors in Friction Caused by Hysteresis . . . . .	26
Normal Load . . . . .	26
Sliding Velocity . . . . .	29
Temperature . . . . .	29
Contamination and Lubrication . . . . .	31
Summary . . . . .	31
 II. FRICTIONAL CHARACTERISTICS OF PNEUMATIC TIRES . . . . .	32
The Role of the Pneumatic Tire . . . . .	32
Tire and Friction Testing . . . . .	34
Mechanism of Tire Friction . . . . .	37
Factors Influencing the Coefficient of Road Friction . . . . .	39
Apparent Pressure . . . . .	40
Pressure Distribution in the Tire Contact Area . . . . .	40
Effect of Wheel Load, Inflation Pressure Constant . . . . .	42
Effect of Inflation Pressure, Wheel Load Constant . . . . .	42
Effects on the Coefficient of Road Friction . . . . .	42
Sliding Velocity . . . . .	44
Locked Wheel . . . . .	44
Rolling Tire . . . . .	47
Tire under Slip . . . . .	48
Some Misconceptions Concerning Slip . . . . .	50
Cornering . . . . .	59
Temperature . . . . .	62
Contamination and Water Film . . . . .	65
Dry versus Wet Conditions . . . . .	65
Transition from Dry to Wet . . . . .	66
Effect of Polishing . . . . .	66
The Problem of Water Removal . . . . .	69
Basic Principles . . . . .	69
The a/b Ratio . . . . .	70
Mechanism of Water Removal . . . . .	71

(CONTINUED)

## CONTENTS (Cont.)

	Page
II. FRICTIONAL CHARACTERISTICS OF PNEUMATIC TIRES (Cont.)	
Factors Influencing the Coefficient of Road Friction (Cont.)	
The Problem of Water Removal (Cont.)	
Channelization . . . . .	72
Drainage of the Center Section . . . . .	74
Planing . . . . .	75
"Best Point" Compromise . . . . .	75
Summary . . . . .	77
REFERENCES . . . . .	79
APPENDIX	
Laboratory Techniques . . . . .	85
Road Friction Testing . . . . .	86
The Penn State Brake Test Trailer . . . . .	89
Remarks on the Stopping Distance Method . . . . .	92

# LIST OF FIGURES

	Page
1 Mechanism of adhesion, schematic from microscopic view . .	5
2 Mechanism of hysteresis . . . . .	5
3 Influence of track roughness on maximum coefficient under dry conditions . . . . .	10
4 Load dependence of coefficient due to adhesion . . . . .	10
5 Influence of sliding velocity on coefficient due to adhesion for two normal loads, constant-velocity method. .	10
6 Influence of pull force on sliding velocity for two normal loads, constant-pull method . . . . .	10
7 Equivalence of results with constant-velocity and constant-pull methods . . . . .	13
8 Influence of sliding velocity, surface roughness, and lubrication on coefficient . . . . .	13
9 Transient adhesive shear as a function of travel distance and sliding velocity . . . . .	13
10 Influence of travel distance on sliding velocity for two different pull forces . . . . .	13
11 Coefficient due to adhesion at low sliding velocities, replot of Fig. 9 . . . . .	14
12 Coefficient due to adhesion at low sliding velocities . .	14
13 Impedance of contact region of rubber slider as a function of time . . . . .	20
14 Effect of electrostatic attraction on sliding velocity, constant-pull method . . . . .	20
15 Sliding velocity of rubber block as a function of temperature, constant-pull method . . . . .	25
16 Effect of temperature on adhesive shear for two sliding velocities, constant-velocity method . . . . .	25
17 Coefficient due to hysteresis as a function of actual pressure . . . . .	28
18 Comparison of coefficients due to adhesion and hysteresis as a function of normal load, constant apparent contact areas . . . . .	28

(CONTINUED)

# LIST OF FIGURES (Cont.)

	Page
19 Accident rate attributed to skidding as a function of seasonal temperature variations . . . . .	28
20 Decrease of hysteresis component with temperature . . . . .	28
21 Coefficient measured with various friction testers on four surfaces, using different tires . . . . .	36
22 Coefficient measured with seven different friction testers on four surfaces, using identical tires . . . . .	36
23 Idealized contact area of treaded tire resting on coarse road surface . . . . .	43
24 Pressure distribution under cone penetrating rubber block . . . . .	43
25 Effect of wheel load on apparent pressure under center and outer ribs of passenger car tire tread . . . . .	43
26 Effect of inflation pressure on apparent pressure under center and outer ribs of passenger car tire tread . . . . .	43
27 Sliding coefficient of tire versus travel distance . . . . .	46
28 Sliding coefficient of tire at very low sliding velocities . . . . .	46
29 Trends of sliding coefficient at higher sliding velocities, for dry, wet, and icy conditions . . . . .	46
30 Typical decay of sliding coefficient as a function of sliding velocity, dry and wet conditions . . . . .	46
31 Coefficient of braked wheel as a function of wheel slip for two vehicle speeds, dry and wet conditions . . . . .	53
32 Deformation, pressure distribution, tangential shear, and local velocity of tire running under brake slip as a function of contact length . . . . .	53
33 Simplified model of pneumatic tire running under brake slip . . . . .	53
34 Critical slip $S$ and slip components $S_e$ and $S_{sl}$ as a function of vehicle speed, assuming $V_{sl}$ crit constant. . . . .	54
35 Critical slip $S$ and slip components as a function of vehicle speed, assuming $V_{sl}$ crit/ $V_v$ constant . . . . .	54

(CONTINUED)

# LIST OF FIGURES (Cont.)

	Page
36 Velocity vectors of two rubber elements in contact area of tire running under brake slip, viewed from above . . .	60
37 Side force coefficient of pneumatic tire running at a slip angle, dry and wet conditions . . . . .	63
38 Deformation of contact area of tire running at a slip angle, and orientation of cornering, drag, and side force and self-aligning torque . . . . .	63
39 Distribution of lateral shear stresses over contact length for three slip angles . . . . .	63
40 Side force as a function of self-aligning torque, replotted from Fig. 39 . . . . .	63
41 Temporary drop of coefficient during transition from dry to wet conditions . . . . .	67
42 Sliding coefficient in left wheel track and center strip of heavily traveled concrete surface, dry and wet conditions .	67
43 Water to be removed and time available for removal versus vehicle speed, normal passenger car tire . . . . .	73
44 Thickness of water layer under loaded 6 by 4 in. elliptical plate, as a function of time . . . . .	73
45 Influence of heel and toe wear of tread elements on sliding coefficient . . . . .	73
46 Effect of grid size and speed on critical coefficient . .	73
47 Deceleration of vehicle under wet conditions as a function of tread openness, smooth surface . . . . .	76
48 Coefficient of braking as a function of wheel slip and inflation pressure . . . . .	76
49 Critical coefficient as a function of vehicle speed and water layer thickness . . . . .	76
50 Decay of critical and sliding coefficients under wet conditions, treaded and smooth tires . . . . .	76
51 Laboratory techniques to determine the coefficient of friction: constant-pull method, constant-velocity method .	84

(CONTINUED)



# LIST OF FIGURES (Cont.)

	Page
52 Penn State brake test trailer, right and left views . . . .	91
53 Coefficient from stopping distance method, and components due to tire-ground friction and air drag . . . .	95
54 Coefficient from stopping distance method and components, averaged over interval $V_1$ . . . . .	95

# NOMENCLATURE

<u>Symbol</u>	<u>Measure</u>	<u>Definition</u>
A	sq in.	Apparent contact area of rubber block
A <sub>a</sub>	sq in.	Actual contact area of rubber block
A <sub>g</sub>	sq in.	Apparent gross contact area of tire (a × b)
A <sub>r</sub>	sq in.	Apparent net contact area of surface
A <sub>t</sub>	sq in.	Apparent net contact area of tire
a	in.	Length of tire contact area
b	in.	Width of tire contact area
D	in.	Travel distance of rubber block or tire
F	lb	Resultant friction force of rubber block (F <sub>A</sub> + F <sub>B</sub> + ...)
F <sub>A</sub>	lb	Friction force due to adhesion (s × A <sub>a</sub> )
F <sub>B</sub>	lb	Resistance due to hysteresis (γ × E <sub>c</sub> )
F <sub>b</sub>	lb	Resultant friction force of braked tire
F <sub>s</sub>	lb	Resultant friction force of cornering tire
f	-	Resultant sliding coefficient of rubber block (f <sub>A</sub> + f <sub>B</sub> + ...)
f <sub>A</sub>	-	Friction coefficient due to adhesion (F <sub>A</sub> /L)
f <sub>B</sub>	-	Friction coefficient due to hysteresis (F <sub>B</sub> /L)
f <sub>b</sub>	-	Resultant coefficient of braked tire (F <sub>b</sub> /L <sub>w</sub> )
f <sub>crit</sub>	-	Critical or maximum coefficient of slipping tire (F <sub>b</sub> max/L <sub>w</sub> or F <sub>s</sub> max/L <sub>w</sub> )
f <sub>s</sub>	-	Resultant coefficient of cornering tire (F <sub>s</sub> /L <sub>w</sub> )
f <sub>sl</sub>	-	Resultant sliding coefficient of tire
H	in.	Height of first rebound
H <sub>0</sub>	in.	Initial or drop height
h	in.	Average thickness of water layer
L	lb	Normal load on rubber block

# NOMENCLATURE (Cont.)

<u>Symbol</u>	<u>Measure</u>	<u>Definition</u>
$L_w$	lb	Static wheel load
$n$	-	Number of tread elements
$p$	psi	Apparent pressure normal to contact area of rubber block or tread element ( $L/A$ or $L_w/A_c$ )
$p_a$	psi	Actual pressure normal to actual contact area
$p_i$	psi	Inflation pressure
$R_r$	-	Contact ratio of smooth tire on coarse surface ( $A_g/A_r$ )
$R_t$	-	Contact ratio of treaded tire on smooth surface ( $A_g/A_t$ )
$r$	in.	Outer radius of undeformed tire
$r_e$	in.	Effective rolling radius of tire at given speed and torque
$r_{e0}$	in.	Effective rolling radius of tire at given speed and zero torque
$s$	psi	Shear strength ( $F_A/A_a$ )
$S$	-	Total slip $(V_v - V_t)/V_v$
$S_e$	-	Slip component due to elastic deformation ( $V_e/V_v$ )
$S_{sl}$	-	Slip component due to mean sliding velocity in contact area ( $V_{sl}/V_v$ )
$T$	°F	Temperature
$t$	sec	Time
$t_c$	sec	Time a single tread element spends in contact area, $a/(V_v \pm V_s)$
$t_r$	sec	Time available for water removal ( $K \times t_c$ )
$V_e$	ips	Lag velocity due to elastic deformation
$V_s$	ips	Resultant slip velocity

# NOMENCLATURE (Cont.)

<u>Symbol</u>	<u>Measure</u>	<u>Definition</u>
$V_t$	ips	Velocity of tire as computed from wheel rpm and effective rolling radius ( $\omega \times r_e$ )
$V_v$	ips, mph	Vehicle speed
$v$	ips	Sliding velocity of rubber block or tread element
$v_x$	ips	Component of sliding velocity in longitudinal or x direction
$v_y$	ips	Component of sliding velocity in lateral or y direction
$y$	psi	Yield strength for metals
$\alpha$	deg	Slip angle (angle between tire plane and direction of vehicle motion)
$\gamma$	-	Hysteresis coefficient, $(H_0 - H)/H_0$
$\delta$	in.	Deformation of center of a tread element in tire-ground plane, with respect to its undeformed position
$\epsilon$	-	Strain in contact area along a given meridian
$K$	-	Drainage factor
$\omega$	1/sec	Angular velocity of tire at given torque
$\omega_0$	1/sec	Angular velocity of tire at zero torque

## PART I

### FRICTIONAL BEHAVIOR OF RUBBER SLIDERS

Certain characteristics of the pneumatic tire in combination with the good frictional grip of rubber on various surfaces have made possible the control of vehicle motion over a large operational and environmental range. The tire, although subject to continuous modifications in material composition, structure, and shape, has not changed basically since its invention and will remain a vital component of roadbound automobiles and conventional airplanes in the foreseeable future.

Economy and safety of transportation depend to a great extent on the friction potential built into tire and road. Owing to increased travel speed and traffic density, the built-in friction potential for wet conditions, where it is needed most, is constantly diminished by the polishing effect of tires upon the road surface and even by localized oil drippings, rubber deposits, and other organic and inorganic contaminants.

This problem can be kept under reasonable control by the joint efforts of road material suppliers, highway building and maintenance organizations, the automotive and rubber industries, and drivers as well. But success in this direction will be determined largely by (a) how well the basic mechanism of friction between tire and road is understood, and (b) how accurately and economically slippery surfaces can be detected. The second of these factors requires a standard method for measuring the coefficient of friction, which has yet to be found.

Although much work has been done on this subject both in the United States and abroad, it has mainly been concerned with full-scale tire and friction testing. Research of this kind is necessary in terms of tire engineering and vehicle performance, but unless it is supplemented by basic research it cannot contribute much toward a better understanding of the mechanism of rubber friction. In England the Road Research Laboratory links basic research and application. In this country, however, there has been little basic research in this field, and conclusions drawn from full-scale test results have led to some fundamental misconceptions concerning the frictional behavior of rubber.

Several factors affect the friction of a given rubber specimen, stationary or sliding, on a given surface. When rubber is bonded to a pneumatic carcass and tested as a tire on a laboratory rig, more factors enter the picture. Still other factors have to be considered when this tire is put on a test trailer or vehicle and subjected to road tests under various operational and environmental conditions. Moyer (1)\* reported thirty or more factors influencing the friction developed between tire and road. Though most of these factors have second-order effects on friction, their presence in combination with the remaining

---

\* See References.

first-order factors is sufficient to override some of the frictional characteristics of a rubber specimen, and may perhaps account for the misconceptions mentioned.

Here the value of laboratory experiments to assist in interpretation of results obtained from full-scale road testing becomes clear. Laboratory experiments or tests reduce the number of factors that must be considered. Moreover, in a well-designed experiment several factors can be selectively eliminated from the investigation, and those remaining can be much better controlled.

Rubber as a flexible and extensible material is often believed to have rather vague and variable properties. This belief is extended to the tire in even greater degree. True, the close tolerances assigned to metal machine parts cannot be applied to rubber components and tires. Moreover, it is familiar knowledge that tire operation is affected by partial slip and yaw, and that local strain, stress, normal load, and relative motion in the contact area are complex matters not yet completely mapped.

But neither rubber nor the tire is unpredictable. Each shows specific behavior under specific operating conditions. If the conditions are broadened to include such variables as rubbers of different composition and tires of different shapes running on various types of surfaces dry and wet, then, of course, only trends rather than exact analytical relations can be given.

The present study relates the frictional behavior of rubber sliders to the characteristics of pneumatic tires by indicating observable and predictable trends, and draws attention to some of the many unsolved problems in this field.

#### THE CLASSIC LAWS OF FRICTION

Leonardo da Vinci was probably the first purposeful investigator of friction phenomena. His notes contain the statement that friction between two solid bodies is independent of the [apparent] contact area and proportional to the load. He related friction to normal load and found a ratio of 0.25 for the materials investigated.

Amontons, about 1700, verified Leonardo's observations but indicated that the frictional resistance was material-dependent. In 1781, Coulomb and Morin found that the force required to move a body at rest (static friction) is greater than the force necessary to maintain motion (dynamic or sliding friction).

These principles, taken together, are known as the classic laws of dry friction. Using Euler's term "coefficient of friction" for the ratio of friction to normal load, they may be restated as follows:

1. Friction is independent of the apparent contact area.
2. The coefficient of friction is independent of the load.
3. The static coefficient is greater than the coefficient for sliding.
4. The coefficient for sliding is independent of velocity.

The classic laws have survived the years unaltered, and within certain limits they are still valid for most engineering applications. Occasionally they have been applied to rubber -- without justification, as will be shown.

#### THEORIES OF FRICTION

The classic laws do not explain the cause or the mechanism of friction. Both Amontons and Coulomb believed the cause to be purely mechanical. Friction was explained as the force required to overcome the interlocking of microscopic roughnesses on the surfaces in contact and to lift the upper surface over the roughnesses of the lower (2). Some workers still advocate this theory (3, 4). Others maintain that the mechanical component is responsible for only a small percentage of the total friction (5).

Of several recent proposals, the most persuasive are the welding-shearing theory, the electrostatic theory, and the molecular attraction theory. Welding-shearing (6) seems to offer the most likely explanation of the main cause of friction, and is substantiated by many workers (2). Developed for metals, it is applicable to nonmetals as well if the term "welding" is replaced by "adhesion." As applied to both metals and nonmetals, it might be called more appropriately the adhesion theory.

According to this theory, friction is due mainly to shearing and hysteresis or plowing. Bowden and Tabor (6) successfully separated these terms and showed that shear resulting from adhesion, or welding in the case of metals, is the more important. A reasonable distribution of friction for metals sliding on each other may be shear due to adhesion, 80%; resistance due to hysteresis, 16%; and resistance due to lifting, 4%. The exact distribution will be a function of material properties and operating conditions. For softer materials sliding on hard and rough surfaces, the hysteresis component increases and the lifting term becomes insignificant.

Generally speaking, a specimen of any material sliding on any clean or contaminated surface develops a resisting force in the plane of contact. Under specific conditions this force may be due to a single term such as adhesive shear or hysteresis, or it may be purely viscous drag. In most practical cases, however, two or more terms are likely to contribute simultaneously.

In the present study, friction is defined as resistance against sliding, regardless of cause unless specified.

#### MECHANISM OF RUBBER FRICTION

Tabor (7) has shown that the two main causes of rubber friction are shear due to adhesion, and hysteresis. Under specific conditions a term related to the cohesive properties of rubber may also be involved in resistance to sliding.

The lifting term becomes small for softer materials, as mentioned earlier, and is zero for soft rubber sliding on a rigid surface. In

view of the speed range of locked tire operation on roads and runways under wet conditions, viscous drag may also be disregarded as a source of frictional resistance.

The friction attributable to the adhesion, hysteresis, and cohesion terms will now be defined and briefly discussed, in the descending order of their importance.

Friction Caused by Adhesion. A rubber block placed on a clean surface makes intimate contact with this surface in small zones  $A_{a1}, A_{a2} \dots A_{an}$  distributed irregularly over the apparent block area (Fig. 1). In these zones, the sum of which is defined as the actual contact area, molecular interaction forms minute adhesive bonds between rubber and surface. To move the block in the plane of contact or to slide it with constant velocity requires force enough to shear these bonds. The shear resistance  $F_A$  caused by adhesion is proportional to the actual contact area, the constant of proportionality being the shear strength  $s$ .

Friction Caused by Hysteresis. When rubber slides on a sufficiently lubricated wavy surface (Fig. 2), direct adhesional contact between rubber and surface cannot develop. As a consequence, the shear resistance due to adhesion must be zero. Any viscous drag is also negligible as long as the lubricating film remains thick enough and the sliding velocity is not excessive. However, a definite resistance  $F_B$  has to be overcome to maintain the sliding of the rubber block.

On a surface such as that shown in Fig. 2, the rubber is subject to continuous deformation. The process of deformation is restricted to a relatively thin layer of the rubber block, and consists of a compression phase and an expansion phase. A certain amount of energy is required to compress the rubber element as it approaches an obstacle. When the block moves on, the element previously compressed can expand, but owing to hysteresis it gives back only part of the stored energy. The difference between compression energy  $E_c$  and expansion energy  $E_e$  is lost to the rubber and converted into its heat equivalent  $\Delta E$ . To maintain energy equilibrium, the loss must be compensated by external work done on the rubber block. Hysteresis is therefore responsible for the resistance against sliding  $F_B$ . This resistance, defined as friction caused by hysteresis, is proportional to the hysteresis value of the rubber and the deformation it undergoes.

Friction Caused by Cohesion. A knife-edge of finite length but negligible thickness and depth slicing through rubber has to overcome molecular cohesion. But because of the finite dimensions of the knife-edge or surface irregularities, this term is always accompanied by adhesion and hysteresis, and it seems impossible to separate the two latter terms from the first. It is likely that cohesion, as such, has very little effect on friction but contributes indirectly by augmenting adhesion and hysteresis resistance.

Under specific surface and operating conditions, rubber particles are torn out of the slider's surface. Estimates based on the known break-energy density of rubber indicate that this contributes perhaps not more than 2% of the total friction (9). The resulting abrasion



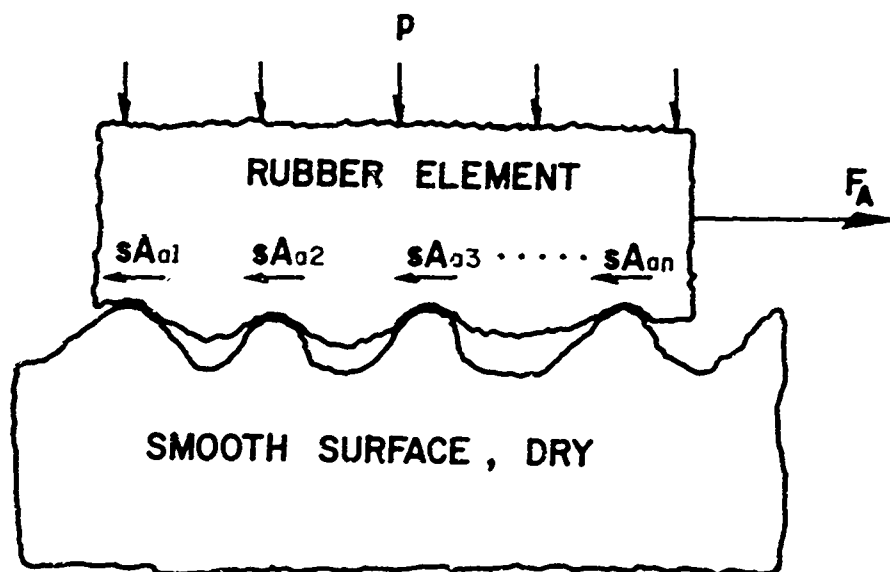


FIG. 1. Mechanism of adhesion, schematic from microscopic view.  $p$ , apparent pressure;  $F_A$ , pull force required to overcome adhesive shear;  $s$ , shear strength;  $A_{a1}$ ,  $A_{a2}$ ,  $A_{an}$ , local contact areas.

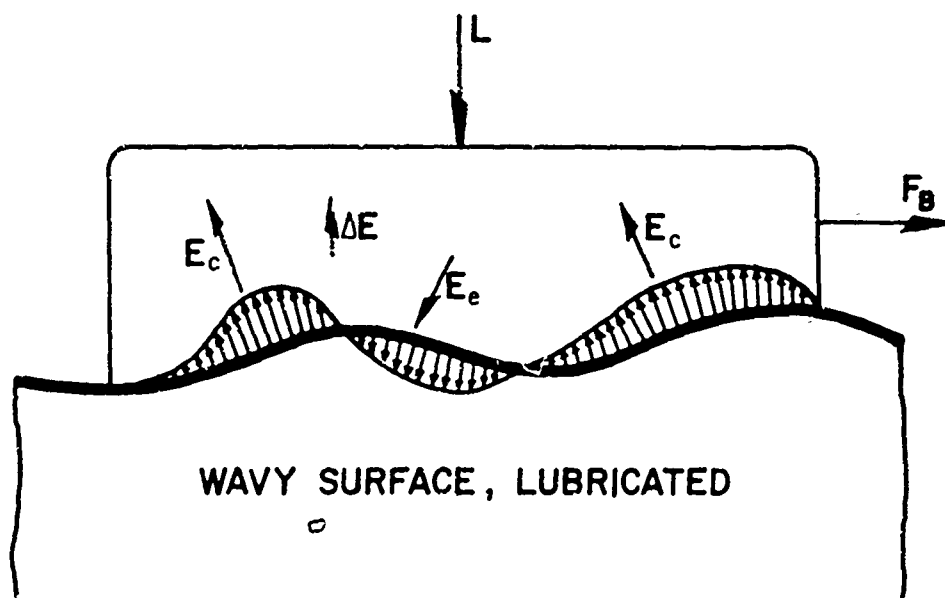


FIG. 2. Mechanism of hysteresis.  $L$ , normal load;  $F_B$ , pull force required to compensate for hysteresis losses;  $E_c$ , compression energy;  $E_e$ , expansion energy;  $\Delta E$ , energy loss (converted into heat).

should be distinguished from the so-called "mild abrasion" that occurs on smooth and polished surfaces and appears to have no detectable effect on friction.

Sometimes the wiping action, and also drainage in the case of tires, are referred to as additional sources of friction. It is certainly true that wiping on dry dusty or contaminated surfaces and drainage and wiping under wet conditions can influence to a great extent the magnitude of friction due to adhesion and hysteresis. But these are mechanical aids to friction rather than causes as are adhesion, hysteresis, and cohesion.

#### FACTORS INFLUENCING FRICTION

The factors influencing the magnitude of the coefficient of friction may be outlined as follows:

- I. Rubber properties
  - A. Composition
    - 1. Type
    - 2. Mix ratios
    - 3. Curing process
  - B. Physical properties
    - 1. Hardness
    - 2. Modulus of elasticity
    - 3. Resilience
    - 4. Thermal and electrical conductivity
    - 5. Decomposition temperature
    - 6. Rate of melting
  - C. Geometric properties
    - 1. Size and shape of slider
    - 2. Surface texture (macro- and microroughness)
- II. Track surface properties and conditions
  - A. Surface composition
    - 1. Aggregate
    - 2. Mix ratio
    - 3. Binder
  - B. Physical properties
    - 1. Hardness and modulus of elasticity (in special cases)
    - 2. Thermal conductivity
  - C. Geometric properties
    - 1. State of smoothness
    - 2. When rough, size and shape of average aggregate
  - D. Contamination and lubrication
    - 1. Type and thickness of contaminating film or type and amount of lubricant
    - 2. Viscosity and its change with temperature
- III. Operating conditions
  - A. Apparent pressure (normal load relative to apparent contact area)
  - B. Sliding velocity
  - C. Bulk temperature of slider

Among these, the most important in relation to friction testing and automobile and aircraft tire applications are apparent pressure, sliding velocity, temperature, and track contamination. The modulus of elasticity, the surface texture of rubber and track, and the apparent pressure specify the actual contact area, at least on a statistical basis, and consequently the resulting friction. It is assumed that the specific shear is only a function of the materials in contact. Therefore, it is not necessary to investigate separately the influence of each of these factors on the magnitude of friction. It is sufficient to know the dependence of the resulting friction, for a given sliding velocity and temperature, on the actual contact pressure. When this dependence is known, the influence of changes in the modulus of elasticity of the rubber or in the texture of the track can be readily deduced.

For example, increasing the load on a rubber block sliding on a polished surface has about the same effect on the coefficient of friction as sliding the block over a slightly rough surface without increasing the load. In both cases the average actual pressure (normal load related to actual contact area) is increased and causes the coefficient to drop, at least in the range of pressures of interest for pneumatic tires.

Although the sliding velocity and the bulk temperature of the rubber slider are related unless the first is very small, separate consideration of these factors makes it easier not only to predict the behavior of the tire but also to understand the reported scattering of results from full-scale friction tests.

In the general case, friction  $F$  is the sum of several components,

$$F = F_A + F_B + F_C \text{ (etc.)} \quad (1)$$

and the coefficient of friction is

$$f = F/L = f_A + f_B + f_C \text{ (etc.)} \quad (2)$$

where  $L$  is the normal load and the subscripts identify the sources of friction:

- A = adhesion
- B = hysteresis
- C = cohesion

Because the mechanism of friction may be different for each term, as is evident especially for terms A and B, the influencing factors cannot be expected to affect each term in the same manner. Consequently, the observation of the resulting friction  $F$  as a function of any such factor is not sufficient to determine the behavior of a single component ( $F_A$ ,  $F_B$ , etc.)

In experiments, however, it is possible to separate the terms by using different surfaces and lubrication (8). Whereas A can develop under either "static" or sliding conditions, sliding is a requirement for

B and C. For deformation of the rubber interface, B also requires a wavy or otherwise irregular surface. C can build up only on rough surfaces of sharp-edged aggregate.

To investigate A, smooth and relatively clean surfaces are required, such as plate glass or highly polished metal. On these surfaces B and C are practically zero. To examine B, the rubber slider is dragged over slightly rough or wavy surfaces, such as pebbled or frosted glass. On these surfaces C is not present, and A can be eliminated by introducing a lubricant. To prevent breakdown of the lubricating film, investigations are restricted with respect to normal load and surface texture. As was pointed out earlier, C can hardly be separated from A and B.

The influence of normal load, sliding velocity, temperature, and contamination will now be examined separately for terms A and B. Term C will not be further discussed, since its contribution is due mainly to adhesive shear and hysteresis, which are covered by the first two terms.

#### FACTORS IN FRICTION CAUSED BY ADHESION

##### NORMAL LOAD

Assuming that the shear strength  $s$  is a constant of the materials composing the rubber and the track, the friction caused by term A can be expressed as

$$F_A = sA_a \quad (3)$$

in which  $A_a$  is the actual contact area, and can be related to the normal load  $L$  by

$$A_a = cL^m \quad (4)$$

For materials having a defined yield strength  $y$ ,  $c = 1/y$  and  $m = 1$ , so that for metals

$$f_A = sA_a/L = s/y \quad (5)$$

indicating that the coefficient due to A is constant regardless of normal load.

According to Hertz's equation (9), for ideally elastic materials with smooth surfaces  $m < 1$ , and for a sphere pressed into such a surface  $m = 2/3$ . Although rubber has no defined modulus of elasticity under tension (10), within a certain pressure range its behavior is quasi-elastic under compression (11) and  $m < 1$ , but owing to microscopic surface roughnesses  $m > 2/3$ . For surfaces with spherical irregularities the exponent was predicted (12) to be 0.89, and was determined by experiments (8) to be 0.87. Using Eq. 3 and Eq. 4, the coefficient of friction due to term A then becomes

$$f_A = csL^{m-1} = C_1 L^{-0.13} \quad (5a)$$

and is load-dependent. Bartenev (21) found that the specific shear  $s$  is also load-dependent, but considers the effect to be of second order.

Equation 5 indicates that for a given normal load the coefficient increases when the actual contact area is increased. This increase can be brought about by substituting a smooth surface for a rough one, and experiments with rubber sliders on smooth and apparently clean glass, plastics, or metal surfaces have shown that coefficients of 2.5 and higher, due solely to adhesive shear, can be obtained (13, 14). The observation that such high coefficients cannot be produced on any coarser surface, where term B can also develop and eventually term C, suggests that no other term and not even the sum of them can compensate for the decrease of term A owing to a shrinkage of the actual contact area (Fig. 3). Reasoning indicates, however, that Eq. 5a can be valid only under specific conditions, that is, for a rubber with a given modulus of elasticity and a small range of apparent pressures.

For very small apparent pressures and a given apparent contact area, it can be assumed that the actual contact area is proportional to the load, so that

$$A_a = cL \quad \text{and} \quad f_A = \text{const} \times s \quad (5b)$$

The coefficient is independent of  $L$ , as for metals. At very high apparent pressures the actual contact area cannot be expected to increase indefinitely with  $L$ . In this case the coefficient is dependent on  $L$  because the actual contact area does not change, and

$$f_A = \text{const}/L \quad (5c)$$

Denny (15) conducted experiments with rubber samples having various moduli of elasticity (defined as the effective modulus under compression not to exceed 10% strain), sliding with a constant velocity of 0.01 cm/sec on a polished steel track lubricated with olive oil. The coefficient of friction was measured as a function of apparent pressure, the latter being varied over the range  $1.4 \times 10^{-3}$  to  $3.1 \times 10^3$  psi. Although this setup suggests that neither complete or dry adhesion between rubber and track nor hysteresis could develop (the viscous term can be neglected because of the low sliding velocity), the friction is proportional to the actual area of contact between the rubber and the layer of olive oil provided the layer is so thin that the shear does not occur within the layer. (The fact that such layers can have elastic rather than viscous properties is discussed later.) Denny's results are in agreement with the findings of Thirion (16), who gave a relation

$$f_A = 1/(c_1 + c_2 p) \quad (6)$$

for the coefficient of friction, where  $c_1$  and  $c_2$  are constants and  $p$  is the apparent pressure. The relation obtained by Denny for the described conditions is

$$f_A = 1/A(1 + Bp/E_0) \quad (7)$$

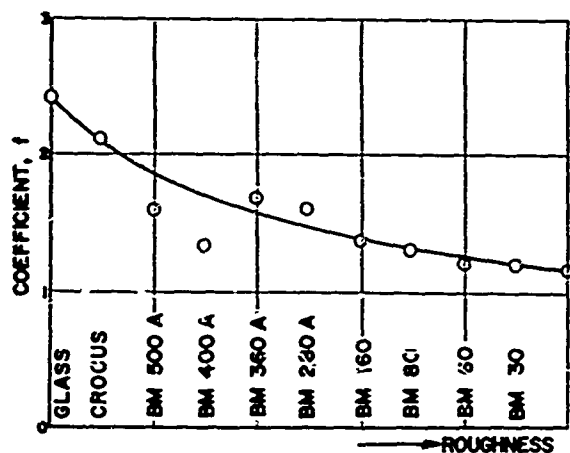


FIG. 3. Influence of track roughness on maximum coefficient under dry conditions. Constant-pull method, synthetic rubber, apparent pressure 1.8 psi, temperature 75° F. Numbers at abscissa refer to grid size of sandpapers used.

FIG. 4. Load dependence of coefficient due to adhesion (15). Polished steel surface lubricated with olive oil; sliding velocity 0.01 cm/sec;  $p$ , apparent pressure;  $E_0$ , modulus of elasticity for rubber under compression.

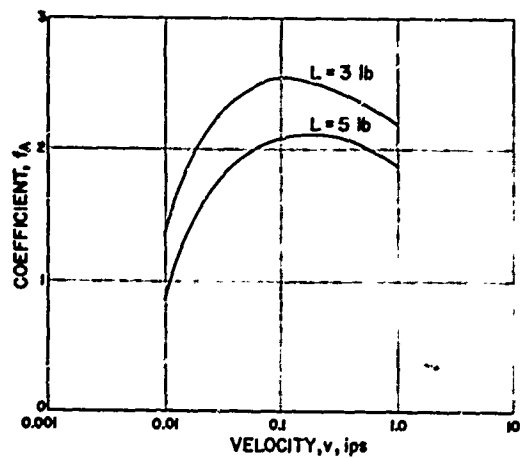
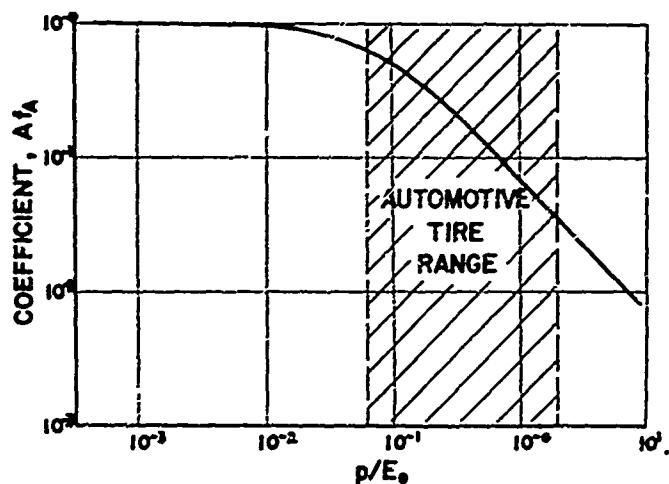


FIG. 5. Influence of sliding velocity on coefficient due to adhesion for two normal loads (18), constant-velocity method. Dry glass surface, apparent contact area 6 sq in., temperature 75° F.

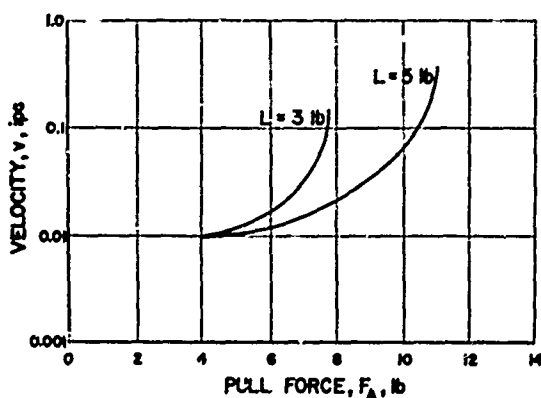


FIG. 6. Influence of pull force on sliding velocity for two normal loads (18), constant-pull method. Dry glass surface, apparent contact area 6 sq in., temperature 75° F.

A and B are constants, A ranging from 1 to 8, B being quasi-constant and approximately 15. The modulus of elasticity  $E_0$  for the samples tested ranged from 14 to 310 psi.

The values of  $Af_A$  versus  $p/E_0$  plotted by Denny (Fig. 4) show the independence of the coefficient from load at small apparent pressures and rapid decay when the latter become high. The dependence of the coefficient on the apparent pressure begins at approximately  $p/E_0 = 1 \times 10^{-2}$ . The corresponding pressures for the lowest and highest moduli of elasticity used by Denny then become

$$E_0 = 14 \text{ psi}, p = 0.14 \text{ psi}$$

$$E_0 = 310 \text{ psi}, p = 3.1 \text{ psi}$$

Average apparent pressures for passenger car tires are about 30 to 65 psi (higher for trucks), at least ten times greater than the pressures deduced from Denny's figures, and consequently in a range where the coefficient of friction is already load-dependent (shaded area, Fig. 4). Within this range a value of  $p/E_0$  can be found for which the coefficient is load-dependent according to Eq. 5a.

#### SLIDING VELOCITY

Rubber placed on a relatively clean dry surface develops the maximum friction at a low sliding velocity, not at rest (static friction). Its behavior has been compared with the shear properties of viscous non-Newtonian fluids (17).

The two means most commonly used to investigate the dependence of the coefficient of friction on the sliding velocity are the constant-velocity and constant-pull methods, described in detail in the Appendix. Using these methods, Foster (18) at Penn State obtained the curves shown in Figs. 5 and 6 for rubber sliding on plate glass. These presentations are equivalent; that is, a decrease of the sliding velocity for constant pull is equivalent to an increase of the coefficient of friction for constant sliding velocity (Fig. 7).

The figures indicate that  $f_A$  rises from a low value (at velocity about zero) to a maximum when sliding has taken place, then drops because of chatter as the velocity is increased. Since the constant-pull method is applicable only as long as the gradient  $df_A/dv$  is positive, no readings can be obtained with this method beyond  $f_A \text{ max}$  (Fig. 6).

The initial increase of  $f_A$  with sliding velocity seems to be characteristic for rubber regardless of composition, surface (as long as it is not lubricated), and apparent pressures. But the rise of  $f_A$ , the magnitude of  $f_A \text{ max}$ , and the corresponding velocity are influenced by those factors. For example, the type and the quantity of filler used in a rubber can have a marked effect on the magnitude of friction and the velocity at which chatter occurs. With increasing surface roughness the rise of  $f_A$  with velocity becomes less pronounced (Fig. 8), and chatter develops at a higher sliding velocity than on smooth surfaces (19).

[Authors' deletion]

Since  $f_A$  for a given apparent load is reduced when the surface roughness increases,  $f$  will become less dependent on sliding velocity, in theory not dependent at all, when a lubricant is introduced (broken line in Fig. 8, viscous term disregarded). The critical velocity for the occurrence of chatter will then become infinite.

Laboratory experiments to investigate the effect of sliding velocity on the coefficient of friction are restricted to a very small velocity range. When the velocity exceeds the order of inches per second, its direct effect on the coefficient under dry conditions cannot be separated from temperature effects on friction, and frictional heating predominates at higher velocities. Sliding velocities that cause melting on the surface cannot be investigated with drums, endless belts, and disks, because the skid marks alter the friction properties of the surface.

In connection with the velocity dependence of  $f_A$ , three questions are of interest: (1) Does rubber have a static coefficient? (2) What causes the initial rise of  $f_A$  with distance and velocity? (3) What causes the chatter of the rubber slider?

Does rubber have a static coefficient? Views expressed in the literature are not uniform. Workers engaged in full-scale tire testing have occasionally assumed that the static coefficient is higher than the sliding coefficient (20). The results of carefully controlled laboratory and road tests performed during the present investigation do not confirm this assumption. Recently the existence of a static coefficient, in the absolute sense, has been questioned for rubber (21) and indeed for all materials (13). The fact that determination of the static coefficient is a matter of some complexity (14, 17) could be interpreted in favor of the latter view.

Figure 9 reproduces results obtained with the constant-velocity method on a glass track (14). The coefficient is plotted versus the travel distance of the rubber block, with sliding velocity as the parameter. It was suggested that extended back to  $v = 0$  the curves would intersect the ordinate at a point corresponding to the static coefficient  $f_{A0}$ . The value of  $f_{A0}$  thus obtained was checked by the same workers with an inclined glass track, and the rubber block would not start sliding when  $\alpha$  was less than  $\tan^{-1} f_{A0}$ . When the angle of inclination was increased above this value, the block started sliding and would continue to do so, although with decreasing velocity, when  $\alpha$  was decreased below  $\tan^{-1} f_{A0}$ .

The curves of Fig. 10 were obtained with the constant-pull method on a ground glass track (17). The normal load applied was 14.1 lb. The velocity of the slider, pulled with 12.8 and 17.2 lb, decreased initially



FIG. 7. Equivalence of results with constant-velocity and constant-pull methods.

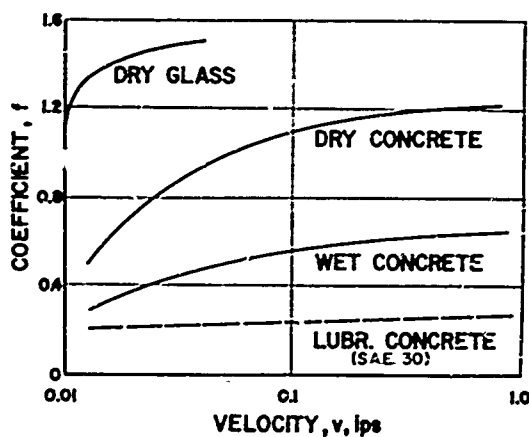
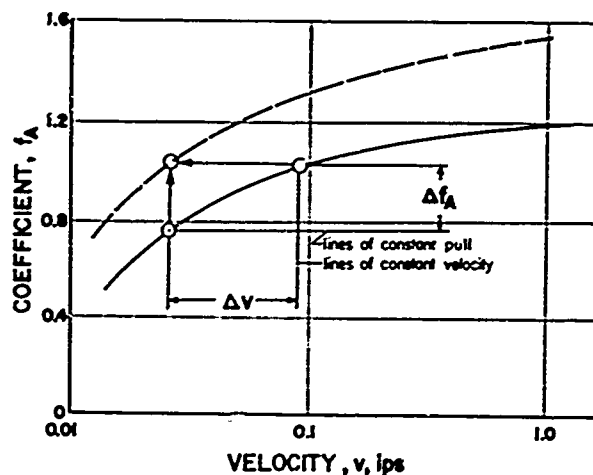


FIG. 8. Influence of sliding velocity, surface roughness, and lubrication on the coefficient (14).

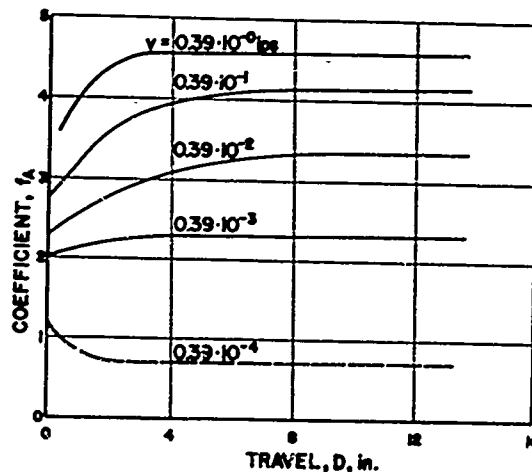


FIG. 9. Transient adhesive shear as a function of travel distance and sliding velocity (14). Dry glass surface.

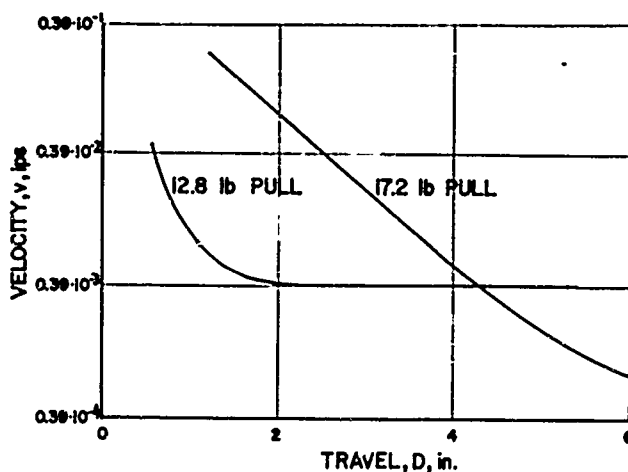


FIG. 10. Influence of travel distance on sliding velocity for two different pull forces (17). Dry glass surface.

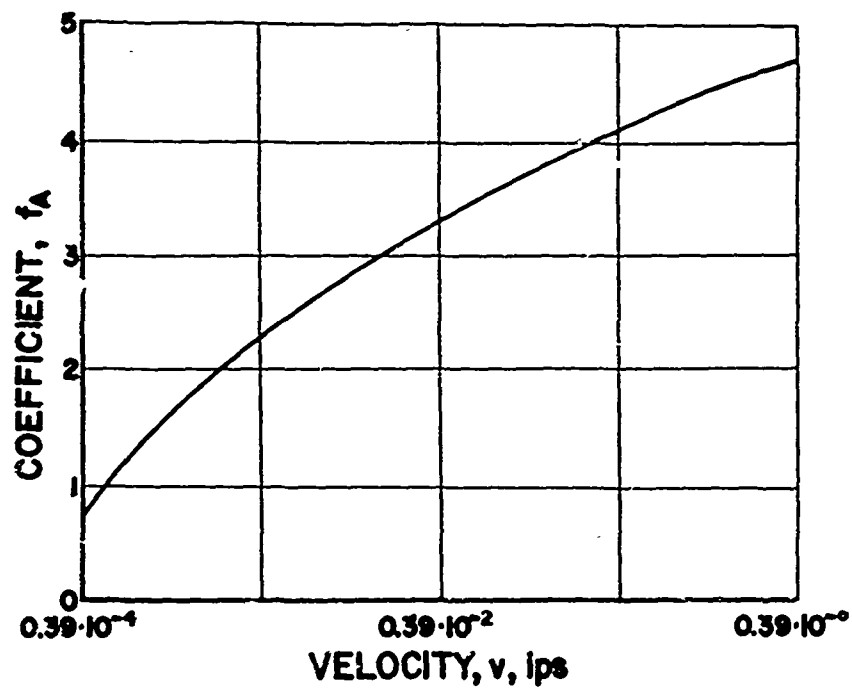


FIG. 11. Coefficient due to adhesion at low sliding velocities, replot of Fig. 9. Values of coefficient taken at steady-state conditions.

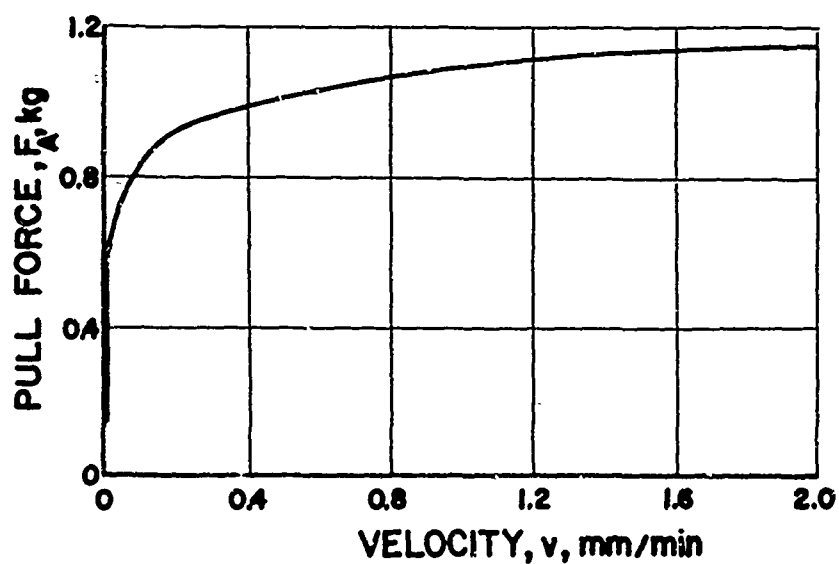


FIG. 12. Coefficient due to adhesion at low sliding velocities (21). Polished steel surface, dry.

with travel. Pulled with the larger weight the slider finally moved along with constant velocity, but when pulled with 12.8 lb it came to an apparent stop after some 8 in. of travel. It was suggested that the lower coefficient,  $f_A = 12.8/14.1 = 0.91$ , would correspond to less than the ultimate static coefficient, and the higher coefficient,  $f_A = 17.2/14.1 = 1.22$ , would be more than the static coefficient.

Although obtained by two different methods, the curves of Figs. 9 and 10 have the same physical meaning and both have been interpreted as evidence for a static coefficient. However, when Fig. 9 is replotted (Fig. 11) with  $f_A$  versus sliding velocity ( $f_A$  taken as the equilibrium value after a certain travel), it appears that  $f_A$  finally approaches zero when the sliding velocity does. Figure 11 is in essential agreement with the interpretation of friction offered by Bartenev (21), who presents a similar graph (Fig. 12). Bartenev's graph, based on investigations of Z. E. Styran, shows the decay of the coefficient with decreasing sliding velocity for rubber on steel.

In experiments performed here, rubber blocks on smooth and rough surfaces would not move for several weeks when the pulling force was increased in small increments from zero and did not exceed a critical value. These results at first seemed to prove the existence of a static coefficient, but it was found that the critical value itself increased when the incremental increases of the pull force were spaced over longer periods of time. If the increase of pull force was halted before the critical value was reached, a detectable force beyond the weight of the block was required to lift it from the track. The separation was accompanied by a sucking noise such as would be expected if the block had been glued to the track with a sticky substance. This bonding effect was observed on both glass and concrete surfaces, but with the same period of contact it was more pronounced on glass. The behavior of the rubber blocks under these conditions can only be explained by assuming that the surfaces, although carefully cleaned at the outset, did not remain clean during the experiments.

Further increase of the pull force resulted in creep, which would also continue when the pull was decreased below the critical value. (Creep rates were observed down to  $1.6 \times 10^{-8}$  ips.) This is in agreement with the experiment carried out on the inclined glass plane, mentioned earlier, and it is likely that the curve for 12.8 lb pull in Fig. 10, if extended to still lower creep rates, would not intersect the abscissa, as the trend of the curve already indicates. Obviously, bonding cannot develop with time where creep occurs.

Detection of minute creep seems to be as difficult as its correct interpretation. In combination with aging, the undefined modulus of elasticity in tension could very well be responsible for limited creep in the rubber sample under stress, even if the rubber molecules in contact with the base would remain stationary. The presence of contaminating films may also contribute in a manner not yet known.

It should be pointed out that initial creep between two materials does not necessarily speak against the existence of a static coefficient.

As long as the rate of creep decays for constant pull, there is a chance that the system comes to rest and will resist a defined tangential force without further motion. Initial creep was also reported for steel sliding on indium (22). It was observed that only minute tangential forces were needed to initiate a relative motion between slider and indium surface, bringing about an increase in actual contact area and a consequent increase in shear stress according to Mises' theory of plasticity ( $p^2 + 3s^2 = y^2$ , where  $p$  is the specific normal load,  $s$  the specific shear, and  $y$  the yield strength of the metal). Apparently the slider will come to rest if the tangential force is not increased.

The important point seems to be that arguments for and against the probability of a true static coefficient arise partly from the difficulty of keeping the contact area clean throughout a long test period, and partly from differences in experimental methods, techniques of measurement, and interpretation of results. The fact that such a coefficient has not been substantiated for rubber under rigorously controlled conditions -- and is not likely to be -- does not mean, however, that the concept of the static coefficient should be abandoned in engineering practice. An automobile left with locked wheels on a ~~critically~~ sloped parking lot will maintain its position there for years.

What causes the initial rise of  $f_A$  with distance and velocity? It has been pointed out that the rise of the coefficient with sliding velocity, as demonstrated in Figs. 5 and 6, must be due to term A, since it is most pronounced on smooth and apparently clean surfaces.

A rubber slider initially at rest but then moved over the track with constant velocity does not develop its steady-state friction immediately. As can be seen from Fig. 9,  $f_A$  increases with travel distance for a given sliding velocity. This behavior of rubber sliders is of interest in relation to the behavior of pneumatic tires, as discussed in Part II, and should be kept in mind. But a minimum creep rate is necessary for this effect, and the travel distance required for  $f_A$  to reach a steady-state value decreases with increasing velocity. The shape of the curves suggests the existence of an activation process that is dependent on both distance and velocity. The terms "conditioning" and "transition from static to dynamic conditions" used in the literature (14, 17) refer to the same phenomena.

When the sliding rubber sample is temporarily stopped, the activation effect is partly or completely lost, depending on the duration of rest. A brief removal of the slider from the track eliminates the effect of activation completely; and for a given sliding velocity, a certain travel distance is required before the original state of activation (coefficient) can be regained (17).

Exactly what causes the increase of  $f_A$  is not fully understood. It is possible that the frictional characteristics observed for rubber sliding on rigid surfaces derive from the kinetic properties of the chain structure of the rubber polymer, as theorized by Bartenev (21). The adhesion term requires contact between molecules of the rubber and the track. The magnitude of adhesion resulting from the summation of shear at the molecular junctions depends not only on the relative mobility of

the molecules (that is, temperature) but also on the orientation of such movement. Bartenev points out that the molecular model for materials with crystalline structure is not applicable to rubberlike materials. The model he proposes for rubber gives the molecule considerable freedom of motion.

When the rubber slider is at rest, with time any of its many molecular chains may change their points of contact with the track molecules in an unorderly fashion; that is, the chains may move in any direction with equal probability. On a statistical basis, these motions cancel one another, and as a consequence a static coefficient cannot exist. It becomes clear that the pattern of motion must change if the slider is to resist any applied stress in the plane of contact. Reacting to a tangential force, the movement of the chains becomes oriented mainly in the direction of such stress. This directed movement causes the rubber to creep, or at higher stresses to slide, and it is believed that the mean speed of the chains is identical with the velocity of the slider. The prevailing motion can perhaps best be compared with the leg movement of a caterpillar. The pattern of motion is oriented mainly in one direction, but it is not synchronous in speed.

The increasing directional orientation of the molecular chains with increased tangential stress can be spoken of as an activation mechanism. This mechanism must be a rate process, because the orientation at any given distance is velocity-dependent. Schallamach (17), investigating the effects of temperature on rubber friction, suggested earlier that the adhesion term is a rate process.

Two other factors may be considered: the presence of contaminating films, and electrostatic charging.

Equation 5 shows that the coefficient of friction caused by adhesion is

$$f_A = F/L = sA_a/L$$

Because  $f_A$  depends on the sliding velocity  $v$ , the shear strength  $s$  or the actual contact area  $A_a$  (or both) may be a function of  $v$  when the normal load remains constant. At the beginning of this section,  $s$  was assumed to be a constant of the materials composing rubber and track. This assumption is justified only as long as both surfaces are absolutely clean so that the two materials can make direct contact.

Experiments performed in relation to the present study indicate, however, that the coefficient of friction for a given sliding velocity on smooth and apparently clean glass and metal surfaces is very sensitive to the type of cleaner used, the procedure for cleaning, and elapsed time after cleaning. This observation argues against the expectation of an absolutely clean surface, and suggests rather the presence of a contaminating film between the rubber and the track surface. Direct contact between the two materials is then replaced by bonding of this film to rubber and track, and at a given sliding velocity this is accompanied by a drop of  $f_A$  due to decreased shear strength. The track can be cleaned

by grinding, as did Schallamach (17), but cleaning the rubber is difficult and the best results are likely to be temporary because some rubber surfaces pick up contaminating film quickly (13).

Contaminating films may have either viscous or quasi-elastic properties, depending on the average film thickness and the chemical composition. In the case of viscous films, shear takes place within the film and Newton's law of viscous shear applies. If the film thickness is assumed to be constant, the specific shear (and consequently  $f_A$ ) would increase linearly with the sliding velocity. The deviation of resulting shear from Newton's law, as observed for increased sliding velocity, could be due to temperature effects on the viscosity, and comparison of the frictional behavior of rubber with the shear properties of viscous non-Newtonian fluids (17) would be reasonable although the order of shear forces involved is quite different. The magnitude of  $f_A$  obtainable from such contaminated surfaces, the initial and distance-dependent rise of  $f_A$  observed for constant sliding velocity, and the occurrence of chatter at elevated sliding velocities would not support the assumption of a truly viscous film.

Thin water films have elastic rather than viscous properties, including yield points when the film thickness drops below a critical value (23). Below this value the shear strength is inversely proportional to the 7th or 8th power of the film thickness. Terzaghi (27) found by experiments that the "viscosity" of thin water films (it is of course misleading to speak of viscosity under these conditions) is a function of the 8th power of the film thickness  $h$ . He gave the empirical formula

$$\eta = \eta_0(1 + a/(h/2)^8) \quad (8)$$

where  $\eta_0$  is the normal viscosity of water and  $a$  is a constant that may take values between  $2.4 \times 10^{-43}$  and  $6.0 \times 10^{-42}$ . The transition from viscous to elastic properties for a pure water film occurs at a film thickness of 150 microns. When the film thickness is decreased to 90 microns, water develops a shear strength of 2860 psi. Impurities in the film raise the critical thickness at which the transition occurs (23).

The increase in shear strength is explained by a rearrangement of the molecules (19). Initial sliding may cause the molecules of the contaminating film to abandon their relative position of equilibrium and form chains oriented in the direction of sliding. The formation of such chains will then decrease the relative mobility of the single molecule, and this is believed responsible for the increase in the effective shear strength. It is evident that this process requires a certain sliding distance. In addition, it must be velocity-dependent, because the reorientation of the molecules is also a rate process.

It is interesting to relate the hypothesized mechanism causing the rise of effective shear strength in thin films to the behavior of rubber elements with sliding velocity. The presence of such films would complicate the picture of molecular movement in the contact plane, but would not alter the effect of sliding velocity on the adhesion term. Because the molecules of the film possess, for the same temperature, a greater amplitude of motion than the molecules of the track, the effective adhesion

at a given sliding velocity would be decreased or a higher sliding velocity would be required to obtain the same resistance as with a film-free track.

Regardless of the presence of contaminating films, the assumption of such an activation process would be in agreement with Fig. 9, which indicates that activation will not take place when the rate of creep is very small, say less than  $10^{-4}$  ips at room temperature. At creep rates below this value the molecules may have sufficient time to escape chain formation and orientation, and the shear strength is not increased.

Two basic experiments in elementary physics are the generation of an electrostatic charge by rubbing two insulators against each other, and the demonstration that two bodies of opposite charge attract each other. The requirements for electrostatic attraction are (a) a mechanism of charge generation (voltage source), (b) good insulating properties in the two bodies involved, and (c) small dimensions, high resistance, and good dielectric properties in the contact region or medium between the two bodies.

These requirements have been met in most of the reported experiments on rubber friction, but few workers have considered the possible additional effect of electrostatic attraction upon the test results. A sliding rubber block can generate an electrostatic charge, and it is reasonable to assume that the voltage generated is proportional to the work done on the rubber slider per unit time; that is, the voltage is proportional to the product of sliding resistance and sliding velocity. Moreover, rubber and most of the track surfaces used experimentally (glass, plastics, various types of sandpaper, and concrete) have good insulating properties.

It has been found (28) that for a given sliding velocity the impedance of the contact region of a rubber slider on a chrome plated brass track is proportional to the pull force needed to maintain constant velocity (Fig. 13). Under these conditions, an electrostatic charge can develop. The main drop of the voltage generated by the slider occurs across the contact region, giving rise to a relatively high-strength electric field and consequent electrostatic attraction. This attraction increases the effective normal load acting upon the sample.

Exploratory experiments in the present investigation, using the constant-velocity method, indicate that a rubber block sliding on a dry surface with insulating properties, and insulated with respect to ground, generates a small voltage that increases roughly linearly with the sliding velocity for a given normal load. The voltage was measured with a high-impedance vacuum voltmeter connected to insulated condenser plates embedded near the rubbing surfaces in the rubber slider and the track. A minimum sliding velocity was necessary to produce a detectable change, and the voltage of the rubber block sliding on glass, plastics, and concrete was always negative.

Based on these findings, another experiment was performed using the constant-pull method. The rubber block and the track were connected

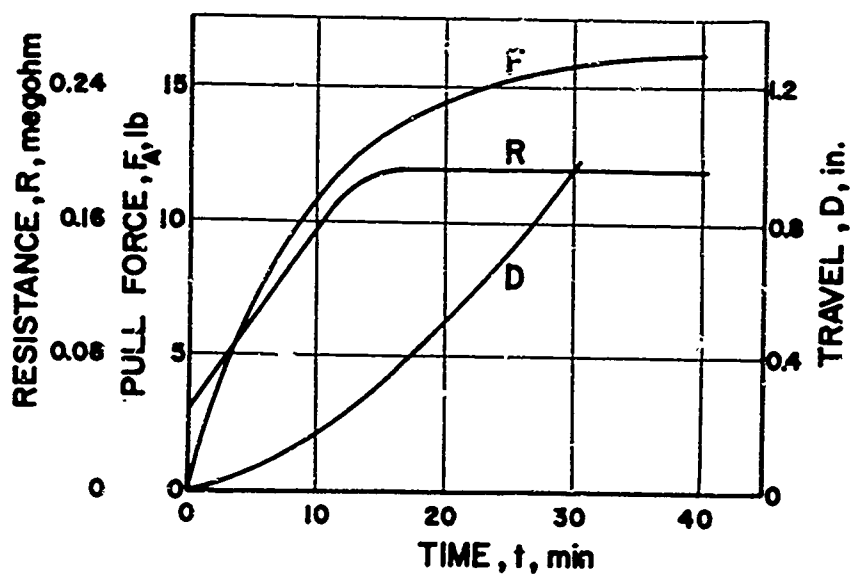


FIG. 13. Impedance of contact region of rubber slider as a function of time (28). Chrome-plated brass surface, dry.

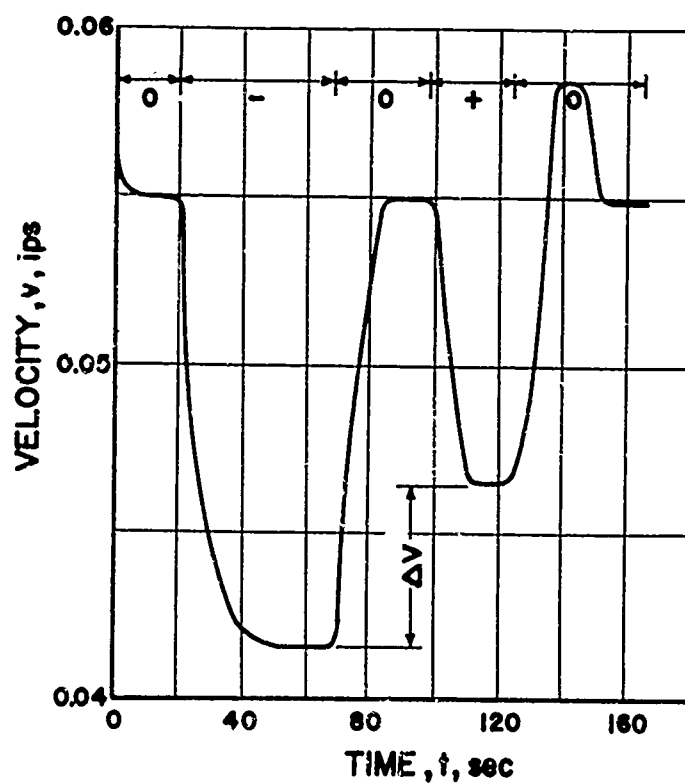


FIG. 14. Effect of electrostatic attraction on sliding velocity, constant-pull method. Dry glass surface, external voltage 200.



intermittently to an external voltage source. Theoretically, this arrangement amplified the effect of the self-generated voltage four times, as can be seen from Eq. 9. The constant-pull method is especially suitable because the velocity/normal-load gradient is large and a small change of the effective normal load owing to electrostatic attraction is indicated by a rather large change in sliding velocity.

As expected, the velocity of the slider dropped when an external charge was applied. The drop was more pronounced, however, when the negative voltage was applied to the slider, because it added to the voltage generated by the latter, whereas positive voltage subtracted from the slider voltage, as shown in Fig. 14. Assuming that the charges on the rubber slider and the track are equal but of opposite polarity, the velocity difference, as indicated in Fig. 14, is proportional to

$$\Delta v = c \left\{ \left[ (e_e + e_r) - (-e_e - e_r) \right] - \left[ (e_e - e_r) - (-e_e + e_r) \right] \right\} \quad (9)$$

$$\Delta v = 4c e_r$$

where  $e_e$  is the voltage superimposed upon the system from the external source and  $e_r$  is the voltage generated by the rubber block.

Under these conditions the rubber slider increases its effective normal load by

$$\Delta L = Q_r Q_t / kd^2 = (1/k)(C e_r / d)^2 \quad (10)$$

where  $Q$  = capacity  $C$  times voltage  $e$   
 $Q_r$  = charge of rubber slider  
 $Q_t$  = charge of track  
 $k$  = dielectric constant  
 $d$  = average distance

Then the effective normal load becomes

$$L_{eff} = L_0 + \Delta L \quad (11)$$

where  $L_0$  is the normal load applied by pressure or weights. But the resulting pull force is usually based on  $L_0$  because  $\Delta L$  can be measured only indirectly by voltage determination or is not considered at all. Owing to this neglect of the change in the normal load, the apparent coefficient of friction is greater than the effective coefficient. It is evident, then, that if electrostatic charging can develop it will amplify the effect of the activation mechanism suggested by Bartenev. To obtain a truer value for the coefficient of friction in such cases, frictional resistance should be based on the effective normal load.

The effective coefficient of friction  $f_A'$  is given by

$$f_A = F/L_0$$

$$f_A' = F/(L_0 + \Delta L)$$

$$f_A'/f_A = L_0/(L_0 + \Delta L)$$

$$f_A' = f_A / (1 + Q_r Q_t / k d^2 L_0) \quad (12)$$

At this time, no attempt was made to determine the various constants as functions of rubber composition, specific pressure, surface properties, and dimensions, or the effects of these on the magnitude of the electrostatic attraction. Further work is necessary to clarify the influence of electrostatic charging and contamination on the coefficient of friction as a function of sliding velocity. It is interesting to note that the presence of electrostatic charging would not contradict Bartenev's hypothesis. When the slider stops, the charge decays because of leakage and the slider again starts with  $L_0$  as its normal load; when the slider is lifted from the track, it discharges completely.

What causes the chatter of the rubber slider? When  $f_A$  reaches its maximum at a critical sliding velocity, a very pronounced chattering may develop in the contact area, causing  $f_A$  to drop. This drop has no direct relation to the observed decrease of the over-all coefficient caused by bulk frictional heating at higher sliding velocities.

The critical velocity at which chatter occurs is a function of the rubber composition, and apparently increases with increasing surface roughness and contamination. Experiments in this study indicate that the critical velocity is of the order of 0.1 to 2 ips for smooth glass, plastics, or polished metal, is sensitive to the relative cleanness of the track, and increases with surface roughness. The high pitch of the noise suggests a high-frequency vibration sometimes called "slip-stick" or relaxation oscillation. This type of oscillation requires that the gradient  $df_A/dv$  must be negative (24, 25).

Motion pictures show that the cycle consists of two phases, the distortion or "stick" phase and the break-loose or "slip" phase (19). The time required to reach maximum distortion is a function of the relaxation obtained in the previous cycle, the bulk or distortion velocity of the slider with respect to the track, and the magnitude of microcreep during the distortion phase. Relaxation oscillations are not necessarily audible, but may be subsonic or ultrasonic (26). Noise should therefore be regarded as a sufficient but not indispensable evidence of chatter.

It can be assumed that the amount of damping due to the hysteresis properties of rubber has an influence on the frequency (audibility) and amplitude (noise factor) of these vibrations. This assumption seems to be supported by the fact that synthetic rubber tires subjected to partial

slippage as the result of high driving or braking torques or cornering forces, squeal very little or not at all when the pavement and the tread are cold. At elevated temperatures, however, the noise generated by the same tire under conditions otherwise the same can become quite pronounced. The magnitude of damping for all known rubber compounds decreases as the temperature rises.

The occurrence of slip-stick has a direct bearing on the friction characteristics of pneumatic tires running under slip, as discussed in Part II, and is undesirable for other reasons than noise generation.

#### TEMPERATURE

Friction between two bodies generates heat, causing the temperature of the contact region to rise. It is assumed that the shear of welding junctions between two metals is accompanied by local temperature flashes. The shear of the minute bridges caused by adhesion between rubber and track may very likely produce similar effects. These flashes cannot be measured with today's temperature sensing devices, which have relatively large thermal inertia, and the bulk temperature of the layer close to the contact region gives no valid indication of the magnitude of local temperatures.

The steady-state temperature of the rubber block reflects the equilibrium between heat generation and dissipation, and can be obtained by energy considerations, using the equation

$$T = T_0 + \beta(f_A v L / \alpha c A_a) \quad (13)$$

where  $T_0$  is the initial temperature when  $v = 0$ ,  $c$  is a conversion factor from mechanical to thermal units,  $\alpha$  is the heat transfer coefficient between rubber block and track, and  $\beta$  is a constant related to the specific heat and conductivity of the track. The equation is based on the assumption that heat transfer from the slider to the track through the actual contact area is the principal means of heat dissipation, neglecting radiation and convection.

Simplification with Eq. 4 yields

$$\Delta T = (\text{const} \times f_A v L^{0.13}) / \alpha \quad (14)$$

indicating that the temperature increase is proportional to the coefficient of friction (which is also a function of the temperature) and to sliding velocity, and inversely proportional to the heat transfer coefficient  $\alpha$ , but is very little affected by the normal load  $L$  for a particular apparent pressure range (see Fig. 4). This is due to the fact that the actual contact area available for heat dissipation also increases with the normal load, according to Eq. 4, although at a slower rate.

For a given rubber and track combination, which fixes the initial value of  $f_A$  and  $\alpha$  and  $\beta$ , the sliding velocity is the determining factor for the temperature developed.

For small sliding velocities up to about 0.5 ips, the temperature rise is negligible and has no significant influence on the frictional resistance. When the sliding velocity reaches the magnitude of 1 fps,  $f_A$  decreases significantly (presumably because the specific shear does, since the actual contact area should increase slightly owing to a decrease in compressive strength), and the coefficient drops to a final value when the melting point of the rubber composition has been reached.

Because the heat generated at low sliding velocities is not sufficient to show the effects of temperature, external heating is necessary for temperature investigations. A heating element was used in experiments, in one case to heat the track and in another to heat the rubber block. The results in both cases were essentially the same. Figure 15 shows the effect of temperature on the sliding velocity for a synthetic rubber slider on a dry glass track, obtained by the constant-pull method. The controllable heating element was placed under the track, as shown schematically in Fig. 15, and the steady-state temperature of the track and the velocity of the slider were recorded.

When the slider approached the heated region, the velocity increased significantly (equal to a drop in the coefficient of friction for a constant sliding velocity). The maximum velocity was reached slightly after the temperature peak, owing to the thermal inertia of the slider.

Schallamach (17) described the relation between sliding velocity and temperature for a constant-pull force by the empirical equation

$$v = \text{const } e^{-(\text{const}/kT)} \quad (15)$$

the form of which suggests the rate process referred to earlier. The dependence of the frictional resistance developed between rubber and a glass track for two sliding velocities is given in Fig. 16.

The effect of temperature on adhesional friction can perhaps be explained as follows. When the temperature rises, the rate of motion in the molecular chains of the rubber block increases. As a consequence, for a given sliding velocity of the block the chains can escape orientation in the direction of tangential stress much more easily than they can under the same conditions but at lower temperatures. To regain the orientation necessary for effective shear, the slider velocity must be increased.

Implementation is now being developed for investigating the effects of higher sliding velocities, and therefore higher temperatures, on the coefficient of friction.

#### CONTAMINATION AND LUBRICATION

As stated previously, the presence of contaminating films or "bloom" decreases the shear strength, with a corresponding reduction of  $f_A$ . Contaminating films seem to be present under all practical conditions, and it is questionable that clean surfaces in the absolute sense can be obtained with available cleaning agents. Schallamach (17) reported that ground glass tracks gave reproducible results.

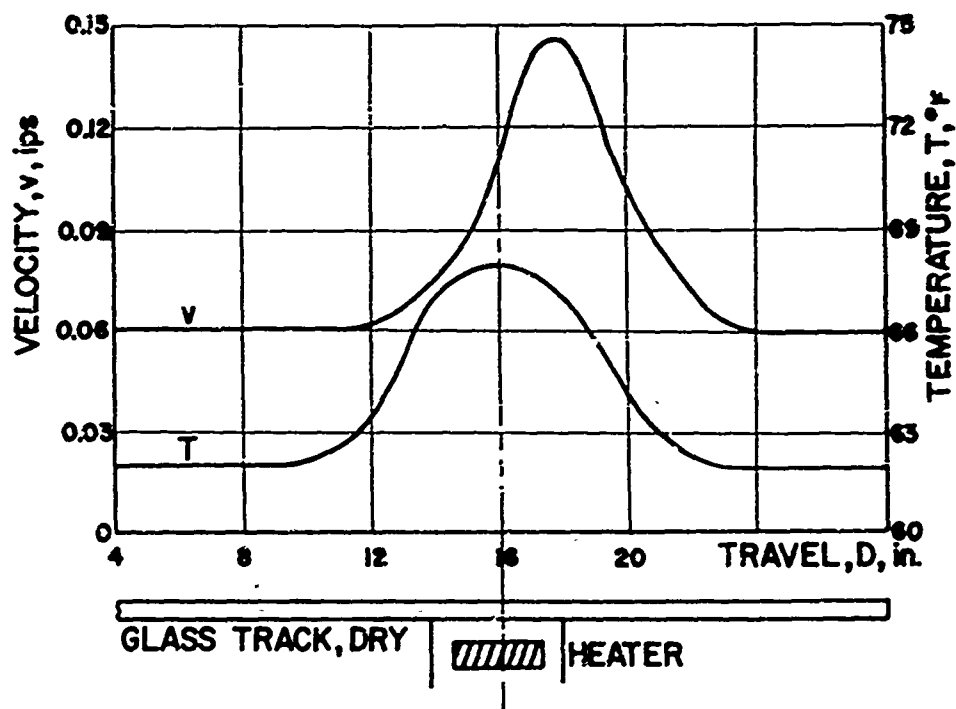


FIG. 15. Sliding velocity of rubber block as a function of temperature, constant-pull method. Dry glass surface with heating element.

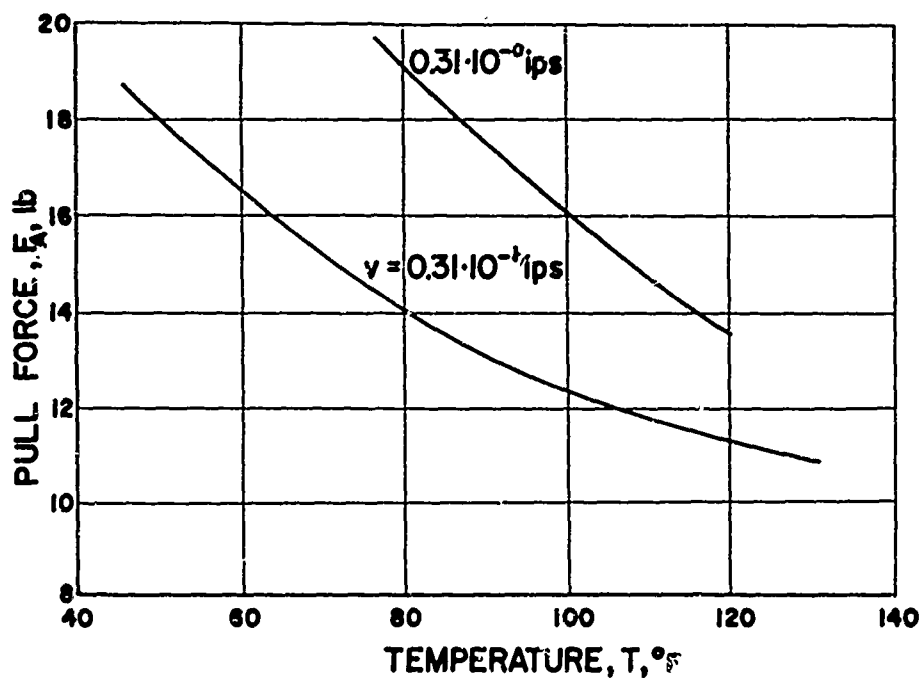


FIG. 16. Effect of temperature on adhesive shear for two sliding velocities (17), constant-velocity method. Dry glass surface.

In experiments conducted here on purposely contaminated and lubricated glass surfaces, the wiping action of the rubber block increased the coefficient of sliding in successive runs at a given sliding velocity. The geometry of the leading edge of the slider appears to be a determining factor. Rounded blocks did not reach the same coefficient as those with relatively sharp edges. The effect of heel and toe wear of tire tread elements on the coefficient of sliding under wet conditions has been reported (29). In that investigation, the coefficient was found to increase approximately 50% when a tread with rounded (worn) leading edges and sharp trailing edges was turned around.

On rougher track surfaces, the wiping action of the slider is less effective because higher local pressures break through the contaminating film. (It is questionable, however, that the wiping action on a smooth but contaminated track completely removes the thin film.)

Further investigation is needed to show whether the shear due to adhesion of a film to the slider and the track occurs in the quasi-viscous transition or in the quasi-elastic region. When the layer between rubber and track is composed of a liquid film, however,  $f_A$  disappears unless the specific normal loads are high enough to enable the rubber to squeeze through the lubricant, or to reestablish the shear properties of a thin film. All other conditions being equal, direct contact between rubber and track is more likely to be obtainable on a coarse track surface than on a surface that is lubricated and smooth.

When effective lubrication is present, the only remaining way to produce reasonable frictional resistance is to use a high-hysteresis rubber and a coarse track surface to ensure continuous deformation of the rubber in the contact region. But the hysteresis term alone can by no means provide sufficient resistance for vehicles moving at medium or high speeds on wet roads. Under such conditions, hysteresis is only a fraction of the adhesion term, as demonstrated by Fig. 18. The adhesion term, although weakened by wet surfaces, still plays the major role.

#### FACTORS IN FRICTION CAUSED BY HYSTERESIS

##### NORMAL LOAD

When a rubber block with defined hysteresis properties slides on a coarse-surfaced lubricated track, there is frictional resistance due to hysteresis (term B) provided the normal load does not exceed a value that causes the lubricant to break down locally. The mechanism of hysteresis is explained in an earlier section and illustrated in Fig. 2.

Tabor (30) showed that the rolling resistance of a sphere traveling on a rubber surface is given by

$$F_R = \text{const} \times L^{1.33} \quad (16)$$

The coefficient of rolling then becomes

$$f_R = \text{const} \times L^{0.33} \quad (16a)$$

When the sphere rolls on a dry surface, the adhesion component is present but trivial because the peeling action of the rolling motion easily overcomes the junctions resulting from adhesion. Hence, the rolling resistance must be due mainly to deformation losses.

If a lubricant is introduced and the sphere is slid over the same surface, the adhesion component again is trivial, although for a different reason, and the resisting force must again be caused by hysteresis. If the normal load is the same on the rolling and the sliding sphere, the rubber will undergo the same deformation in each case. The coefficient of rolling due to term B must therefore be equal to the coefficient of sliding due to term B. Indeed, Tabor (7, 8) showed that  $f_R = f_B$  over a wide range of conditions, so that

$$f_B = \text{const} \times L^{0.33} \quad (17)$$

The increase of  $f_B$  with load is due to a larger than proportional increase of the penetration depth of the sphere into the rubber, and is the main parameter describing the magnitude of deformation.

Theoretically, Eq. 17 can be linearized by introducing the average actual pressure  $p_a$  as  $p_a = L/A_a$ , where  $A_a = cL^{0.67}$  from Eq. 4. Then

$$L^{0.33} = c p_a \quad (18)$$

and with Eq. 17

$$f_B = \text{const} \times p_a \quad (19)$$

The constant is given by the product of the input energy per unit distance  $E_{in}$  and the fractional loss  $\gamma$  due to hysteresis, so that

$$f_B = \gamma E_{in} p_a \quad (19a)$$

Tabor (8), calculating the input energy for a sphere rolling forward a unit distance, found  $\gamma$  to be approximately 0.35 by simple loading and unloading experiments, and derived the relation

$$f_B = 1.4 \times 10^{-4} p_a \quad (19b)$$

His investigation showed that the complex stress cycle to which each rubber element is subjected in rolling leads to higher hysteresis losses, so that  $\gamma$  is approximately 0.7, which changes Eq. 19b to

$$f_B = 3 \times 10^{-4} p_a \quad (19c)$$

Figure 17 shows that  $f_B$  plotted versus  $p_a$  follows Eq. 19c closely up to actual pressures of 400 psi. Above this value the coefficient increases nonlinearly owing to a breakdown of the lubricant and eventual tearing of the rubber.

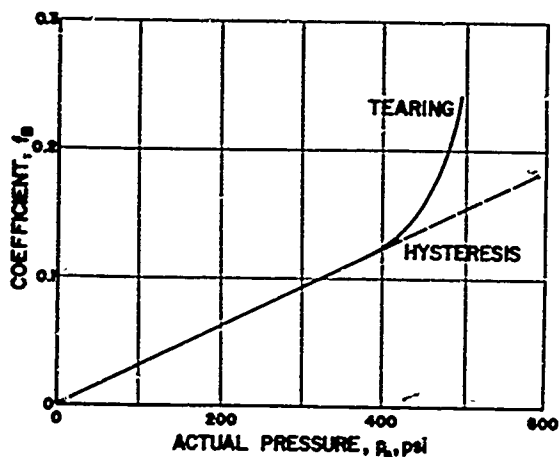


FIG. 17. Coefficient due to hysteresis as a function of actual pressure (8).

FIG. 18. Comparison of coefficients due to adhesion and hysteresis as a function of normal load, constant apparent contact areas (8).

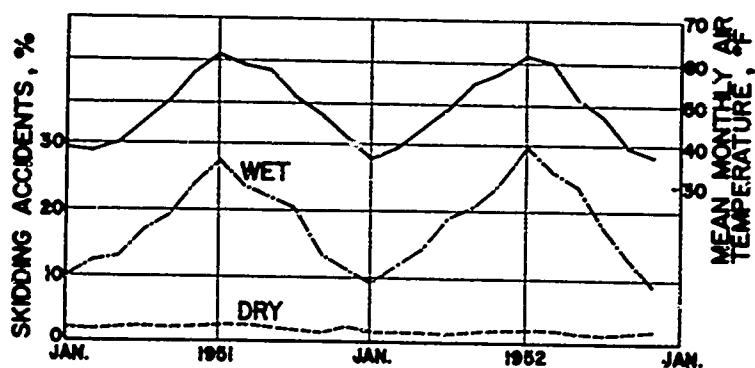
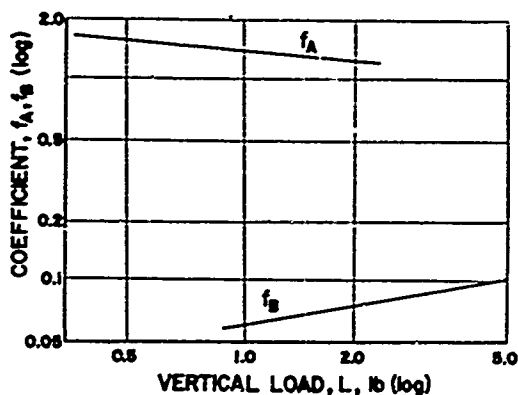
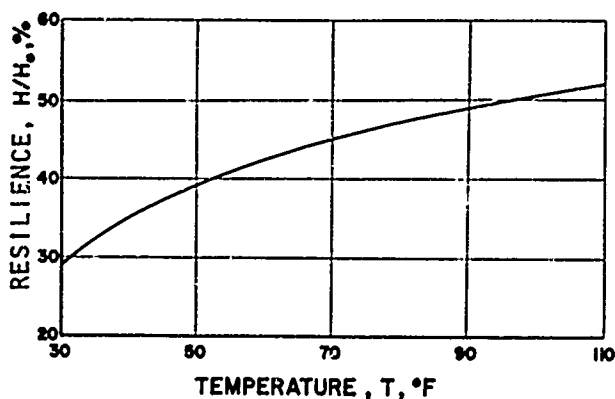


FIG. 19. Accident rate attributed to skidding as a function of seasonal temperature variations (32).

FIG. 20. Decrease of hysteresis component with temperature (33).  $H$ , height of first rebound as percentage of initial height  $H_0$ .





From the foregoing it is clear that in the pressure range beyond 400 psi the presence of  $f_A$  and  $f_C$  can also be expected. Tabor's experiments were extended to a sliding velocity of 6 fps by Sabey (31). At this sliding velocity, water is adequate as a lubricant. The trend of the curves obtained is essentially the same as that indicated in Fig. 17 except that the effective losses increase to more than 70% ( $\gamma > 0.7$ ).

It was shown before that  $f_A$  decreases with increasing load. Comparing the coefficients due to term A and term B as functions of normal load, it is easily seen that their behavior is diametrically opposed, as indicated by Fig. 18.

#### SLIDING VELOCITY

Within limits, the sliding velocity does not alter the deformation loss  $\gamma$  as substantiated by Tabor's loading and unloading experiments (8). As a consequence,  $f_B$  for a rubber slider remains essentially constant within a certain range of sliding velocities, and in this respect the behavior of rubber is similar to that of metals. But hysteresis losses in metals are constant with respect to amplitude and frequency, mainly because of low internal damping ( $\gamma \ll 1$ ) and excellent heat dissipation owing to high thermal conductivity, whereas the conductivity of rubber is low and large  $\gamma$  values produce a high rate of heat generation even in low-hysteresis natural rubbers.

By reasoning, one would expect that amplitude and rate of deformation would eventually influence  $f_B$  in rubber, as demonstrated by the following simple example involving a single cycle of compression and expansion. When a small plunger penetrates a rubber surface at a very slow rate, the energy loss, converted into its heat equivalent, does not increase the temperature of the rubber surrounding the plunger, because sufficient time is available to dissipate the heat by conduction. If the plunger is forced into the rubber quickly, the temperature around the plunger will rise, decreasing the energy given back to the plunger in its return stroke and thus increasing the effective  $\gamma$ .

The results of Sabey's experiment (31) seem to verify such a hypothesis, but there is as yet very little data to support it.

#### TEMPERATURE

In 1934 Moyer (4) reported a definite increase of the coefficient of friction with decreasing temperature under wet conditions. Recent studies made by Giles and Sabey (32) on seasonal variations in skid resistance again showed the dominant effect of temperature on skid resistance under wet conditions.

The decrease of the over-all coefficient with increasing temperature of the water film is directly related to seasonal variation in the rate of accidents chargeable to skidding on wet roadways, as indicated in Fig. 19. The attempt of several workers to explain the temperature behavior under wet surface conditions on the basis of decreased hardness of the rubber, which was known to have an influence on the coefficient of

friction, was not satisfactory because the hardness changed too little with temperature. Now that the relative importance of term B is recognized, a better explanation is possible.

[Authors' deletion]

Giles and Sabey (33), investigating the skid resistance of various rubber compounds as a function of temperature on wet road surfaces, found a decay of the coefficient at increasing temperatures. They also made simple tests of resilience as a function of temperature, using the same rubber mixtures. A steel ball was dropped on the rubber specimen from the constant height  $H_0$ , and the height of the first rebound  $H$  was measured. The relation

$$\gamma = (H_0 - H)/H_0 \quad (20)$$

gives the effective loss  $\gamma$  directly. The height of the first rebound, in percentage of the drop height, is plotted versus temperature in Fig. 20. The temperature-dependence of the hysteresis term suggests again that resistance owing to this term should eventually become deformation-frequency dependent, that is, dependent on sliding speed.

Stegemann (34) also found a definite decrease of the coefficient of friction with rising temperature under wet conditions, but he believed that it was due to change of the surface tension of water with change of temperature. His results show that hydrophile rubber compositions (mixtures that have a good affinity to water) produce a higher coefficient than do hydrophobe mixtures, and he found that synthetics have a good affinity to water, whereas natural rubbers are hostile to wetting.

Simple rebound tests show that synthetic rubbers have much higher hysteresis losses than their natural counterparts. It is therefore likely that Stegemann's experimental measurements revealed more about the hysteresis properties of his rubber sliders than about the effects of the surface tension of water. This follows also from the fact that he used an inclined track with a concrete runway, on which the sliders would be deformed and therefore subject to internal losses. His conclusion that a tire with high skid resistance will skid on road surfaces that are water repellent would be acceptable only if it could be shown that such surfaces were smooth. Nevertheless, it is possible that a definite relation exists between the affinity of various rubbers to water and their hysteresis properties.

The possible application of high-hysteresis rubber for further improvement of skid resistance has been considered (8). In practice, the use of materials with very high hysteresis properties for tires is limited by other considerations, such as rolling friction, tire temperature, wear rates, ride qualities, and cornering. It has been reported that airplane tires skidded on wet grass showed no visible destruction but were damaged just below the contact area, owing to excessive heat. The high temperatures built up in tires on heavy-duty vehicles while in service are directly related to the hysteresis properties of the rubber used in the tires.

If the wheels of vehicles can be positively prevented from locking and if rubber mixtures are improved to provide better conductivity and greater ability to dissipate heat, it is possible that the hysteresis value of all or part of the running band of pneumatic tires can be increased.

#### CONTAMINATION AND LUBRICATION

From the description of the mechanism of hysteresis it is evident that contaminating films can have no effect on  $f_B$ . To a certain extent this is true also for liquid lubricants.

Liquid lubricants can influence  $f_B$  in two ways. When the sliding velocity of the rubber sample is modest and no hydrodynamic effect is present, the liquid may act as a coolant, limiting the drop of  $f_B$  caused by frictional heating. When the thickness or the viscosity of the liquid layer is considerable or the sliding velocity increases, the liquid is not readily displaced and acts as a cushion, decreasing or eliminating the deformation of the rubber contact region with the result that  $f_B$  decreases or drops to zero.

The interrelation of specific normal load, sliding velocity, thickness and viscosity of the liquid layer, drainage from track or road surface and rubber, and the wiping action of the rubber slider is not yet completely understood, nor is the effect of this interrelationship on  $f_A$  and  $f_B$ .

#### SUMMARY

In general, friction is the result of resistance forces of different origins. The adhesion term A predominates under dry conditions. The hysteresis term B predominates when the track is wet, provided the normal pressures are not sufficient to break down the lubricating film. It must be stressed, however, that the hysteresis term alone cannot provide the frictional grip essential for safe operation of vehicles. Whereas the coefficient of adhesion  $f_A$  decreases with normal load, the coefficient of hysteresis  $f_B$  increases.

The adhesion term is particularly dependent on velocity. Contrary to common belief,  $f_A$  reaches its maximum not at rest but at certain low sliding velocities, but  $f_B$  seems to remain fairly constant with respect to a limited range of deformation frequencies if temperature effects are neglected.

The dependence of  $f_A$  and  $f_B$  on temperature is similar. Both coefficients decrease when the temperature is increased.\*

The effect of contaminants and lubricants on  $f_A$  is quite pronounced. On  $f_B$  their effect is insignificant if the thickness of the liquid layer, its viscosity, and the sliding velocity remain small.

\*More recent investigations by the senior author indicate that this statement is not generally true for term A.

## PART II

### FRICTIONAL CHARACTERISTICS OF PNEUMATIC TIRES

#### THE ROLE OF THE PNEUMATIC TIRE

The advantage of wheels rimmed with rubber-coated pneumatic hose over those running on wood or iron was first recognized by Dunlop, who began the manufacture of bicycle tires in Ireland about 1890. Dunlop did not know how important his invention would be to progress in vehicular traffic, nor did he anticipate the complexity of pneumatic tires and the problems related to them.

The first automobile owners did not demand fancy performance of their vehicles. They were satisfied if the car would start, would not break down within the next mile, and would stay on the road however the road might look. But even these early vehicles needed wheels that could transmit to the ground sufficient frictional force to enable the driver to accelerate, drive, climb hills, corner, and brake without regularly inducing a skid.

The pneumatic tire provided a good grip with its flexible and therefore adaptable contact area, and it had excellent lateral holding abilities because it developed large lateral forces under small slip angles. For these reasons it not only relieved the critical problem of vehicle control but also gave a less bumpy and noisy ride.

The modern tire, which is subject to many more and far more rigid demands, represents a complicated but well-balanced compromise. The principal requirements for today's passenger car tire can be listed as follows:

- (1) Adequate transmission of frictional force for a broad range of road surfaces, surface conditions, and speeds.
- (2) Safe operation (elimination of failures due to puncture, tread separation, or bursting) within the design limits of tread life, speed, load, inflation pressure, and temperature.
- (3) Specific cornering characteristics essential to vehicle stability and control.
- (4) Good riding qualities (effective spring rate and damping characteristics), since the tire is an integral part of the vehicle's suspension system.
- (5) Even tread wear and adequate tread life (abrasion resistance) under normal operating conditions.
- (6) Low rolling resistance and heat generation.
- (7) Acceptable noise level.

(8) Resistance to aging, especially freedom from cracking and deterioration under exposure to the atmosphere (ozone, sunlight, etc.).

(9) Low impedance of the rubber compound to prevent the buildup of an undesirable static charge on the vehicle under dry driving conditions.

(10) Close control of dimensions to ensure dynamic balance, and of the properties of all materials used.

The tire designer must be able to satisfy still other requirements, but optimization of only the characteristics listed here is difficult enough. Very expensive experimental programs are set up to verify the acceptability of any chosen solution. In practically all cases a change in tire cross section, structure, rubber composition, tread pattern, design load, or inflation pressure to improve the tire with respect to one characteristic is disadvantageous with respect to one or several of the others.

For example, the persistent demand for a better ride and the recognized advantages of a lower center of gravity have resulted in a reduction of inflation pressure from 35 psi in 1933 to 24 psi in 1960 and a decrease of the outer tire diameter. To support the same load the tire cross section had to increase. These trends have made life more difficult for the brake designer, but they have also brought rolling resistance and heat generation closer to acceptable limits. Relatively low side forces and high self-aligning torques have led to poorer cornering characteristics. It was therefore predicted by French and Gough (35) that tire pressures for standard passenger cars will ultimately level off at 20 psi.

For road vehicles up to 20 tons gross weight (and for airplanes up to 100 tons), tires are expected to provide stability and control at speeds of 60 to 80 mph under dry and wet conditions and 40 to 60 mph on snow and ice. Racing cars and commercial aircraft reach or exceed ground speeds of 200 mph, and jet planes and land vehicles designed for world's record speed competition approach 400 mph. Tires subject to such extreme conditions cannot be expected to provide the same lateral stability as those built for conventional use; they are required to be durable for a prescribed period of time, but stability and control must be secured by aerodynamic means.

The average tread life of a good American passenger tire is approximately 25,000 miles. During this life span each tire section is deflected 20 million times as it comes in contact with the road. After the original tread is worn off, the recapped carcass is expected to run another 15,000 to 20,000 miles.

A few special-purpose tires are now on the market, each of them emphasizing certain properties at the expense of other. Good examples are the thinly coated, treadless high-speed tire, the boxy and treadless "dragster" tire, and the heavily rubbered and open-treaded mud tire. The dragster tire gives the highest possible traction on dry pavement, but it would be extremely dangerous on wet bleeding asphalt. Mud and snow tires, performing well under the conditions for which they are designed, have relatively high wear rates, heat generation, and noise level on dry

pavement. They also have comparatively poor friction characteristics on dry surfaces, but owing to their excellent drainage patterns they may be superior performers at high speed on roads swamped with water, though they are not meant for such use. Many more types of special-service tires will become available in the future. Manufacturers in the United States already offer a choice of passenger car tires for light, medium, or heavy driving, each designed to give the best dollar value for its intended application.

Although the tire industry provides tires incorporating the best current design knowledge, by the choice and use of his tires the operator himself decides whether he gets full advantage of the potential designed into them. He controls inflation pressures and wheel loads, and therefore the life of the carcass; he determines the tread life, and perhaps his own life span, by his driving habits, particularly those involving cornering and speed; he decides when the tire is worn enough to be replaced.

Accidents never just happen; they result from a certain combination of primary and secondary causes. In almost all accidents in which tire-road friction plays a role, the driver is a contributing factor. Under the prevailing conditions, he exceeded the technically safe speed (which usually has very little or no relation to the posted speed limits), attempted a harsh vehicle maneuver exceeding the available friction potential, or drove with one or more bald or underinflated tires at speeds that might have been safe for properly inflated tires with good treads.

Mills and Shelton (36) reported that between 35% and 41% of all accidents in rural districts of Virginia during 1956 and 1957 involved skidding, and that in 35% of these cases the skid occurred before the brakes were applied. Such accidents show clearly that the motoring public is generally unaware of the physical limitations of vehicle, tire, and road, and the dangerous consequences of excessive speed or underinflated, overloaded, and worn tires, especially when driving under wet conditions. Drivers are sometimes misled by surfaces that appear to offer a good grip but actually have a very low coefficient of friction. (The expert's guess of the prevailing coefficient is usually not much better.)

#### TIRE AND FRICTION TESTING

A review of the literature shows that until 1925 knowledge of the mechanism of friction transmission was very limited and largely empirical. The demand for safe handling of more powerful and faster cars, and in particular the problem of shimmy, started more active research in this field. Between 1930 and 1945 a better, though still incomplete, understanding was obtained of longitudinal and lateral tire characteristics as related to deformation in the contact area. This led to various theories forwarded by Temple, Von Schlippe, Rotta, and Fromm (38, page 35).

In addition, dynamic vehicle stability (or full stability, which includes consideration of aerodynamic forces) was studied by Kamm and

coworkers (37). A literature survey by Hadekel (38) covers the bulk of such work up to 1950. Since then an impressive amount of both theoretical and experimental work has been done on pneumatic tires and their many related problems. The problems of vehicle stability and control are similar to those of flight stability and control for airplanes. Researchers of the Cornell Aeronautical Laboratory investigated lateral, nonsteady tire behavior and vehicle stability, using analytical and experimental methods developed for aircraft (39). A fairly complete review of knowledge as of 1958 can be found in the Proceedings of the First International Skid Prevention Conference, conducted by the Virginia Council of Highway Investigation and Research, Charlottesville, Virginia.

During the past 10 years, five of the major United States tire companies have spent approximately \$25 million, destroyed more than 250,000 tires, and run many millions of test miles in the process of developing, designing, and improving tires and controlling their quality.

The reasons for this activity and its continuation are that the tire is a complex structure and its motion and deformation are not easily analyzed or measured. Furthermore, the "footprint" of the tire, which basically results from the contact of a resilient toroid with a solid plane surface, imposes a complex stress and strain cycle on the ever-changing section of the tire passing through the contact area. The load distribution in the footprint obeys no simple law; it is affected by the structural stiffness of the tire carcass, and at higher speeds, the centrifugal and inertial forces acting on each tire element.

Additional parameters introduced by road and vehicle further complicate the problem. A toy tire with a diameter of 1 in. has qualitatively the same characteristics as the 7-ft tire of an earth moving machine with respect to fore and aft forces and slip, side forces and slip angle, and camber. But quantitative differences and deviations from idealized curves make an over-all dimensionless treatment impractical. The vehicle designer must have exact data concerning effective rolling radius, power consumption, cornering force, and self-aligning torque, and these can be obtained only by statistical methods from tests. Each entire series of experiments must be repeated whenever one or more of the tire characteristics is changed.

Although reported research on the pneumatic tire is now impressive in quantity, its general usefulness is limited by differences of purpose and method among the several groups engaged in experimentation. The tire industry is interested in the tire for its own sake. Highway engineers use tires in determining the skid resistance of new and old road surfaces. The automobile engineer is interested in vehicle performance. In full-scale tests he analyzes the tire in terms of power consumption, cornering properties, and the stopping distance of the vehicle under various road conditions. The road materials industry has recently begun to use tires in the laboratory and on the road to obtain data on the rate of polishing of various aggregate types and consequent changes in the coefficient of friction.

Results obtained by any one of these groups are directly useful to another in a few special cases only. Moreover, each group has developed

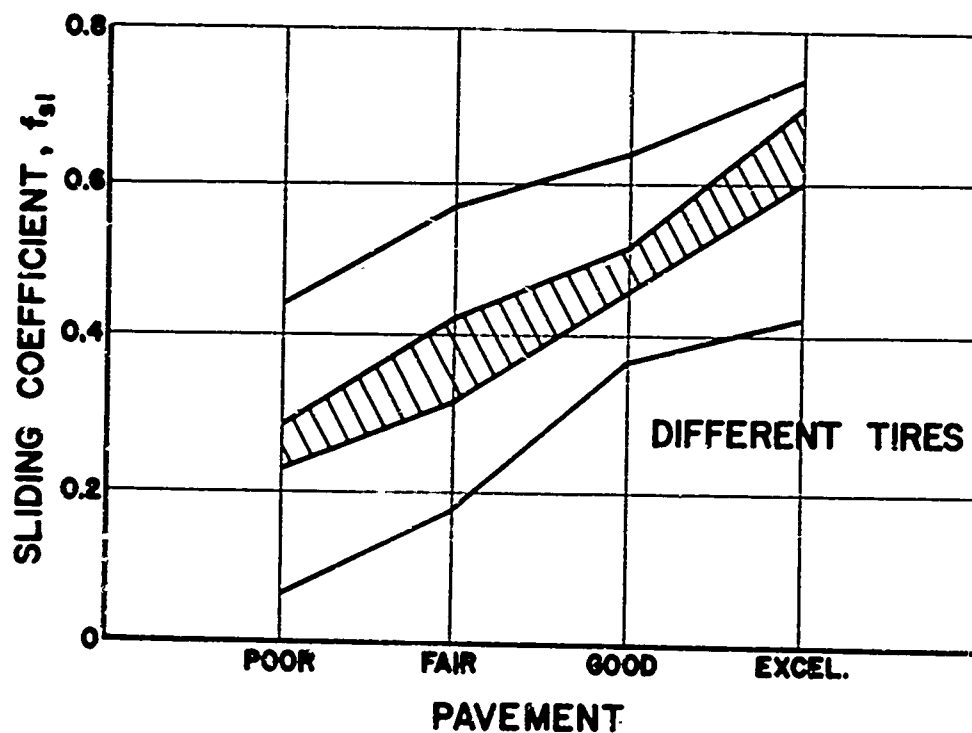


FIG. 21. Coefficient measured with various friction testers on four surfaces, using different tires (40).

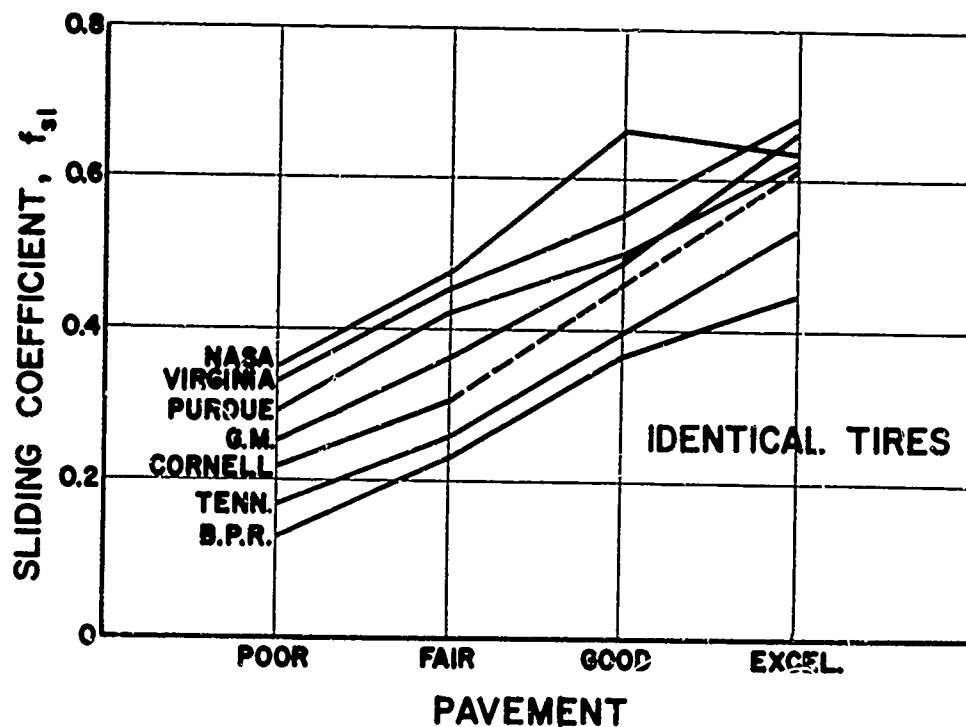


FIG. 22. Coefficient measured with seven different friction testers on four surfaces, using identical tires (40).



its own nomenclature, and even within a single area of investigation comparison of results is sometimes difficult because terms and parameters are too loosely defined. The term "coefficient of friction," for example, is used to describe the coefficient (a) "at rest," (b) during an impending skid, (c) in sidewise sliding, or (d) in forward sliding with the wheel locked. In many experiments, factors needed for full evaluation of the results or for comparisons are either not measured or not reported.

A correlation study conducted prior to the First International Skid Prevention Conference showed clearly that differences in equipment and methods of recording alone accounted for significant variations in results obtained from carefully controlled tests conducted on the same section of road with different and identical tires (40). Friction testers of various design measured the coefficient of road friction on four kinds of pavement under wet and otherwise controlled conditions. The results reproduced in Fig. 21 were obtained with different tires. The use of identical tires decreased the spread of the data only slightly (Fig. 22). The remaining discrepancies are due primarily to variations in equipment design and methods of measuring the friction forces in the tire-ground plane. As long as some machines measure extremely slippery conditions where others indicate a safe surface, comparison of data obtained with these machines at different locations throughout the nation is certainly unwarranted.

A standard friction test method is urgently needed, but much work must be done before such a method can be developed and widely adopted. Meanwhile, reporting of friction experiments could stand improvement.

#### MECHANISM OF TIRE FRICTION

The correlation study mentioned in the preceding section emphasized the significant influence of methods of measurement and design of test devices on coefficients of friction. Experience also seems to indicate that a given test device is unable to produce the same coefficient in successive runs, even though all conditions are apparently kept constant. This would be quite discouraging except for the fact that the reasons for the variations are definite and explainable.

The objective of the following paragraphs is to show (a) that some important tire characteristics can be related directly to the frictional behavior of a sliding rubber block, and (b) that a few basic experiments and application of their results can help to decide whether measured quantities are actually caused by tire friction or by the apparatus and the method of measurement.

As explained in Part I, the mechanism of rubber friction involves principally adhesion and hysteresis. These two terms, and especially adhesion, govern the ability of rotating pneumatic tires to resist longitudinal as well as lateral forces of the order of magnitude of the normal load without letting bodily sliding occur. The manner in which a specific tire deforms in the contact area is also a factor in resistance to sliding.

The mechanism of force transmission is more complex for tires than for a single rubber block, because more variables are involved and tire elements undergo complex stress and load cycles on passing through the contact area, and because rubber friction as a rate process takes place under nonsteady-state conditions in the case of a slipping tire.

Before discussing the main factors that influence the magnitude of the coefficient of friction, some terms must be clarified. In the few instances where the static coefficient enters the picture, it should be understood as limited by the discussion in Part I (page 14). In the laboratory, friction experiments are conducted on level tracks. Fluctuations of the normal load due to dynamic effects are therefore absent, even when the rubber block is suspended by a vibratory system. The coefficient obtained from road tests is usually computed by relating the friction force measured in the tire-road contact plane to the static normal load of the tire. Depending on the suspension characteristics of the friction tester, the levelness of the road surface, and speed, the actual normal load fluctuates around this static value. These fluctuations do not change the coefficient significantly if it is based on the mean value of the friction force recorded over a given time period.

Aerodynamic drag and lift forces can have a more serious effect on the coefficient, since they shift the mean value of the normal load away from the static value. Depending on the aerodynamic shape of the test apparatus and the testing speed, the error thus introduced can be quite large if the friction force is again related to the static normal load.

It is necessary, then, to distinguish between the coefficient of road friction, which is the coefficient obtained by relating the average friction force to the static normal load, and the actual coefficient, which represents the ratio of the friction force to the actual normal load of a given rubber element in the contact area at any instant. The actual coefficient resembles more closely the coefficient obtained in the laboratory under the same conditions of normal load, speed, temperature, and so forth, and is generally higher. The definition for the coefficient of road friction does not distinguish whether the coefficient is attained by a tire slipping fore and aft or sidewise, or by a sliding tire.

The highest obtainable coefficient (sometimes called the impending skid coefficient, which is due to a certain slip in braking or slip angle in cornering, is referred to as the critical coefficient, and the word "critical" also identifies the slip or slip angle at which it develops. The term sliding coefficient requires no definition.

Small motions of individual rubber elements in the contact area of the tire are called creep. When rubber elements move with a velocity greater than 1 ips relative to the road surface, such motion is arbitrarily called sliding. That part of the contact area in which local sliding accompanied by slip-stick occurs is identified as a disturbance area. The term slip is reserved for a dimensionless ratio of slip speed to vehicle speed. Skidding denotes the involvement of a vehicle in an uncontrollable motion.

Normal load is the wheel load normal to the contact area. Apparent pressure relates the normal load to the apparent contact area. Gross contact area is the apparent contact area of a smooth tire in contact with a smooth road surface. It is the maximum contact area obtainable. Net contact area is the apparent contact area of a treaded tire in contact with a smooth road surface, a smooth tire in contact with a coarse road surface, or a treaded tire in contact with a coarse road surface. The net contact area is always smaller than the gross contact area.

#### FACTORS INFLUENCING THE COEFFICIENT OF ROAD FRICTION

Tire and vehicle factors that influence the coefficient of road friction, in addition to those given on page 6 of Part I, are indicated in the following outline. Some of these have only slight effect on the coefficient, but they are included so that the picture may be complete.

##### I. Tire

###### A. Size and shape

1. Width to depth ratio
2. Width to diameter ratio
3. Width of running band
4. Length of footprint

###### B. Tread design

1. Apparent tread-contact area
2. Number of ribs, slots, or sipes
3. Depth of tread

###### C. Carcass

1. Strength of cord material
2. Cord angle
3. Number of plies
4. Longitudinal and lateral stiffness
5. Effective spring rate and damping
6. Hysteresis
7. Thermal conductivity

##### II. Vehicle

###### A. Power train

1. Drive characteristics
2. Brake torque characteristics
3. Steering geometry

###### B. Suspension system

1. Vibration modes and frequencies
2. Roll-steer ratio
3. Stiffness of frame

###### C. Body design

1. Location of center of gravity
2. Load shift due to accelerating, braking, and cornering
3. Aerodynamic resistance and lift

When special devices are employed to measure the coefficient of road friction, they may introduce additional factors that must be taken into account in analyzing the measurements.

The maximum coefficient of friction obtained on a sliding rubber block in the laboratory can be duplicated with a pneumatic tire only when it is locked and provided all pertinent variables are the same. When the tire runs under slip fore and aft or sidewise, the maximum value of the coefficient for a rubber block cannot be reached, for reasons that will later be explained.

The influence of apparent pressure, sliding velocity, temperature, contamination, and lubrication on the two main terms of friction, adhesion and hysteresis, was discussed in Part I. The influence of these same factors on the coefficient of road friction will now be considered.

#### APPARENT PRESSURE

Pressure Distribution in the Tire Contact Area. The pneumatic tire does not act like an air spring, as is often assumed. Under deflection it carries the additional load mainly through an increase of the apparent contact area (and, of course, the actual contact area). Deflection as such has no significant influence on the internal pressure of the tire, since the change in air volume is rather small, but temperature and water vapor content do influence inflation pressure to a high degree (35). It has been reported that the running band of a rolling tire can easily reach a temperature of 212° F (41).

Assuming an initial tire temperature of 70° F and a constant-volume state of change, the initial air pressure within the tire is increased by 13% when the air temperature inside the tire rises to 140° F. Under certain conditions such a rise is possible, especially when the vehicle is continuously braked and the rim and brake assembly fail to act as a heat sink. This automatic pressure adjustment as a function of temperature (which is a function of road surface temperature, vehicle speed, and hysteresis of carcass and tread), is an important safety feature because it counteracts the heat generated by carcass flexing. The increase in inflation pressure makes the tire stiffer in the longitudinal and lateral directions, which is desirable for vehicle control and the generation of standing waves at high speeds.

If the tire were a thin, perfectly flexible inflated hose making contact with an absolutely smooth surface, the apparent pressure  $p$  acting upon the hose from the surface would be identical with the inflation pressure  $p_i$ . In this case the gross contact area is given by  $A_g = L_w/p_i$ , where  $L_w$  is the normal load on the wheel. But when the tire is treaded, the apparent area of contact decreases and the apparent pressure is increased. If the road surface is textured, the apparent pressure rises still more. Hence, the apparent pressure in the tire contact area is always higher than the inflation pressure.

Figure 23 shows schematically a cross section through the contact area of a tire resting on a coarse surface. The tread is assumed to consist of quadratic buttons, and the coarse surface is similarly idealized. The distribution of the tire and surface buttons is assumed to be uniform. It is convenient to relate the net contact areas of tire  $A_t$  and surface  $A_r$  to the common gross contact area  $A_g$ , and so derive the contact

ratios  $R_t$  and  $R_r$ . For the treaded tire on a smooth surface,

$$R_t = A_g/A_t \quad (21)$$

For the coarse surface under a smooth tire,

$$R_r = A_g/A_r \quad (21a)$$

Here,  $A_g$  is defined as the product of the contact length  $a$  and the width of the running band  $b$ , so that  $A_g = ab$ .

The gross contact area  $L_w/p_1$  derived for the thin flexible hose is not reached by the tire, because the carcass is capable of transmitting bending stresses. It should be noted, however, that the carcass stiffness and its effect on the pressure distribution lose significance when the inflation pressure becomes high. The value  $ab$  then approaches the limits of  $L_w/p_1$ . For a treaded tire on a smooth surface, the resulting pressure in the contact area is

$$p = (A_g/A_t)p_1 \quad (22)$$

For a bald tire on a coarse surface,

$$p = (A_g/A_r)p_1 \quad (22a)$$

Combining both cases

$$p = (A_g^2/A_t A_r)p_1 = R_t R_r p_1 \quad (23)$$

The contact ratios for passenger car tires range from about 1 to 2 for bald tires to snow tires. Surfaces may vary from about 1 to 3 for bleeding asphalt to coarse asphaltic concrete. The average contact pressure can therefore be as much as six times higher than the inflation pressure, even for the idealized situation of Fig. 23. Actual pressures are still higher, if only because of the geometry of the aggregate. Investigations by Giles and Sabey (42) employing the pressure sensitivity of x-ray film showed local pressures of 1000 psi on the peaks of the aggregate. Work by Sabey (43) on the pressure distribution under spheres and cones forced into rubber gives evidence that local peak pressures of 5000 to 6000 psi may be obtained for cone angles of 90 degrees ( $\alpha = 45$  degrees) or less (Fig. 24). The pressure distribution produced by the penetration of a road surface asperity into a tire appears to be similar.

Sabey also found that under wet conditions the sliding coefficient is proportional to the average pressure developed in the actual contact area. The main factor under such conditions is apparently the average tip angle of the asperity. If the angle is equal to or smaller than 90 degrees, a high coefficient of sliding can be predicted under wet conditions.

Weber (44) showed that approximately 10% to 15% of the tire's design load is carried by the carcass. Because carcass stiffness has its greatest effect on the outer ribs of the tread, the pressure is highest under these ribs. The uneven distribution of the apparent pressure across a tire can be observed in skid marks under dry conditions and from the water pattern left by the tire on a wet road. The water is more thoroughly displaced in the strips at the outer edges of the tracks than it is in the center.

When a tire is rolling at higher speeds, the pressure distribution is further changed by the inertia of the rubber elements moving into the contact area.

The foregoing implies that a change of the normal load at constant inflation pressure and a change of the inflation pressure at constant load must have different effects upon the pressure distribution in the contact area. The two cases are therefore discussed separately.

Effect of Wheel Load, Inflation Pressure Constant. An increase in wheel load causes an increase in contact area, but also increases the local pressure at the outer ribs because the bending of the carcass has become more severe. The pressure at the center is hardly affected; here the tire behaves like a membrane and the pressure under this area can be changed only by inflation pressure. Figure 25 is a replot of data presented by Hofelt (45), showing the effect of wheel load on the local pressure at two characteristic locations. The pressure distribution in the contact area was measured with miniature load cells. As can be seen, an increase of wheel load at constant inflation pressure increases the differences in local pressure across the contact area. It is believed that such differences are undesirable from the standpoint of wear, the critical coefficient attainable, and water removal.

Effect of Inflation Pressure, Wheel Load Constant. Increased inflation pressure at constant wheel load decreases the contact area. When Hofelt's data for this case (Fig. 26) are compared with Fig. 25, it is evident that the share of the load carried by tire elements in the center of the contact area increases about linearly with inflation pressure. The pressure under the outer ribs is very little affected, perhaps even showing a slight tendency to decrease. Increasing inflation pressure decreases the differences in the shares of the load carried by the center and outer ribs.

Effects on the Coefficient of Road Friction. It is obvious that the influence of wheel load and inflation pressure on the coefficient of road friction can be investigated only when the tire is run with unchanging slip, slip angle, or sliding velocity.

The footprint of a typical standard passenger car tire has the same net contact area whether it carries a 1085-lb load at 16 psi or a 1515-lb load at 24 psi. In the latter case, however, the average pressure in the contact area is higher. As was pointed out in Part I, the coefficient of friction due to term A decreases with increasing pressure. This implies that the coefficient of road friction at a given slip or slip angle

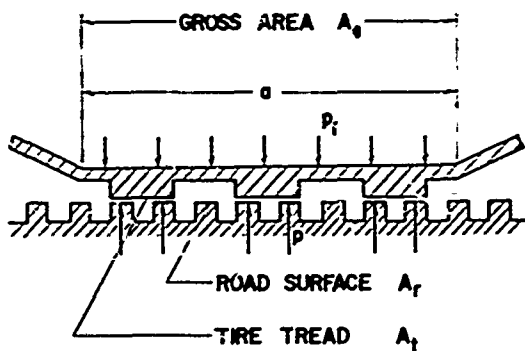


FIG. 23. Idealized contact area of treaded tire resting on coarse road surface. Depth taken as unity.

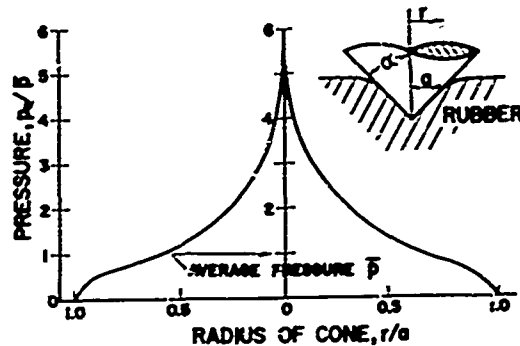


FIG. 24. Pressure distribution under cone penetrating rubber block (43).  $p_a$ , actual pressure.

FIG. 25. Effect of wheel load on apparent pressure under center and outer ribs of passenger car tire tread (replotted from Ref. 45). Inflation pressure 24 psi.

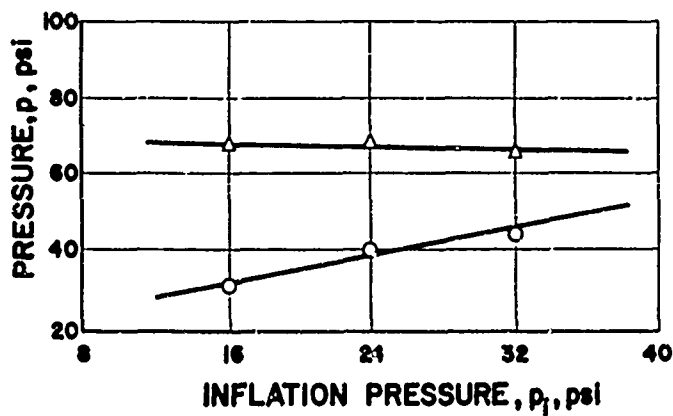
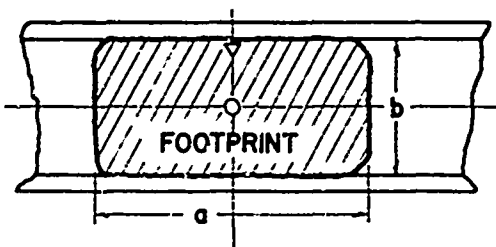
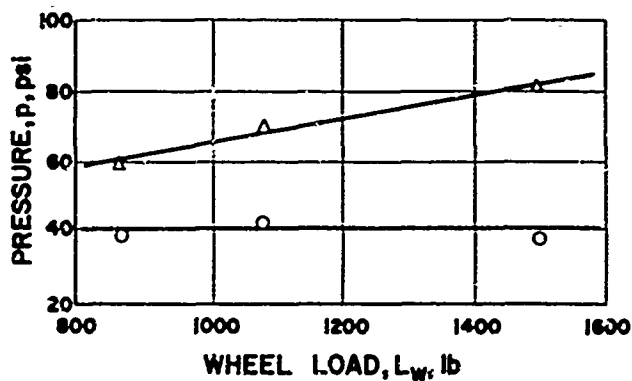


FIG. 26. Effect of inflation pressure on apparent pressure under center and outer ribs of passenger car tire tread (replotted from Ref. 45). Wheel load 1085 lb.

and the coefficient of sliding for a given sliding velocity should be smaller for the more heavily loaded tire with higher inflation pressure, provided the adhesion term predominates. Experiments on dry and smooth surfaces have borne this out.

The normal load on a wheel is generally constant if changes due to suspension dynamics and aerodynamic effects are not considered. What can change significantly is the inflation pressure. The coefficient of road friction will therefore be greater when the tire is cold than after it has run long enough to reach an elevated inflation pressure. But this is due not only to the increase of inflation pressure but also to the direct influence of temperature on adhesion and hysteresis.

Adhesion and hysteresis are affected differently by changes of the contact pressure. Whereas the adhesion term decreases, the hysteresis term increases with increased pressure. Because both terms are present on nearly all road surfaces, changes in either will balance each other to a certain extent. Road tests conducted by several researchers have revealed differences in the coefficient when the inflation pressure was increased while the normal load was held constant, but the differences were always small.

An increase in wheel load at constant inflation pressure and a decrease of inflation pressure at constant wheel load have more serious effects on the cornering characteristics of tires (35), but that is a consideration beyond the scope of the present study.

#### SLIDING VELOCITY

Locked Wheel. The frictional behavior of a tire when the wheel is locked presents a relatively simple situation, since there is very little, if any, relative motion of the tire elements within the contact area. All elements slide with essentially the same velocity. The sliding tire is directly comparable to a rubber block sliding at corresponding velocity, temperature, and contact pressure.

Experiments conducted by the authors show that a standard passenger car tire develops its maximum coefficient of friction not at rest but at some definite though low velocity, just as does a rubber block. The frictional behavior of a locked tire sliding at high velocity cannot readily be duplicated with rubber sliders in the laboratory, because under dry conditions the surfaces of drums, belts, or disks become contaminated by abrasion and melting of the rubber.

Low-speed locked wheel experiments were performed with the Penn State test trailer (see Appendix) towed by a 3/4-ton pickup truck on dry and wet asphaltic concrete and concrete roads, at various wheel loads and inflation pressures. A free-rolling control wheel trailed by the truck drove a potentiometer that gave on the oscillograph record a deflection of 0.2 in. per inch of travel on the road. This provided an accurate means to determine the travel as well as the sliding velocity of the test wheel at low speeds.



Before each experiment the test wheel was locked, and it was kept locked during the entire test. The driver started the tow truck by carefully engaging the clutch, aided by a meter that indicated the force tending to rotate the locked brake assembly. As the clutch engaged, the towing force increased steadily, deforming the tread rubber and carcass elastically. The tire eventually started to slide, and the vehicle was permitted to accelerate slowly to 5 mph. The speed of the test wheel, the towing force, and the wheel load were recorded simultaneously by an oscillograph.

Figure 27 shows the averaged results of several sliding test on dry asphaltic concrete. The coefficient of sliding friction is plotted against the log of the distance traveled by the wheel from the start of motion. The coefficient reaches a maximum after approximately 35 in. of travel, then drops due to audible chatter and eventual temperature effects.

In Fig. 28 the coefficient is plotted against sliding velocity on a concrete surface, which gave very similar results. The curves for two different wheel loads and inflation pressures are nearly identical, again illustrating the relative unimportance of these two factors in this situation.

The results on wet surfaces were qualitatively similar, but the maximum coefficient of sliding on both types of surfaces occurred at lower velocities in the case of asphaltic concrete, at 8 ips as against 14 ips for the dry condition.

In interpreting these results it must be understood that the graphs represent nonsteady-state conditions. The temperature in the contact area is lower than the steady-state temperature at the same velocity. As a consequence, the steady-state curves would plot slightly below those of Figs. 27 and 28, with the peak value of the coefficient occurring at slightly lower velocities. It was reported in the literature (20, for example) that the static coefficient exceeded low-speed friction coefficients. This can be explained only by the fact that the method for measuring velocity would not record small transient values, thus making it appear as though the observed peak occurred with the wheel still at rest.

The locked wheel experiments were not extended to higher velocities, because numerous data are available for the range of 5 to 100 mph. Figure 29 gives the trend of the sliding coefficient as a function of velocity under dry and wet conditions, based on data from various sources (45). An important point is that under both conditions the coefficient decays with speed, although for different reasons.

On dry surfaces the coefficient drops after reaching its maximum value, owing to slip-stick and temperature effects. The drop becomes more pronounced when the melting temperature of the rubber is reached. There are, however, reported instances of an increase of the coefficient with speed under dry conditions (45, 46). This unusual behavior cannot be explained on the basis of rubber characteristics. Since such results

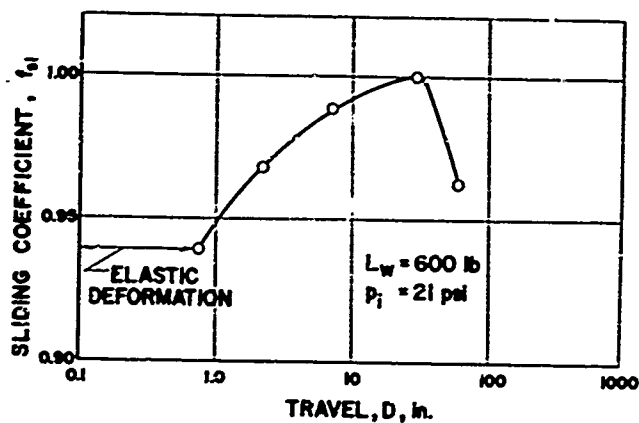


FIG. 27. Sliding coefficient of tire versus travel distance. Dry asphalt surface.

FIG. 28. Sliding coefficient of tire at very low sliding velocities. Dry concrete surface, two combinations of wheel load and inflation pressure.

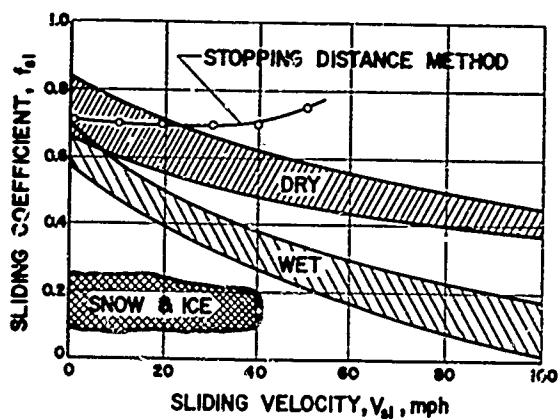
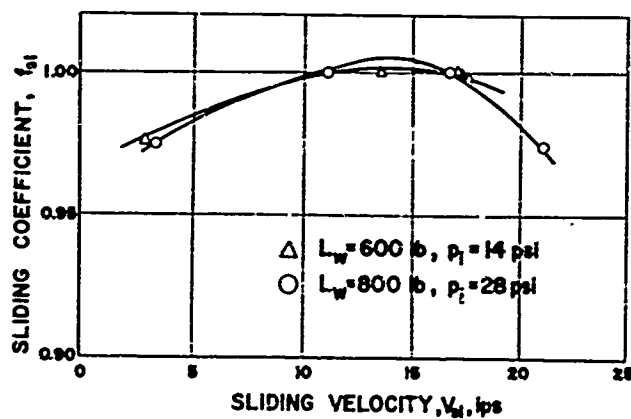
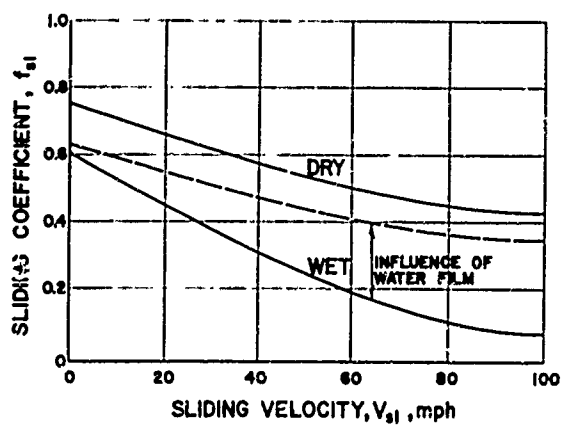


FIG. 29. Trends of sliding coefficient at higher sliding velocities, for dry, wet, and icy conditions (45).

FIG. 30. Typical decay of sliding coefficient as a function of sliding velocity, dry and wet conditions.



were obtained by the stopping-distance method, it is suggested that this method measures a coefficient that has a physical meaning other than the coefficient of road friction.

The coefficient obtained by the stopping-distance method is found by equating the kinetic energy of the vehicle at initial speed with the work done in braking it down to zero speed. The latter is the product of the average decelerating force (including air resistance) and the stopping distance. At relative velocities (vehicle speed plus or minus wind velocity) below about 20 mph, aerodynamic resistance has no significant effect on the stopping distance, but at higher relative velocities its influence increases progressively. Between 20 and 30 mph the decrease of the road friction coefficient due to temperature effects appears to be just about compensated by the increase in aerodynamic drag, whereas above 30 mph the air resistance increases more rapidly than the temperature effects decrease the tire-road friction (see analysis in the Appendix). Hence a correction for air resistance would bring the coefficients obtained by the stopping-distance method into agreement with the trends shown in Fig. 29.

When the road is wet, the coefficient has a lower value because the adhesional shear strength is reduced by the presence of a liquid film. More importantly, the decay of the coefficient with speed is more pronounced. In this case the cause for the decrease is not so much the temperature but the increasing hydrodynamic lift imparted to the tire by the water film.

Figure 30 indicates the typical decay of the coefficient of sliding under dry and wet conditions. Comparing the drop of both curves, the more rapid decay of the "wet" curve might at first appear to be due to the water film, and it may seem that this curve would run parallel to the upper one if allowance were made for hydrodynamic effects. But because of the lower coefficient and better cooling, the footprint temperature is lower and increases much less with speed than it does under dry conditions. Consequently, temperature effects contribute much less to the decay of the sliding coefficient than in the dry case (dotted line), and hydrodynamic effects are responsible for the drop from the dotted curve to the lower curve in Fig. 30. Actually, the situation is much more complex, and it will be the task of a later section to examine the influence of water more fully.

Rolling Tire. The running band of a pneumatic tire represents a section of a toroid (38, page 23), provided the vertical deflection of the tire remains small. When a thin elastic shell of spherical or toroidal contour is forced into contact with a plane, it buckles inward, as a simple experiment with a hollow rubber ball will demonstrate. Whether or not the center section of a tire will buckle inward depends on carcass design, wheel load, and inflation pressure. Buckling has been measured in an underinflated standard tire (47), but with normal inflation pressures the center section is pressed down. The stress in the carcass must then be relieved in some other manner, and the tread elements are forced to spread away from the center.

When the tire rolls, the elements entering the contact area have a tendency to spread outward and to return to their original position upon leaving it. This implies that in pure rolling the tread elements must creep, the rate and direction of creep being dictated by compression stresses within the carcass, shear stresses within the tread elements, the local contact pressure, and the prevailing local coefficients of friction. The creep rates seem to remain below 1 ips. The directions at low rolling velocities are known from rolling tests on a glass plate (48).

The important fact that can be deduced from the foregoing is that the tread elements in the contact area are not stationary but are in continuous motion, with changing rates and directions. For this reason, the footprint would be no place to look for a static coefficient even if rubber did have a true static coefficient. This is even more true when the tire transmits driving, cornering, or braking forces.

The creep pattern of a straight tire rolling at low velocities seems to be quasi-symmetric with respect to the plane through the center of the footprint and the axis of rotation of the tire. The resultant force developed in the plane of the footprint is therefore small, although adhesion and hysteresis forces perpendicular to that plane are present. The adhesion term is trivial for rolling motion, as has been shown by Tabor and Eldredge (49), since it is easily overcome by the peeling action in the outgoing section of the footprint. Hysteresis losses occur in any rubber element subject to deformation. The tread elements laid down at the incoming section of the footprint are compressed vertically, and in the exit zone they expand. Because the compression energy is higher than the expansion energy, an upward force is produced in the forward section of the footprint. This force, together with that due to carcass hysteresis, builds up a torque with respect to the wheel axis which is responsible for the rolling resistance. The hysteresis in the tread and in the tire structure is also responsible for the temperature buildup that occurs as the tire rolls.

Tire under Slip. Whether a wheel is quasi-rigid like a railroad wheel or rimmed with a flexible pneumatic tire, it runs under slip as it transmits driving, braking, or cornering forces to the ground. Slip is defined as the ratio of the effective slip velocity in a specific direction to the forward ground speed of the vehicle. The direction is forward or aft in driving and braking, and sideways in cornering. In braking,

$$S = (V_v - V_t)/V_v \quad \text{or} \quad S = V_s/V_v \quad (24)$$

where  $V_v$  is the vehicle speed,  $V_t$  the forward velocity of the tire, and  $V_s$  the difference of the two, or slip velocity. The fact that a wheel cannot transmit forces to the ground without slippage is puzzling and cannot be reconciled with the assumption of a static coefficient in the contact area. That conditions in the contact area are not static has already been discussed. In the case of rolling, the superposition of a driving or braking torque or cornering force creates still higher creep rates, orientated mainly in the direction of force transmission. The creep eventually leads to sliding and loss of brake and steering control.

An interrelated and complex picture is formed by the actual distribution of strain and the consequent stresses, the exact magnitude and direction of creep and sliding, the contact pressure distribution, and the resulting local coefficient. Except for the case of cornering, the interrelation of these quantities has not been determined either by experiment or by analytical models.

The complexity of the situation explains why the friction properties of a slipping tire are only related to and not identical with the behavior of a simple rubber slider. The simulation of a slipping tire by rubber sliders in the laboratory would require an elaborate setup. The friction could be duplicated only by dragging a fair number of interconnected rubber elements over a distance that resembles the contact length, at the same time varying the normal load and creep velocity of each element to match the pressure and creep distributions of the slipping tire. The pendulum tester is perhaps the only existing laboratory equipment that even approximately simulates the mechanism of a slipping tire, since the rubber block attached to the pendulum goes through a normal load and velocity cycle similar to that of the tire element. From this standpoint, the pendulum method deserves more attention.

The operating modes of driving, braking, or cornering can be looked upon as special cases of the same phenomenon, that is, transient friction relative to a rotating flexible rubber body. McConnel (20) showed that the relation of the coefficients of traction and braking to slip is a continuous curve, symmetrical about the point of zero slip. It is sufficient, then, to limit the following discussion to two cases, braking and cornering.

Figure 31 shows typical curves of the coefficient of friction as a function of wheel slip during braking, as verified by numerous experiments. The shape of the curves is qualitatively valid for all types of tires, for most surface conditions, and for the range of vehicle speeds so far investigated.

As the figure indicates, the braking coefficient rises from zero approximately linearly with slip, to a maximum termed the critical coefficient. The coefficient developed at a given slip within the range from zero to critical depends only on tire stiffness and is not influenced by the limiting friction of rubber and surface. The magnitude of the critical coefficient depends, of course, on the latter. Under most surface conditions the curve decreases to a value smaller than the critical at 100% slip, owing to slip-stick and temperature effects. At 100% slip, the coefficient of sliding takes over. The critical value for railway wheels under average conditions has been found to occur at 0.28% slip (50), whereas the pneumatic tire develops its critical coefficient within the range of 8% to 20% slip (48, 59).

Published slip curves are usually extended beyond the critical slip, often to 100%. This extension is of dubious value because a coefficient beyond the critical value cannot be measured with ordinary vehicles or friction testers. When the critical slip is exceeded, the equilibrium between brake and road torque is disturbed and the wheel immediately

slows down and locks. Friction beyond the critical slip can be measured only with special devices permitting forced rotation, such as the NACA friction cart (51) or the machine of the Swedish Road Research Laboratory (52).

Some Misconceptions Concerning Slip. Three points require detailed discussion because they have evoked considerable misunderstanding: (a) the question of whether the slip velocity of a tire running under slip, as suggested by Eq. 24, is real; (b) the question of whether the critical coefficient occurs at the same slip regardless of vehicle speed or at a constant slip velocity; and (c) the question of why the critical coefficient is significantly smaller at all vehicle speeds than the coefficient of a locked tire sliding at a low velocity.

(a) Is the sliding velocity suggested by slip real? When a dynamometer trailer is towed at 50 mph and the wheels are braked to operate at 10% slip, Eq. 24 suggests a slip velocity of 5 mph between tire and road. This suggested velocity is by no means representative for the local velocities in the contact area. To understand this better, one has to remember how slip is actually measured.

Values for slip-torque or slip-coefficient curves are obtained by running tires at progressively higher driving or braking torques and measuring the wheel revolutions  $u$  for a given distance or the angular velocity  $\omega$ . Such test series are run at constant vehicle speeds to eliminate centrifugal force effects on the effective rolling radius. The values for  $u$  and  $\omega$  as functions of torque are compared with those of zero torque  $u_0$  and  $\omega_0$ , and slip values are obtained by

$$S = (u_0 - u)/u_0 \quad \text{or} \quad S = (\omega_0 - \omega)/\omega_0 \quad (24a)$$

In the case of free rolling, the angular velocity  $\omega_0$  is directly related to vehicle speed  $V_v$  by

$$V_v = \omega_0 r_{e0} \quad (25)$$

where  $r_{e0}$  is the effective rolling radius for zero torque. The tire operating under brake slip superimposes upon the angular velocity a small sliding component  $V_{sl}$ , so that

$$V_v = \omega r_e + V_{sl} \quad (26)$$

Solving these equations for  $\omega_0$  and  $\omega$  respectively, insertion into Eq. 24a yields

$$S = 1 - (r_{e0}/r_e)(1 - V_{sl}/V_v) \quad (27)$$

This equation shows that slip as defined by Eq. 24 or 24a is not only a function of the ratio  $V_{sl}/V_v$  but is also dependent upon the ratio of

the effective radii. (It should be mentioned that the latter has no direct relation to the geometric radius  $r$  of the tire.)

Hadekel (38) points out that the effective radius of a tire operating under slip depends on the tangential strain in the contact area, and he arrives at the relation

$$r = r_{e0}(1 - \epsilon) \quad (28)$$

where  $\epsilon$  is the strain in the contact area along a given meridian. Substituting this in Eq. 27,

$$S = 1 - [1/(1 - \epsilon)](1 - v_{sl}/v_v) \quad (29)$$

is obtained. This expression has general validity. In the special case of a rigid wheel,  $\epsilon$  must be zero ( $r_{e0} = r_e$ ) and Eq. 29 would reduce to

$$S = v_{sl}/v_v$$

indicating that a slip-suggested sliding velocity is real. But wheels are never rigid, and even the small slip of a railway wheel (see page 49) is partly due to elastic deformation. Since the effective modulus of elasticity of a wheel rimmed by a pneumatic tire is very much lower than that of a steel wheel, the mentioned effect for a given stress is much more pronounced.

That slip is due to sliding as well as the elastic properties of the wheel can perhaps be demonstrated more clearly in another way. Figure 33 represents a simplified model of the pneumatic tire shown in Fig. 32, with "n" rubber elements equally spaced at the circumference. The elements are elastically deformable and are held in place by radially arranged spring-loaded plungers that simulate the retention of the elements by the rim. It is assumed that the ratio of radius  $r$  and contact length  $a$  is large, so that throughout the contact length the normal load on the rubber elements is quasi-vertical with respect to the road surface. It is also assumed that movement of the plungers does not change the spring force significantly, that is, the apparent pressure of the elements on the road is constant.

With these assumptions, a uniform normal load distribution is obtained. The axis of the wheel proceeds with  $V_v$ , the angular velocity is  $\omega$ . For the time being, let it be assumed that the elements do not slide on the surface but behave as if they were pinned down at the entry and released at the exit. In braking, the tread elements in contact with the surface must deform to transmit shear forces. Let  $\delta$  be the deformation of the center of the contact zone of the second element with reference to the undeformed position. In the position shown, element 1 enters the contact area undeformed, elements 2 and 3 are deformed by  $\delta$  and  $2\delta$  respectively, and element 4 is leaving the ground and has snapped back into its undeformed position.

The rim lags behind the center of element 2 by  $\delta$ . Since the rim is delayed by this amount for each entering element, the lag per wheel revolution becomes  $n\delta$ . The resulting lag velocity  $V_e$  is

$$V_e = 30n\delta\omega/\pi \quad (30)$$

and the corresponding slip  $S_e$  is

$$S_e = 30n\delta\omega/\pi V_v \quad (31)$$

This slip is due entirely to elastic deformation, since it was assumed that the rubber elements do not slide. It will be referred to as deformation slip.

The result would be the same if, in addition to the rubber elements, the plungers (equivalent to the carcass) and the guidance (equivalent to the rim) were permitted to deform. The deformation slip for a given brake torque would simply be larger. Equation 31 suggests that inflation pressure, depth of tread, and stiffness of carcass must have an influence on the deformation slip, because those factors have a bearing on  $\delta$ . Tread depth and carcass stiffness are, of course, subject to change during the lifetime of the tire.

So far this model has ignored the sliding that in reality occurs between the tread elements and the road surface. Assuming Bartenev's theory (21, see also 53) to hold, the tread elements can be deformed only when creep or sliding takes place between rubber and surface. As a consequence the slip for a given brake torque is further increased by the slip component due to  $V_{sl}$ . The total slip then becomes

$$S = S_{sl} + S_e = (V_{sl} + 30n\delta\omega/\pi)/V_v \quad (32)$$

That fraction of slip due to actual sliding deserves closer inspection. The sliding velocity suggested by  $S_{sl}$  is the average, not the local velocity in the contact area. In the latter, relative motion of the single rubber elements can take place as stated before. Stroboscopic observation of a tire running under brake slip indicates that the sliding velocity is small at the entry, builds up towards the center, and reaches a maximum close to the exit. The sliding velocity  $V_{sl}$  in Eq. 32 is related to the local velocity  $v$  by

$$V_{sl} = 1/a \int_0^a v \, da \quad (33)$$

The velocity distribution as described in text and shown in Fig. 32 holds for the driven or cornering wheel as well. The latter case was extensively investigated by Gough (54).

To the authors' knowledge, no attempt has ever been made to isolate deformation slip. Hence no numbers exist for its contribution to the total slip. Until knowledge of the various phenomena involved has been



FIG. 31. Coefficient of braked wheel as a function of wheel slip for two vehicle speeds, dry and wet conditions.

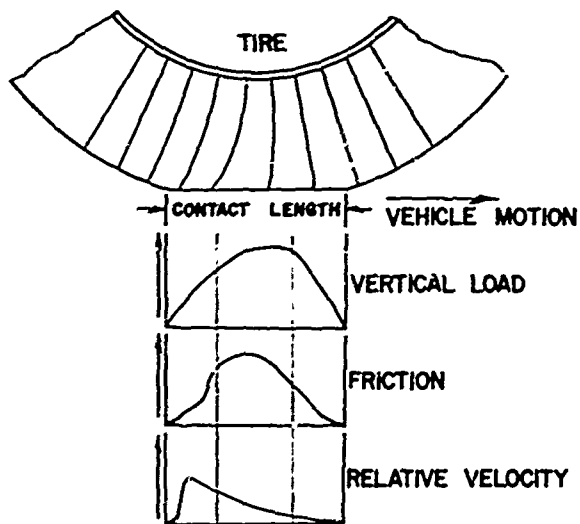
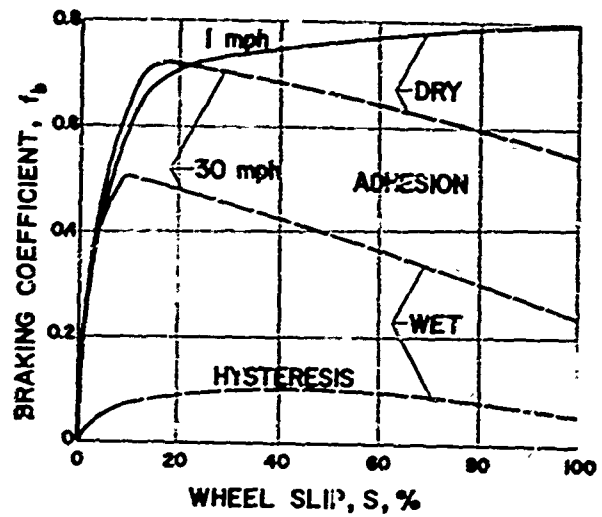
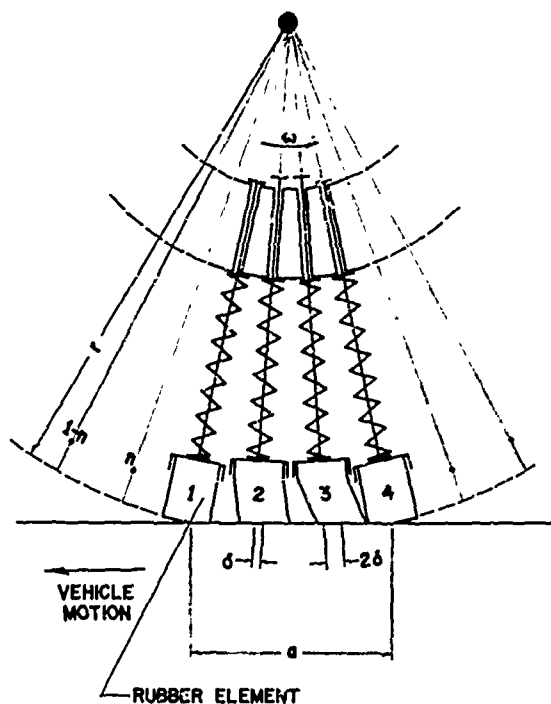


FIG. 32. Deformation, pressure distribution, tangential shear, and local velocity of tire running under brake slip as a function of contact length.

FIG. 33. Simplified model of pneumatic tire running under brake slip.  $\delta$ , deformation (see text).



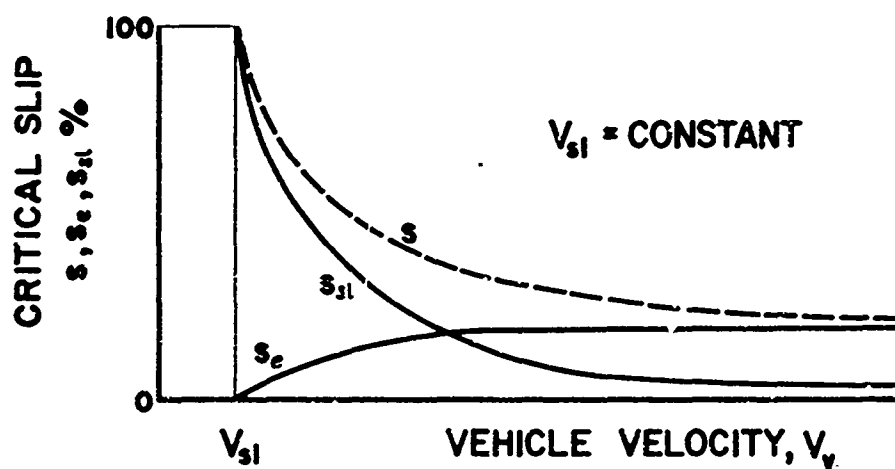


FIG. 34. Critical slip  $S$  and slip components  $S_e$  and  $S_{sl}$  as a function of vehicle speed, assuming  $V_{sl}$  crit constant.

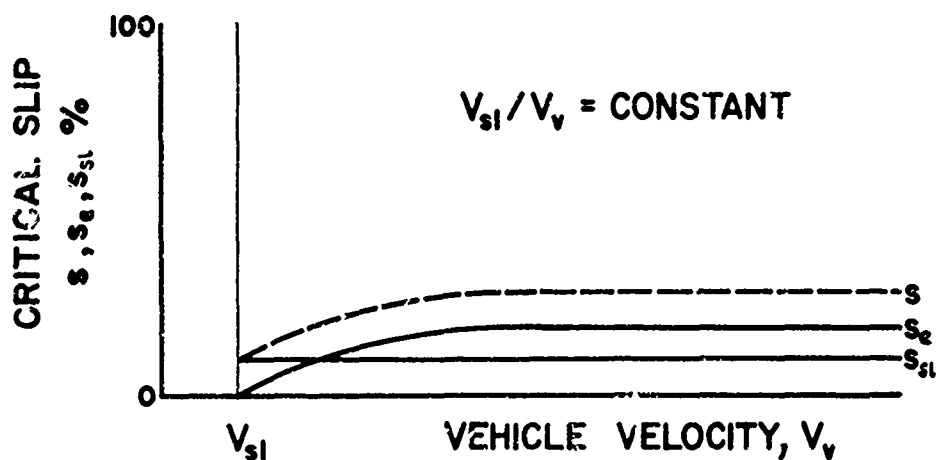


FIG. 35. Critical slip  $S$  and slip components as a function of vehicle speed, assuming  $V_{sl}$  crit/ $V_v$  constant.

deepened, only qualitative analyses are possible. With this restriction in mind we may now attempt to answer the second question.

(b) Does the critical coefficient occur at constant slip or at constant sliding velocity throughout the range of vehicle speeds? As pointed out in Part I, the rise of the coefficient of sliding friction with velocity is characteristic for rubberlike materials under all surface conditions where the adhesion term develops. For example, if the maximum steady-state coefficient of friction for a locked tire is obtained at a sliding velocity of 6 ips, one might expect that the critical coefficient of a slipping tire would occur at a slip velocity of 6 ips, regardless of vehicle speed. If this were so, the corresponding slip component ( $S_{sl} = V_{sl}/V_v$ ) would have to decrease hyperbolically with vehicle speed, according to Eq. 32. But the findings of other workers and road tests with the Penn State test trailer indicate that the critical coefficient is usually obtained at approximately constant slip, though its magnitude decreases with increasing vehicle speed under dry conditions and even more under wet conditions.

Slip was shown to be composed of a sliding component and a deformation component. A velocity balance requires that

$$V_v = r_e \omega + V_{sl} + V_e \quad (34)$$

Replacing  $V_e$  by Eq. 30 and solving for  $\omega$  gives

$$\omega = (V_v - V_{sl}) / (r_e + 30n\delta/\pi) \quad (35)$$

By combining the latter expression with Eq. 32, slip can be expressed in terms of vehicle speed and sliding velocity, the elastic properties of the wheel, and the corresponding effective rolling radius:

$$S = S_{sl} + S_e = V_{sl}/V_v + [30n\delta/(\pi r_e + 30n\delta)] [(V_v - V_{sl})/V_v] \quad (36)$$

Let it first be assumed that  $V_{sl}$  is independent of  $V_v$  and is identical with the sliding velocity at which a locked tire develops its maximum coefficient. Since we are concerned here with the critical slip,  $\delta$  and  $r_e$  are constants because their maximum value is governed by the critical coefficient.

The two slip components  $S_{sl}$  and  $S_e$  are plotted against  $V_v$  in Fig. 34. Whereas  $S_{sl}$  drops from 100% at  $V_v = V_{sl}$  and approaches the abscissa asymptotically,  $S_e$  starts at zero and becomes asymptotic to the line:

$$\lim_{V_v \rightarrow \infty} S_{e \text{ crit}} = 30n\delta/(\pi r_e + 30n\delta) \quad (37)$$

The dotted line shows the resultant slip.

Gough (53) points out that application of Bartenev's theory to a slipping tire suggests that the sliding velocity at which the critical

coefficient occurs is a function of vehicle speed, so that the ratio  $V_{sl}/V_v$  remains constant. The curves for the slip components  $S_{sl}$  and  $S_e$  for this case are plotted in Fig. 35.

Comparison of the two graphs shows that the curves for the resulting slip are similar at higher vehicle speeds. In both cases the critical slip is practically independent of  $V_v$ , although its magnitude may be slightly larger (depending on  $\delta$ ) where the ratio  $V_{sl}/V_v$  remains constant.

At low vehicle speeds, however, the curves are dissimilar. As stated at the outset, experiments have shown the constancy of critical slip in the range of vehicle speeds so far investigated, with two exceptions. One of these occurs when the vehicle speed is of the magnitude of the sliding velocity at which a locked tire develops its maximum coefficient; hence the critical coefficient clearly cannot be reached at low slip values. As Eq. 36 indicates, the slip component due to sliding is unity or slightly smaller than unity, and the deformation slip is zero or almost zero. Figure 31 shows that the curve for the coefficient versus slip at a vehicle speed of about 1 mph continues to rise until 100% slip has been reached. (The curve was obtained on a dry asphaltic concrete surface that produced the maximum locked wheel coefficient at 14 ips or 0.8 mph.) From the standpoint of wheel-lock control systems, this curve is stable.

Test results obtained with the Penn State trailer indicate that under given conditions and otherwise comparable circumstances the critical slip changes from 14% on a dry surface to 9% on a wet surface ( $f = 0.72$  and  $0.5$  respectively), as shown in Fig. 31. The two friction curves coincide at low slip values, proving again that in this range the coefficient of friction is independent of the friction properties of tire or road.

That the critical coefficient is obtained at a lower slip under wet conditions has already been reported by French and Gough (48). The locked wheel tests described earlier showed that the maximum coefficient occurs also at a lower sliding velocity (8 ips when wet and 14 ips when dry, other conditions identical). There is no explanation as yet why the velocity for the maximum coefficient of a sliding tire should drop owing to the presence of water. For a slipping tire, one factor is suggested by Eq. 36: the water film causes the adhesion term to decrease. Since  $\delta$  depends on the local friction,  $\delta$  wet is smaller than  $\delta$  dry, reducing the deformation slip.

The 30 mph curves are unstable. At this speed a slight disbalance of brake and road torque makes the wheel slow down and lock. The shape of these curves beyond the critical coefficient can only be obtained with equipment allowing forced rotation. Reasoning indicates that at low and medium vehicle speeds and on dry and comparatively smooth surfaces, a significant drop in  $f$  must occur immediately following  $f_{crit}$  because of the onset of slip-stick. Under these conditions, temperature effects can be expected to play a minor part. At higher vehicle speeds and on coarse surfaces where slip-stick is less pronounced, temperature becomes the overriding factor and the drop immediately beyond the critical

coefficient should be more gentle. Between these extremes different combinations appear possible, suggesting numerous types of curves connecting the critical with the sliding coefficient.

The second exception occurs on the rare occasions when hysteresis predominates over the adhesion term. If conditions are such that the adhesion term can be neglected while hysteresis is still effective, the curve for friction versus slip will no longer have the typical shape with a maximum at a critical slip; it will be similar to the bottom curve in Fig. 31. Such a curve would not readily lead to wheel lock. That this is so was accidentally noted in a heavy rain on a moderate grade swamped with water. Under these conditions the wheel of the test trailer could be run with more than 60% slip without locking.

A thorough and systematic investigation to obtain quantitative data on the effects of the many variables influencing tire behavior in the whole range of slip is obviously warranted. It will require extensive laboratory experiments, since the many variables cannot be controlled accurately enough on the road.

(c) Why is the critical coefficient at normal vehicle speeds lower than the maximum coefficient for a locked tire at small sliding velocities? Workers have tried in vain to reach the value of the maximum coefficient of sliding with a slipping tire (20). There seem to be two principal reasons why the critical coefficient is lower in driving, braking, or cornering.

In discussing the frictional behavior of a locked wheel it was pointed out that all elements remain in contact with the road surface and slide at essentially the same velocity. The contact time  $t_c$ , as defined by Eq. 38, is therefore infinite:

$$t_c = a/(V_v \pm V_{sl}) \quad (38)$$

The positive sign indicates driving; the negative sign, braking. (Contact time as the term is used here does not refer to the molecular interaction of rubber and surface. The time available for the rubber molecules to interact with molecules of the surface is finite, even for a locked wheel; in fact, it is usually shorter for a locked wheel than for a slipping tire.)

The mechanism is very much different for a slipping tire, since the local sliding velocity changes from entry to exit and the contact time is finite; that is, each rubber element remains in contact with the ground a limited time only.

The velocity dependence of the coefficient, discussed in Part I, is shown in Figs. 5 and 6 and for different surfaces in Fig. 8. This dependence, although most pronounced for smooth surfaces favoring the adhesion term, is still observable on coarser surfaces (Fig. 8).

Let it be assumed that the vertical pressure distribution across the contact area is uniform. Then, whereas each element of a locked tire slides at the same velocity and therefore produces the same

coefficient, the elements of a slipping tire slide at velocities that differ from entry to exit, producing different coefficients locally. For instance, at critical slip the low creep velocity in the entrance zone stays below the velocity required to reach the maximum coefficient. This velocity is reached in the center, whereas the exit zone is already operating under slip-stick. It is evident that neither the entry nor the exit zone carries the same friction load per unit area as the center does. This is even more pronounced when the vertical pressure distribution deviates from its assumed constancy across the contact area.

The foregoing explains at least qualitatively why the critical coefficient in slip is lower than the maximum coefficient in sliding. There is, however, another aspect to be considered. So far, it has been assumed that the local coefficient is only velocity-dependent, that is, it increases without delay in accordance with curves of Fig. 8 when the velocity is increased. But Fig. 9 shows that a rubber element subject to a velocity step input enters a distance-dependent transient before the steady-state coefficient corresponding to the prevailing velocity is reached.

Since the velocity of any rubber element in the contact area changes continuously from entry to exit, it does not quite reach the steady-state coefficient suggested by Fig. 8 for a given surface, but lags behind. The nonsteady-state behavior of a slipping tire seems to be responsible for another reduction in the overall coefficient. It is true that the transient aspect of rubber friction loses significance when the adhesive term is weakened by increasing surface roughness, sliding velocity, or a water film. As a consequence the activation process (see page 18) has less significance for a slipping tire operating on a wet and coarse road surface.

To summarize, the contact area can be divided into a transient zone at the entry, and active zone in the center, and a disturbance zone at the exit (Fig. 32). The identification of these zones is of course arbitrary, because the locally developed friction changes continuously with the contact length rather than in a stepwise fashion. But this idealization helps to visualize how the first zone is narrowed and the other two move gradually forward as the slip increases. The picture is also valid for the driving and cornering tire. In all three cases the critical coefficient is reached when the center zone of the tire, which carries the heaviest normal load, is operating at the verge of slip-stick velocity.

A third effect may contribute to the discrepancy between the critical and the maximum coefficient. The direction of the friction force of a sliding element is always opposed to the direction of the sliding velocity. A rubber element dragged over the track in the laboratory has only one velocity and therefore one friction vector. This is also the case for a locked tire sliding on a road surface. For the elements in the contact area of a slipping tire, however, both the velocity and the direction of sliding change from entry to exit, since the tire is a toroidal body that can adapt to the road surface only by spreading and contracting its elements in a transverse direction.

Figure 36 shows two element in the contact area of a tire operating under brake slip. In the position shown, the elements proceed with a longitudinal velocity  $v_x$  and a transverse component  $v_y$ . Let the coefficient for a given set of conditions be related to the sliding velocity by a function  $g$ , so that

$$f = g(v) \quad (39)$$

The maximum coefficient of a single element is reached for a specific sliding velocity, so that

$$f_{crit} = g(v_{crit}) \quad (39a)$$

In the case of the slipping tire the critical velocity is the resultant of the velocity components in x and y directions.

$$v_{crit} = (v_x^2 + v_y^2)^{1/2} \quad (40)$$

As can be seen from Eq. 39a and 40, the corresponding coefficient in x direction is reduced:

$$f_{x\ crit} = g(v_{crit}^2 - v_y^2)^{1/2} < f_{crit} \quad (41)$$

The sum of the y components of friction on a straight rolling tire is of course zero, since the transverse motions of the elements are symmetrical with respect to the long axis of the contact area and their effects cancel one another.

The effect of the presence of a y component on the friction in x direction must be small compared to the effect of the nonuniform velocity distribution and the velocity changes in the contact area, because  $v_y$  as function of x,y is not always present. For example, the component must be zero for  $y = b/2$  and  $0 \leq x \leq a$  and for  $x = a/2$  and  $0 \leq y \leq b$ . The transverse friction component can decrease the component in x direction only near the exit zone of a tire running under critical slip, since the critical sliding velocity is not reached in the entrance zone (see Fig. 36) and the  $v_y$  component in the center zone is almost zero.

Cornering. On the subject of cornering, much information is available in the literature. It is taken up here only to show the similarities in cornering and braking characteristics of a tire. The buildup of the cornering force in relation to rolling distance, the pattern of motion, and lateral stress distribution was extensively investigated by Gough and coworkers (48, 54).

The increase of side force with slip angle for dry and wet conditions is shown in Fig. 37. As in the case of fore and aft slip, both curves coincide at small slip angles, indicating that in this range the side force is again independent of the limiting friction properties of the tire-surface combination. It is dependent on only the deformation pattern within the contact area, which is a function of the overall lateral stiffness of the carcass and tread rubber. Figure 38 is the top view

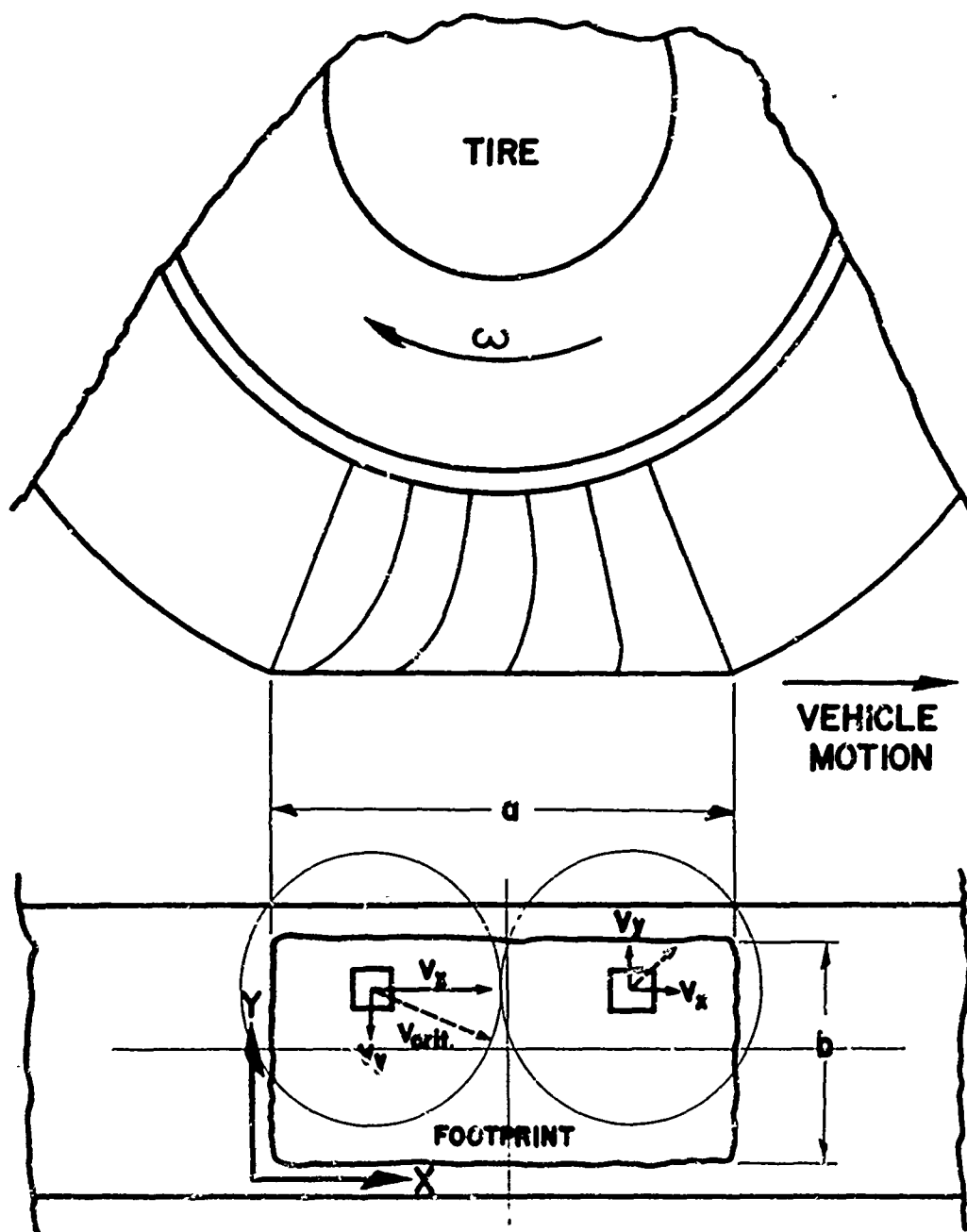


FIG. 36. Velocity vectors of two rubber elements in contact area of tire running under brake slip, viewed from above.



of a tire, showing the deformation of its contact area due to running at a slip angle and the orientation of cornering, drag, and side force and self-aligning torque.

In Fig. 39 the lateral stress distribution is plotted against the length of the contact area for three different slip angles. The characteristic curve in Fig. 40 shows the side force versus self-aligning torque for these three cases. The torque is due to unsymmetric lateral stress distribution at small and medium slip angles with respect to the wheel axis, as indicated in Figs. 32 and 39. Figure 39 demonstrates that the resulting lateral force  $F_s$  acts behind the center of the tire to produce the self-aligning torque (SAT), which tends to decrease the slip angle of the wheel and align it in the direction of motion.

$$\text{SAT} = F_s e \quad (42)$$

where  $e$  is the effective lever arm, sometimes referred to as pneumatic trail. When this torque is not obscured by friction in the steering mechanism or by power-assisting devices, it can give the driver a very useful clue to the magnitude of lateral friction.

Interesting here is the similarity of stress distribution in the contact area of braked and cornering tires, and the fact that the ratio of apparent lateral creep or slip velocity to forward velocity determines the magnitude of the side force as long as the slip angle does not exceed the critical value. For the cornering tire the contact area can again be divided into an activation zone at the entry of the running band, a zone of maximum friction slightly behind the center (when the slip angles are small), and a disturbance zone in which the slip-stick velocity will be reached first. As the slip angle is increased, the disturbance zone moves gradually forward until the whole contact area is involved in bodily sliding. At this instant the vehicle is thrown into a side skid.

The simplified model of a tire running under brake slip, Fig. 33, was used to show that the tire can slip without requiring a movement of the rubber elements in the contact area, and that the overall slip (that is, the measured slip) is only partly due to actual sliding of the rubber elements. By analogy to that case, the lateral slip velocity  $V_s$  suggested by the slip angle  $\alpha$  (Fig. 38)

$$V_s = V_v \sin \alpha \quad (43)$$

represents not only the sliding velocity of the rubber elements in the lateral direction but also the deformation velocity in this direction.

As for the tire running under brake slip, the critical coefficient sideways is virtually unaffected by the vehicle velocity over a wide range of velocities if temperature effects are neglected. When the critical slip angle is exceeded and bodily sliding occurs, the resulting friction is increasingly velocity-dependent. At a slip angle of 90 degrees the coefficient of sliding governs entirely, as in the case of 100% slip.

Superpositions of driving or braking and cornering follow the same trends, but the resulting friction determines the magnitude of both slip angle and side force. As long as the friction does not exceed the critical values obtained under braking, driving, or cornering, brake or driving force and side force can exist together. When a higher frictional demand is placed on one of the components, however, the other breaks down and bodily sliding of the vehicle occurs in a direction tangent to the path of the vehicle at the instant of break-away.

#### TEMPERATURE

The effect of temperature on the friction of a sliding rubber block was discussed in Part I. Since the critical coefficient for a pneumatic tire is proportional to the maximum coefficient measured for the rubber block in the laboratory, a similar dependence upon temperature can be expected.

The temperature dependence of the coefficient of road friction was observed by Moyer (4) in 1934, but at that time no satisfactory explanation was at hand. Now that the relative importance of the hysteresis term is recognized, several workers believe the drop of the coefficient of road friction to be due entirely to the decrease of the hysteresis term with temperature. The reduction of  $\gamma = (H_0 - H)/H_0$  with rising temperature was observed in the laboratory, and is shown in Fig. 20 in terms of the increasing height of the first rebound.

The relative magnitude of the adhesion and hysteresis terms was compared in Fig. 18. Since the hysteresis term is only a fraction of the adhesion term under dry conditions and usually also remains smaller under wet conditions, it still appears unsatisfactory to explain the pronounced temperature dependence of the coefficient of road friction by the hysteresis term alone. It must again be stressed that the adhesion term is also a function of temperature and may decrease significantly when the temperature is raised (compare Figs. 15 and 16).

The temperature rise and the decrease in contact time resulting from an increase in vehicle speed appear to be the two principal reasons for the measured decay of the critical and sliding coefficients under dry conditions. The increase of the average apparent pressure in the contact area owing to a rise of inflation pressure and inertia forces is another contributor, but it seems to be of second order.

Three factors influence the temperature of the running band: (1) the ambient temperature, (2) the pavement temperature, and (3) the heat generated by the tire. The ambient temperature is the initial level from which the tire starts to build up its temperature and inflation pressure, and as the tire becomes warmer the ambient temperature controls the heat that will be dissipated by convection and radiation. The pavement temperature of a blacktop or bleeding asphalt surface, which can exceed 140° F on a sunny day (1), largely determines the operational temperature of the tire.

The heat generated in a rolling tire by hysteresis losses in tread rubber and carcass raises the temperature of the running band above that

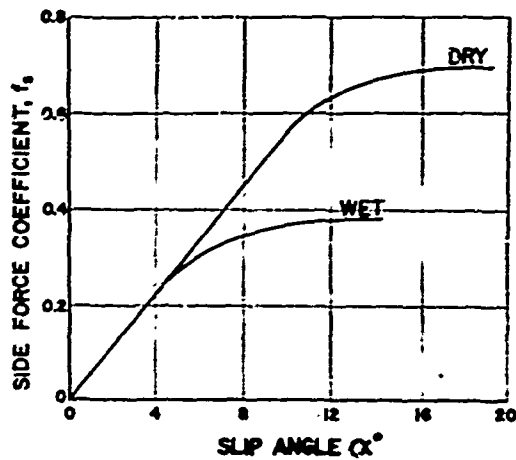


FIG. 37. Side force coefficient of pneumatic tire running at a slip angle, dry and wet conditions.

FIG. 38. Deformation of contact area of tire running at a slip angle, and orientation of cornering, drag, and side force and self-aligning torque.

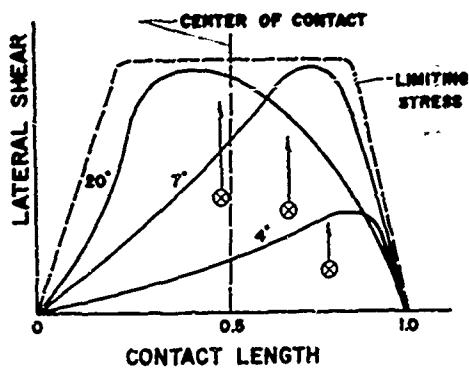
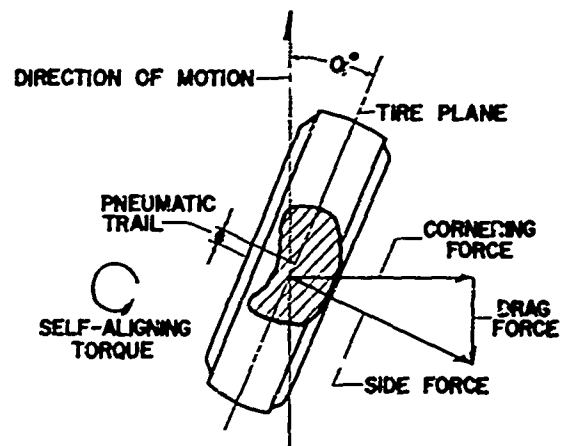
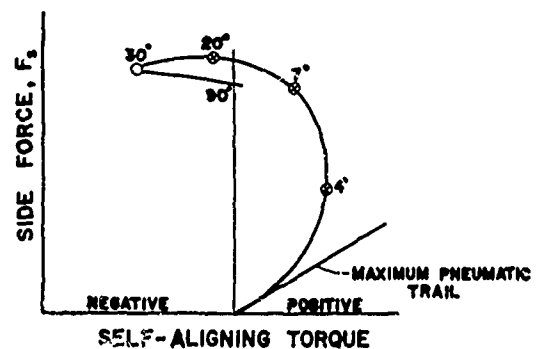


FIG. 39. Distribution of lateral shear stresses over contact length for three slip angles (based on Ref. 48).

FIG. 40. Side force as a function of self-aligning torque, replotted from Fig. 39.



of the pavement. On a new asphaltic concrete surface with an average temperature of 78° F, ambient 69° F, the outer rib of a styrene-butadiene rubber (SBR) passenger car tire showed temperatures 27° and 45° F above the pavement temperature at 30 mph and 45 mph respectively (wheel load 1000 lb, inflation 25 psi).

The temperature of a tire running under partial slip or yaw rises still more because the heat input is greater, owing partly to additional hysteresis resulting from the more severe deformation in the contact area, and partly to external frictional heating.

The most extreme temperature conditions are produced by the sliding tire. In this case the frictional heating in the contact area overrides the combined influence of ambient and pavement temperatures. Under dry conditions, contact area temperatures of more than 400° F (1) and close to 1000° F (55) have been recorded. It is obvious that under such conditions the tread rubber will reach its decomposition temperature and melt, causing the familiar skid marks.

Under wet conditions the cooling and lubricating properties of the water film generally keep the temperature below the decomposition level. In some instances, however, skid marks of the outer ribs can be detected on wet roads (56), owing to the unequal distribution of apparent pressure. When contamination or a thin liquid film eliminates the adhesion term, the tire is still subject to severe hysteresis heating if the speed is high. It has been reported that a locked airplane wheel sliding at high speed on wet grass showed local blistering below the surface of the contact area and damage due to separation of tread and carcass (57).

The effect of temperature on the obtainable coefficient explains why synthetic rubber compositions, beside having better hysteresis properties, are superior to natural rubber at high sliding velocities. Most of the synthetic rubbers have higher decomposition temperatures. Government rubber styrene (GRS), now called styrene-butadiene rubber (SBR), decomposes at approximately 670° F, which is about 100° F higher than natural rubber and 70° F higher than Butyl (58). The difference in the decomposition temperatures of natural and synthetic rubber tires is directly observable in their skid marks, which are decidedly heavier for natural rubber tires, all other conditions being equal.

Experiments with rubber blocks in the laboratory verify the sensitivity of the coefficient of friction with respect to temperature. Similarly, in a pneumatic tire the coefficient of road friction shows a pronounced decrease as the temperature increases.

Road tests with the Penn State test trailer support the belief that changes in tire and surface temperatures can be responsible for the wide variation in reported results said to have been obtained with the same friction machine on a given surface under closely controlled conditions. Keeping the inflation pressure and the wheel load within exact limits was found to be less important than recording the ambient temperature and the temperature of the road surface and running the tire, under test conditions, prior to a test until the inflation pressure had stabilized, indicating a steady-state temperature for the tire.

Results from road tests made on different dates were in better agreement on overcast than on sunny days, a further indication of the influence of temperature on friction. Since the temperature picture changes with such variables as the time of day, weather conditions, the color of the road surface, and operating conditions, the elimination of temperature-related errors in road friction measurements may not always be possible, but consistency and reproducibility of data can be improved by more attention to the prevailing temperatures and their effects.

#### CONTAMINATION AND WATER FILM

Dry versus Wet Conditions. The decrease of the sliding coefficient with increasing vehicle speed under dry and wet conditions is demonstrated in Figs. 29 and 30. Curves for the critical coefficient follow much the same trend, but they plot higher than the curves of Fig. 30 (see Fig. 50). On dry surfaces the effect of temperature on the predominating adhesion term is the principal factor in reducing the coefficient at higher vehicle speeds. Under wet conditions, increasingly effective hydrodynamic support is responsible for the reduction.

The initial drop of the coefficient at very low speeds, shown in Fig. 30, is due to weakening of the adhesive shear strength by a contaminating film, by an emulsion of organic and inorganic deposits and water (such as that formed at the beginning of rain after a long dry spell), or by plain water. At low speeds hydrodynamic effects are practically absent. This drop must be accepted as unavoidable.

Although hysteresis aids the adhesion term whenever the rubber elements in the contact area are deformed, the magnitude of the friction obtained at low and medium speeds on most road surfaces under wet conditions suggests that the adhesion term still plays the major role. When a water film is present, its thickness becomes another independent variable. As the vehicle speed increases, the water film makes it more and more difficult for the adhesion term to develop locally, and at the same time it reduces the deformation.

At very high speeds on wet surfaces, both terms eventually become trivial due to hydrodynamic effects. The rubber elements then lose the "feel" of the road texture, and the tire locks and starts planing at the slightest brake application. Trant (59) mentions NACA tests with a C-123 airplane touching down under a heavy rainfall, in which Sawyer and Kolnick found that the wheels once locked would not resume rotation even when the brakes were completely released. Similar planing was observed on the NACA treadmill. Planing is unlikely for passenger cars and trucks under normal driving conditions, but it is dangerously within reach of a speeding motorist driving worn and underinflated tires on a smooth road surface with a water film thickness above 0.5 mm.

The decrease of the critical and sliding coefficients with increasing vehicle speed can be controlled to some extent by design factors related to tire geometry, openness of tread and road surface (that is, contact ratios  $R_t$  and  $R_r$ ), and inflation pressure.

Transition from Dry to Wet. An important aspect of contamination and wetness is the transition from dry to wet, but very few data are available on this subject. Accumulations of abrasive particles from the road surface and from tires, together with other organic and mineral substances, can form a very effective lubricating film when a small amount of water is added. The effects of such films are very pronounced on well-polished surfaces. The coefficient is known to recover when enough rain has fallen to flush the slippery layer away. The change of the coefficient during a rain spell after a long dry period is shown in Fig. 41.

Figure 41 also suggests some interesting considerations in the evaluation of coefficient measurements. To show the lowest possible coefficient, locked wheel tests must be made in the wheel track most polished after a long dry period, using very little water (water film thickness 0.1 mm or less). To reveal the frictional properties of the surface under conditions otherwise the same, the track must be thoroughly flushed (water film thickness 0.5 mm or more).

Italian experience (60) indicates, moreover, that a thorough wetting of the surface prior to locked wheel friction measurements produces readings only slightly below those obtained under dry conditions, whereas slight wetting such as might be caused by very damp weather, fog condensation, or a brief spell of rain can result in a dangerously low coefficient.

Further study of the coefficient during this transition is certainly warranted.

Effect of Polishing. Surface films decrease the adhesion term, but they have no effect on hysteresis. The drop in the former is most pronounced when the surface is smooth (polished metals, glass, etc.). Surface finishes of this kind are practically nonexistent on the road, however, except when there is glare ice. When the coarseness of the surface increases, the adhesion for a given apparent pressure decays, as discussed in Part I; but because under sliding the interface is macroscopically deformed by the surface asperities, hysteresis enters the picture. On surfaces composed of sharp angular aggregate, very high local pressures are set up, the magnitude of which is dependent on the modulus of elasticity of the rubber and the average peak angle of the individual asperity. Existing contaminating films are likely to be penetrated locally, so that at least in the high-pressure zones the adhesion term can fully develop. As a consequence, contaminants on such surfaces have less effect on the reduction of adhesion.

Intuition would predict a marked change in the coefficient of friction when an oil-spattered road is cleaned. But friction tests conducted by the British Road Research Laboratory on surfaces contaminated with oil drippings showed little or no increase in the coefficient after the surfaces had been cleaned with a detergent and flushed with water (61). Since oil drippings occur mainly in the center strip between the wheel tracks, an area not subject to polishing, the hazard of this type of contamination is usually not acute. Nevertheless, the effects of road film on the coefficient at heavily traveled intersections remain open to question and should be investigated.

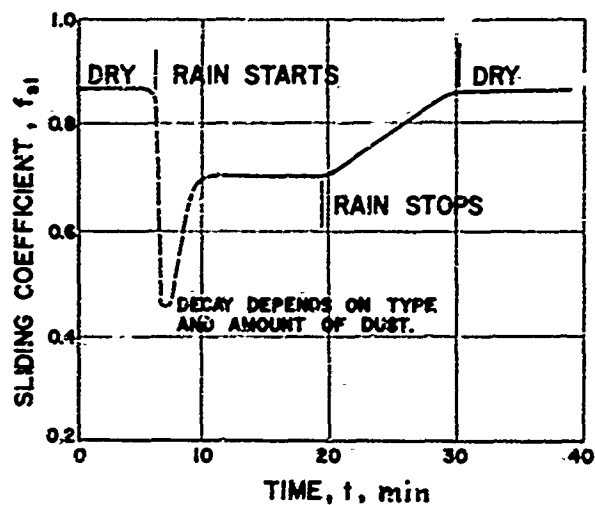


FIG. 41. Temporary drop of coefficient during transition from dry to wet conditions.

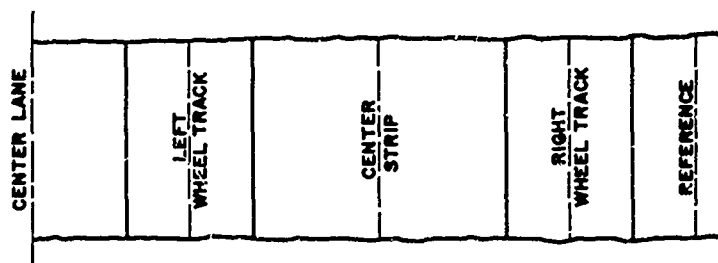
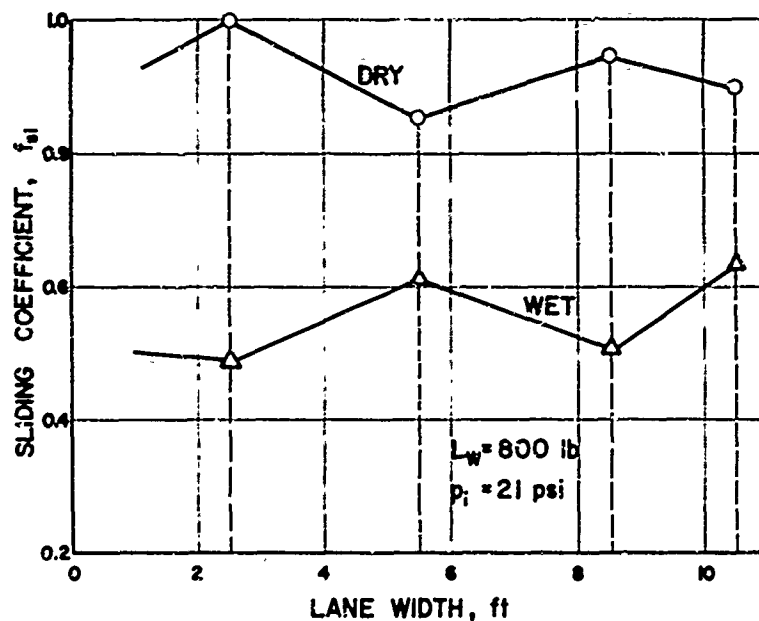


FIG. 42. Sliding coefficient in left wheel track and center strip of heavily traveled concrete surface, dry and wet conditions. Sliding velocity 5 mph, road surface temperature 68° F.

Results of locked wheel tests conducted with the Penn State test trailer on a lane of concrete road, dry and wet, are shown in Fig. 42. The wheel tracks of this surface were polished, and the center strip appeared heavily contaminated after a long dry summer. The tests were run at a sliding velocity of 5 mph, with constant wheel load and inflation pressure. The sliding coefficients of the polished left wheel track and the center strip were measured. For reference purposes, the surface close to the shoulder was also measured, as indicated in the figure.

The upper curve, obtained under dry conditions, shows a higher coefficient in the wheel track and a lower coefficient in the center strip. When the lane was wet, the shape of the curve was reversed. The high coefficient on the polished and relatively clean dry surface was to be expected. The lower coefficient in the center strip was due mainly to greater roughness, which raised the local pressures for the same wheel load and inflation pressure. Tests near the edge of the pavement, where the surface was neither polished nor contaminated, showed a coefficient slightly higher than that in the center. This difference can be attributed to the contaminant.

On the wet lane the low coefficient in the wheel track is typical for a relatively smooth surface and shows the dangerous effect of polishing. The coefficient in the center strip is now higher, because the greater coarseness, with its effect on local pressures, permits high local adhesion and also brings hysteresis into play. Hence the oiliness of the surface interferes with adhesion to a relatively insignificant extent.

Experience indicates that reversal of the curves, as shown in Fig. 42, can be expected on straight single lanes with a coarse surface. On multilane highways, where vehicles change lanes frequently, and on curved road sections, the reversal is less pronounced or cannot be found at all. In these cases the wheels do not follow a common path, but polish across the whole lane more or less uniformly. The reversal is also absent on lanes with surfaces constructed smooth; here the polishing action of the wheels has little or no effect.

From the foregoing it is apparent that under wet conditions a single-wheel trailer running in the center strip may measure a higher critical or sliding coefficient than a two-wheel trailer running in the wheel tracks. Under conditions where the reversal occurs, the additional measurement of the coefficient in the center strip or on the shoulder can be used as a reference to evaluate the progress of polishing.

A tire does not have to slip to cause polishing; rolling alone is sufficient. The relative motion between the peaks and flanks of the aggregate as they penetrate into and retract from the rubber at the entry and exit of the contact area is enough to produce surface wear. How much the rate of wear is intensified by a slipping tire is not known. British findings seem to indicate that the presence of fine mineral dust is needed for the polishing process (62).



Weathering and its seasonal variations also influence the micro-roughness of the aggregate surface. Giles (32) surmised that seasonal changes in the rate of skidding accidents, as shown in Fig. 19, might not be due solely to temperature changes. He found that fine-textured aggregate is more smoothly polished in summer than in winter. Measured with a pendulum tester under wet conditions, his mean coefficient for such a surface at the same temperature was 0.53 for summer and 0.69 for winter.

Present knowledge indicates that only actual friction measurements can show whether or not a road is dangerously slippery. But such measurements are difficult, expensive, and somewhat uncertain, and most states have no suitable equipment for obtaining them. The common method of dealing with the problem is to plant SLIPPERY WHEN WET signs after several accidents have occurred at a particular site. That this is the least effective and most costly method requires no emphasis here.

#### THE PROBLEM OF WATER REMOVAL

Most published reports concerned with tire-road friction under wet conditions touch upon the problem of water removal (or drainage). In a few instances tests have been devised to clarify specific points, but no thorough experimental or analytical investigation has yet been conducted. No other aspect of the tire-road friction problem demonstrates so clearly the dependence of the magnitude of friction on the interaction of tire, road, and operating conditions rather than on any of these individually.

The mechanism of water removal is complex, and since more experimental information must be obtained to guide any realistic analytical approach, the following discussion attempts only a qualitative description of the problem.

To make local adhesive contact and secure sufficient deformation to produce a net force in the tire-ground plane, the bulk of the water encountered by the tire must first be removed. At low vehicle speeds this presents no problem, regardless of water layer thickness, tread design and tire wear, or the road surface. At high speeds the magnitude of adhesive and hysteresis resistance depends entirely on how much water can be removed and how fast. To the extent that contact between the tread element and the road surface can thus be restored, the friction-producing mechanisms of adhesion and hysteresis take over as before.

Basic Principles. Three different actions of the tire contribute to the removal of water from the road. Part of the water is displaced ahead of the contact area by the wedge formed between the incoming tread and the road. The remaining water can be displaced by the squeezing and wiping action of the tread elements in the contact area. The water so displaced or wiped off must be discharged through channels provided by the tread and road surface.

It is necessary to differentiate between the volume of water to be removed per unit time and the amount that is actually removable by the three actions mentioned. Obviously, the capacity to remove water must be great enough to handle the anticipated volume in a fraction of the time a single tread element spends in the contact area, or the tire will

plane. The volume per unit time is determined by the average water film thickness on the road, which is a function of the amount of rain; the surface geometry (slope and crown); the width of the running band; and most importantly, vehicle speed.

The capacity to remove water is determined by the geometric shape of the tire; the arrangement and effective cross section of the channels in the running band and the road; the viscosity of the water layer; in the case of squeezing action, the driving force or pressure gradient within the contact area; in the case of wiping, the heel and toe wear of the single tread element and its motion relative to the road surface; and, again, vehicle speed.

The basic problem of water removal as a function of speed is illustrated by Fig. 43. The volume of water  $q$  to be displaced per unit time is given by

$$q = hbV_v \quad (44)$$

where  $h$  is the average thickness of the water layer,  $b$  is the width of the tire tread, and  $V_v$  is the vehicle speed. The time available to remove water from the contact area is given by

$$t_r = Ka/(V_v - V_s) \quad (45)$$

where  $a$  is the length of the contact area,  $V_s$  is the slip velocity, and  $K$  is a drainage factor smaller than unity.

The curves are based on a standard passenger car tire, with  $a = 5$  in.,  $b = 4$  in., the initial thickness of the water layer assumed as 0.02 in., and  $K = 0.3$ . Reasoning indicates that the drainage factor  $K$  should be of the order of 0.3, or preferably less, since a tire cannot be expected to transmit any significant forces in the ground plane if its tread elements have not touched the ground within the second third of the contact length.

Figure 43 shows that the volume of water to be removed at a given time increases linearly with vehicle speed, whereas the time available for its removal decreases hyperbolically. Owing to inertia and viscous effects, water resists displacement and discharge, making the mechanism of water removal time-dependent.

The  $a/b$  Ratio. Since the slope or crown of a road surface is dictated by other considerations, the amount of water experienced by a tire can be influenced only by varying the tire width and the vehicle speed. Assuming that it is not desirable to change the inflation pressure and the contact ratio  $R_t$ , a decrease of  $b$  to half the width value of a conventional tire would double the length of the contact area. From Eq. 45 it is apparent that the time available for water removal would then be doubled, suggesting that tires with a large  $a/b$  ratio should be superior in braking or driving under wet conditions.

Tabor (7) mentioned that a tire with a narrow and long contact area is advantageous from the standpoint of built-in hysteresis. High rolling resistance, internal heating, and wear are the usual objections to the

use of high-hysteresis rubber in the running band. A sliding tire with a large a/b ratio will provide the same hysteresis resistance in the tire-road plane as a conventional tire with the same contact area and inflation pressure, but rolling resistance and internal heating will be less.

Although there are considerations that argue against such a tire shape, it is worth noting that any increase of the a/b ratio, other conditions remaining the same, would (a) decrease the amount of water to be removed, (b) increase the time available for its removal, and (c) permit the use of high-hysteresis rubber in the running band without the penalties of higher rolling resistance and heating. Increasing the a/b ratio by reducing the inflation pressure would be no improvement, since the pressure difference between the center of the tire and the outer ribs would increase (see Fig. 26). From the standpoint of squeezing and drainage, the pressure difference should be as small as possible.

That a reduction in vehicle speed is the simplest but most often neglected way to improve the frictional grip of a tire on a road surface need not be discussed.

Mechanism of Water Removal. The three actions of water removal and some of the factors that influence their efficiency will now be examined more closely.

The amount of water that can be displaced by the wedge formed between the incoming tread and the surface depends on the initial thickness of the water layer and the geometric shape of the wedge; that is, the ratio  $r/a$ , where  $r$  is the radius of the undeflected tire. If the asperities of the surface are not completely submerged, a tire with a small  $r/a$  ratio will not, of course, displace water to any significant extent. The tread elements that have entered the contact zone must cope with the water not removed by the wedge.

In 1936, Saal (63) pointed out that water films are difficult to expel when they are merely a few thousands of an inch thick. If sufficient time is available, the film may eventually reach a critical thickness below which the apparent viscosity increases sharply (see page 20). Saal calculated the decrease of the thickness as a function of time for an elliptical plate sinking through a water film, assuming an initial film thickness of 0.020 in. and an apparent load of 32 psi. Figure 44 plots his relation

$$1/h^2 = 1/h_0^2 + 2/3(p/\eta)[(a^2 + b^2)/a^2b^2]t \quad (46)$$

where  $h_0$  is the initial film thickness,  $p$  is the apparent pressure,  $a$  and  $b$  are the major and minor axes of the ellipse, and  $\eta$  is the viscosity of the liquid film. Although the initial decay of the film thickness is rapid, the time axis is approached asymptotically.

A similar relationship appears to exist between the thickness of a water layer and the time required by a tread element seeking contact on a smooth surface. If the surface is composed of fine sharp-angled

aggregate, high local pressures are reached quickly, the time depending on the relative statistical height of the water layer and the surface asperities. The horizontal branch of Saal's curve is then of no concern.

The effectiveness of the squeezing action in removing water ahead of and within the contact area is not affected by relative motion of the tread elements in the tire-ground plane, but the wiping action depends on such motion. The slipping tire satisfies this condition for wiping, and the sliding tire even more so.

Experiments performed with a rubber slider on a contaminated track showed that the coefficient increased more in consecutive runs if the leading edge of the slider was sharp. Gough (29) pointed out that the heel and toe wear of tread elements has a bearing on the sliding coefficient (Fig. 45). Other conditions being equal, the sliding coefficient for a tire was found to increase 50% when the leading edges of the tread elements were sharp, but it is difficult to decide what part of this improvement is due to the wiping action as such and what part is due to a negative angle of attack, which prevents hydrodynamic support. The upper portion of Fig. 45 suggests that in this case each tread element can act as a Mitchell bearing, because the angle of attack is positive.

Since tires which normally transmit driving torques develop heel and toe wear favorable to the wiping action under braking, tires on a drive axle should produce a higher sliding coefficient than tires simply rolling. This does not hold, however, for tires subject to stop-and-go driving. Under such conditions the leading and trailing edges of the tread elements are rounded evenly.

Channelization. The water displaced by squeezing and wiping action must be discharged through channels in the tire and in the road surface. If the tire and the road surface were made of materials having the same modulus of elasticity, it should not matter whether the required cross section was made available in one or the other or in both. Accordingly, a smooth tire should develop the same coefficient in contact with a coarse surface as a ribbed tire on a perfectly smooth surface, provided  $R_t = R_r$ . Although experiments indicate such a tendency, the friction obtained in both cases is not equal. At low vehicle speeds a smooth tire slipping or sliding on a sandpaperlike surface gives a higher coefficient than a treaded tire on a polished surface, because local pressures are much higher in the first case and the hysteresis term is absent in the second case.

Theoretically, hysteresis resistance will be the same whether it is due to severe deformation in a few spots or moderate deformation in many spots, as long as the total deformation remains constant. Adhesion favors many small asperities rather than a few large peaks. Book (64) conducted tests with a smooth 10 X 2.5 tire on a treadmill. The tire was run on abrasive belts of three grid sizes, with three different water settings, at belt speeds from 5 to 70 fps. Figure 46 shows the critical coefficient as a function of grid size, with belt speed as a parameter. The water slot setting was constant. Since the  $r/a$  ratio of this tire was small, the water was displaced mainly by squeezing it out through the irregular channels provided by the belt surfaces. The rapid decay of

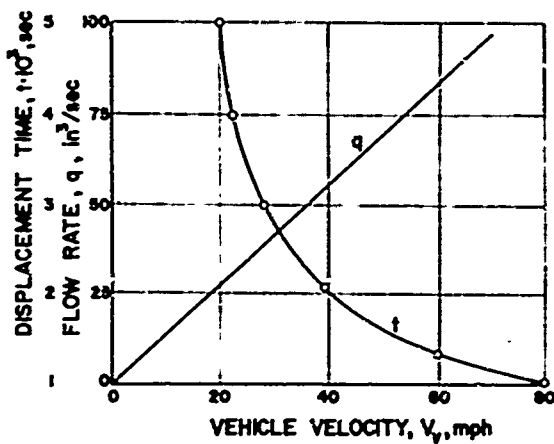


FIG. 43. Water to be removed and time available for removal versus vehicle speed, normal passenger car tire.

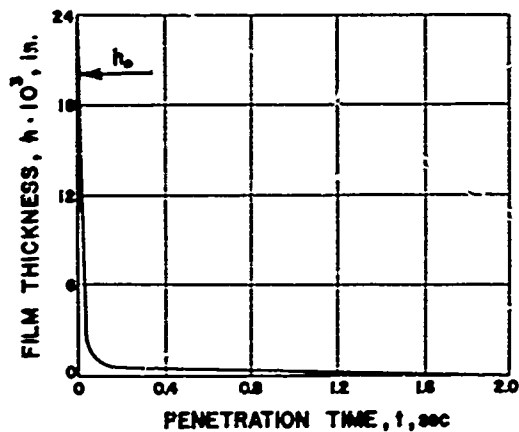


FIG. 44. Thickness of water layer under loaded 6 by 4 in. plate as a function of time (63). Initial thickness, 0.02 in.; pressure, 32 psi.

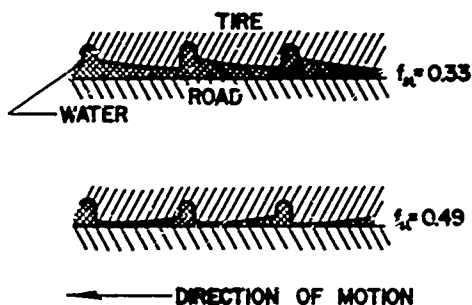
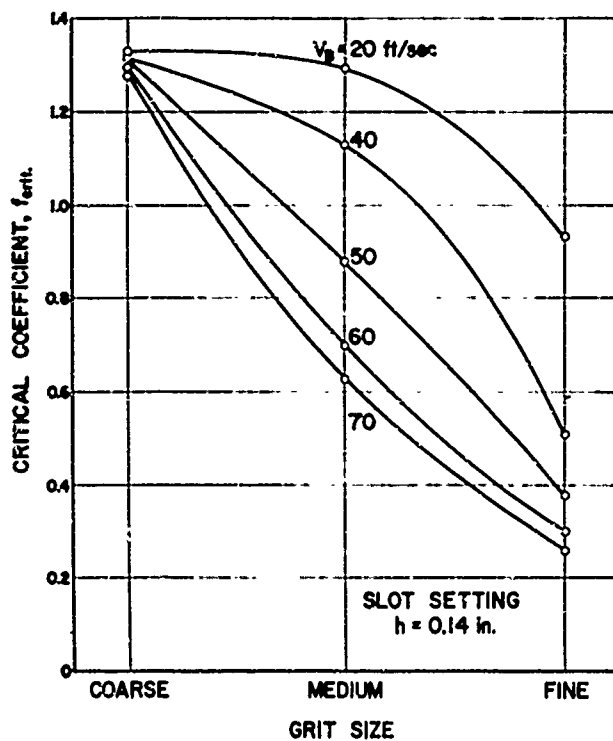


FIG. 45. Influence of heel and toe wear of tread elements on sliding coefficient (29).

FIG. 46. Effect of grid size and speed on critical coefficient (64). Belts, water-proof Behr-Manning, 24-X, 150-X, and 400-X; model tire, 10 x 2.50, 2 ply; wheel load, 22 lb; inflation pressure, 16 psi; water slot setting, 0.14 in.



the coefficient with decreasing grid size for a given speed (and vice versa) is typical for surfaces where channelization is inadequate. As shown in Fig. 46, only the coarsest grid permitted the tire to discharge the water in time at 70 fps, that is, proved adequate for the volume of water to be removed. When the belt speed was increased beyond 70 fps in one exploratory experiment, the highest coefficient was obtained with a ribbed and slotted tire on the same coarse grid.

Grime and Giles (63) measured the effect of different tread designs, other conditions constant, on vehicle deceleration (Fig. 47). It is significant that the deceleration increases when the ratio of the circumference of the gross contact area to the square root of the net contact area becomes larger. This ratio can be changed for the same tire geometry (that is, the shape of the gross contact area) by varying the openness of the tread, as was done by Grime and Giles. It can also be influenced to a certain extent, however, by changing the geometric shape of the tire. For a smooth tire, for example, the lowest value obtainable for a circular contact area is 3.54. A square contact area gives a value of 4.0, and a rectangular footprint with  $a = 2b$  gives 4.23.

Improved channelization, regardless of whether it is due to a change in the road surface or the tread design or both, is accompanied by an increase of the average apparent pressure, according to Eq. 22, 22a, and 23.

If the modulus of elasticity of rubber were sufficiently high, the necessary cross section for drainage could be obtained by relatively narrow but deep channels, thus preserving a large contact area. In practice, the arrangement and dimensions of channels in the tire are dictated by numerous other requirements. The tire must not be too noisy and must have good abrasion resistance. The individual ribs must be sufficiently rigid so that they will not collapse. Although the channels of modern tires look adequate, their effectiveness for drainage is greatly reduced by their tendency to squeeze shut under the normal pressure and tangential stresses in the contact area.

Drainage of the Center Section. Because of the peculiar apparent pressure distribution in the contact area, the pressure gradient is not always negative along lines connecting the center of the contact area with points on its perimeter. It can happen that the higher pressures under the outer ribs squeeze the water outward as well as towards the center of the tire. Observation of the water trace left by a fast-rolling tire indicates a more thorough removal of water at the shoulders. This suggests that the center portion of the footprint is more difficult to drain and will eventually lose contact with the surface before the shoulders do.

An improvement of the frictional grip of the center section of the contact area (and therefore of the whole tire) could be achieved in two ways. The channels provided in the fore and aft direction could be enlarged (a) to facilitate the discharge of water in the direction already favored by the vertical pressure distribution, and (b) to raise the pressure under the tread elements. Trant (59) reported that the highest critical coefficient obtained from several tires with identical geometry but

different treads was produced by an arrangement of peripheral grooves. This observation verifies the statement made earlier about the importance of the  $a/b$  ratio, since such a tire can be thought of as consisting of several tires with a very large  $a/b$  ratio, placed in parallel. Or the pressure gradient in the fore and aft direction could be made steeper simply by increasing the inflation pressure. Trant reported a marked increase of the coefficient measured at low slip values when the inflation pressure was increased (Fig. 48).

Planing. Figure 49, from Trant (59), shows the effect of vehicle speed and water film thickness on the critical coefficient obtained with a treaded passenger car tire. It can be seen that the tire will reach the planing stage at approximately 60 mph when the water film thickness is 0.3 in. During a heavy rain such a condition may be experienced by the motorist, at least on turnpikes or straight sections of highways. It should be noted that planing will occur earlier if the tire is locked. Moyer (65) investigated the effect of vehicle speed and tread design on the critical and sliding coefficient (Fig. 50). Typical, again, is the more rapid decrease of the critical as well as the sliding coefficient when the tread is worn smooth. At lower speeds, the curves for the treaded and the smooth tire approach each other and may even cross over, indicating that the surface on which the tests were made was alone adequate to handle the water to be removed from within the contact area.

"Best Point" Compromise. The problem of friction transmission at higher vehicle speeds under wet conditions demonstrates the compromising role the tire must play, since no tire can provide maximum friction through the entire range of vehicle speeds, road surfaces, and water film thickness. Each tire has a "best point," determined by the interaction of tire factors (geometry, tread design, etc.), road surface, water thickness, and operating conditions (wheel load, inflation pressure, speed).

It is likely that a dimensionless number can be found that will govern the occurrence of this best point, which may take the form of

$$(a/b)^u (p/p_1)^v (t_r/t)^w \quad (47)$$

where  $u$ ,  $v$ , and  $w$  are exponents to be determined. The first ratio describes the geometry of the tire (the significance of the  $a/b$  ratio was mentioned earlier in this section). The second ratio represents the product of the contact ratios  $R_t$  and  $R_r$  (Eq. 23), and is a measure of apparent pressure as well as channelization. The third ratio compares the time  $t_r$  available for water removal, as defined by Eq. 45, and the time  $t$  actually required for a single rubber element to squeeze through a liquid layer of a given initial thickness and viscosity (compare Eq. 46 when solved for  $t$ ).

A better understanding of the mechanism of water removal could lead to a special-purpose tire especially effective at higher speeds under wet conditions. The standard tire could also benefit from this understanding, undergoing changes that would make it more effective under adverse conditions without impairing its performance in other respects.

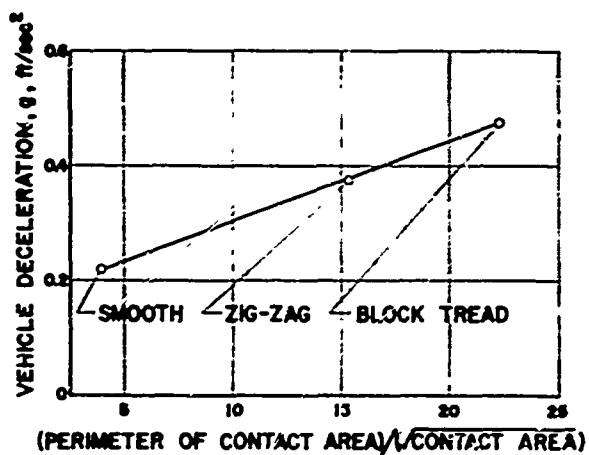


FIG. 47. Deceleration of vehicle under wet conditions as a function of tread openness (63), smooth surface.

FIG. 48. Coefficient of braking as a function of wheel slip and inflation pressure (59). Water depth 0.3 in.

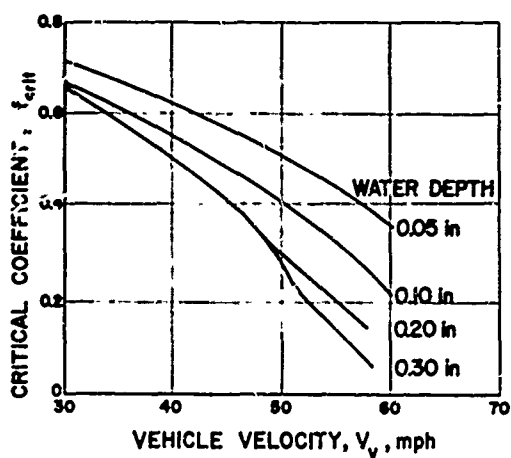
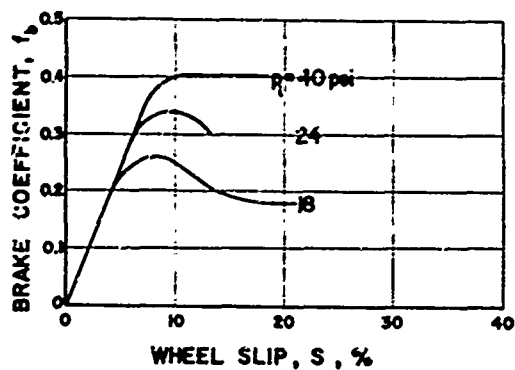


FIG. 49. Critical coefficient as a function of vehicle speed and water layer thickness (59).

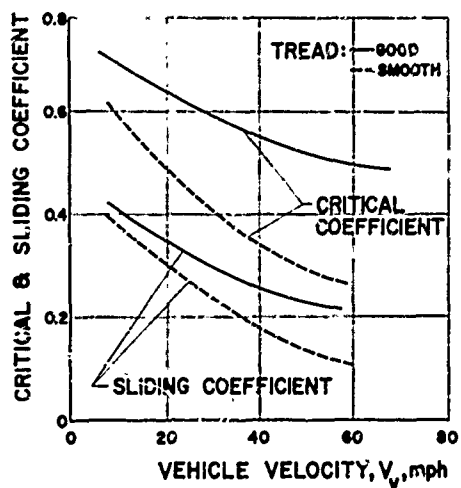


FIG. 50. Decay of critical and sliding coefficients under wet conditions, treaded and smooth tires (65).



## SUMMARY

The friction characteristics of a pneumatic tire are related to but not identical with those of a simple rubber block. The surface texture of most roads and the relative motion of the tread elements within the contact area of a slipping or sliding tire permit hysteresis to be present simultaneously with adhesion. The adhesion term is the main contributor to the total frictional resistance developed by a slipping or sliding tire under dry conditions. When the road surface is wet, the adhesion term is reduced by weakening of the shear strength, but it is still dominant in most situations.

The sliding coefficient of a rubber block changes perceptibly with variations of the apparent pressure. The effect of wheel load on the coefficient of road friction is less pronounced for a tire, partly because wheel load variations are not entirely translated into apparent pressure changes, and partly because of the opposing trends of the adhesion and hysteresis terms.

Under bulk creep or at low sliding velocities, the tire behavior is identical with that of rubber slider. Therefore, the maximum coefficient of a locked tire is obtained at a low sliding velocity, which is of the order of several inches per second and appears to be lower under wet conditions.

Slip, as usually measured in road tests, is composed of a component due to elastic deformation and another due to the mean sliding velocity in the contact area. Experiments indicate that throughout a wide range of vehicle speeds the critical coefficient occurs at essentially constant slip. This is in agreement with theory proposed for medium and high vehicle speeds, regardless of whether the sliding velocity of the contact area was assumed to be a function of or independent of vehicle speed.

The critical coefficient is lower than the maximum coefficient obtained from a locked tire sliding at low velocity. It is proposed that the difference is due primarily to the nonuniform distribution of the sliding velocity over the contact length and the transient behavior of the adhesion term in the presence of rapid velocity changes.

Temperature effects on the coefficient of friction, sliding or critical, are as pronounced for a pneumatic tire as they are for a simple rubber slider. They are progressively more severe for rolling, slipping, and sliding tires. Under dry sliding conditions the decomposition temperature of rubber is easily reached, and there are indications that decomposition is partially attainable under wet conditions. Measurements of tire and road temperature and ambient temperature are indispensable in evaluating friction data.

The effects of oil drippings on the coefficient of road friction appear to be of second-order importance as long as the oil deposits are not excessive and the surface is not polished. The transition from dry to wet, especially after a long dry spell, is known to cause a temporary drop of the coefficient. Neither of these subjects has yet been adequately explored.

Polished surfaces reduce the coefficient under wet conditions and are particularly dangerous at higher speeds. The magnitude of friction obtained on a wet surface at higher vehicle speeds depends primarily on tire geometry, tread design, texture of road surface, thickness of water film, and operating conditions (most importantly speed and inflation pressure.) A more thorough investigation of the problem of water removal is needed.

## REFERENCES

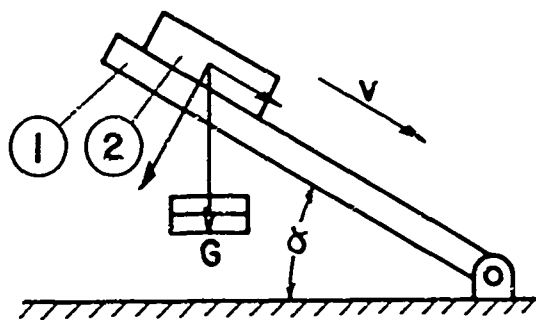
1. Moyer, R. A., A Review of the Variables Affecting Pavement Slipperiness, Proceedings First International Skid Prevention Conference, Virginia Council of Highway Investigation and Research, University of Virginia, 1958, Part II, p. 411.
2. West, A. C., Friction and Boundary Lubrication, Lubrication Engineering, 9(4):211-216 (1953).
3. Bikerman, J. J., Friction and Adhesion, Philosophical Magazine, (7)32:67-76 (1941).
4. Moyer, R. A., Skidding Characteristics of Automobile Tires on Roadway Surfaces and Their Relation to Highway Safety, Iowa Engineering Experiment Station, Bulletin 120, 1934.
5. Strang, C. D., and Lewis, C. R., On the Magnitude of the Mechanical Component of Solid Friction, Journal of Applied Physics, 20:1164-1167 (1949).
6. Bowden, F. P., and Tabor, D., The Friction and Lubrication of Solids, Oxford University Press, London, 1950.
7. Tabor, D., Friction between Tire and Road, Engineering, 186:838-840 (1958).
8. Tabor, D., The Importance of Hysteresis Losses in the Friction of Lubricated Rubber, Proceedings First International Skid Prevention Conference, Virginia Council of Highway Investigation and Research, University of Virginia, 1958, Part I, p. 211.
9. Schallamach, A., Load Dependence of Rubber Friction, Proceedings Physical Society, London, 65B:657-661 (1952).
10. Hütte I, Gummi, 27th ed., 1952, p. 978.
11. Gough, V. E., and Parkinson, D., Dunlop Fatigue Test for Rubber Compounds, Transactions Institution of the Rubber Industry, 17:168-239 (1941).
12. Archard, J. F., Contact and Rubbing of Flat Surfaces, Journal of Applied Physics, 24:981-988 (1953).
13. Gough, V. E., A Simple Direct-Reading Friction Meter, Journal of Scientific Instruments, 30:345 (1953).
14. Roth, F. L., Driscoll, R. L., and Holt, W. L., Frictional Properties of Rubber, Bureau of Standards Journal of Research, 28:439 (1942).
15. Denny, D. F., The Influence of Load and Surface Roughness on the Friction of Rubber-like Materials, Proceedings Physical Society, London, 66B:721 (1953).

16. Thirion, P., Coefficients of Adhesion of Rubber, *Revue générale du caoutchouc*, 23:101-106 (1946).
17. Schallamach, A., The Velocity and Temperature Dependence of Rubber Friction, *Proceedings Physical Society, London*, 66B:386 (1953).
18. Foster, R., Friction of Rubber at Low Sliding Velocities, M.S. thesis, Department of Mechanical Engineering, The Pennsylvania State University, 1961.
19. Papenhuyzen, P. J., Friction Experiments in Connection with Slipping of Automobile Tires, *De Ingenieur, Utrecht*, 53(45):V, 75-82 (1938).
20. McConnell, W. A., Traction and Braking Characteristics of Vehicles, *Proceedings First International Skid Prevention Conference, Virginia Council of Highway Investigation and Research, University of Virginia*, 1958, Part I, pp. 81-87.
21. Bartenev, G. M., Some Questions Concerning the Surface Friction of Rubbers, *Colloid Journal, USSR*, 18(6):627-628 (1956).
22. McFarlane, J. S., and Tabor, D., Adhesion of Solids and Effect of Surface Films, *Proceedings Royal Society, London*, A202:224-243 (1950).
23. Derjaguin, Shear Elasticity of Water Films, *Zeitschrift für Physik*, 84:657 (1933).
24. Dudley, B. R., and Swift, H. W., Frictional Relaxation Oscillations, *Philosophical Magazine*, (7)40:849-861 (1949).
25. Andronow, A. A., and Chaiken, C. E., *Theory of Oscillations*, Princeton University Press, Princeton, 1949.
26. Blok, H., Fundamental Mechanical Aspects of Boundary Lubrication, *SAE Journal*, 46:54-68 (1940).
27. Terzaghi, K., *Erdbau Mechanik auf bodenphysikalischer Grundlage*, F. Deuticke, Vienna, 1925, pp. 124-125.
28. Schallamach, A., Surface Condition and Electrical Impedance in Rubber Friction, *Proceedings Physical Society, London*, 66B:817-825 (1953).
29. Gough, V. E., Hardman, J. H., and Maclaren, J. R., Abraded Tire Treads, *Transactions Institution of the Rubber Industry*, 32:46 (1956).
30. Tabor, D., Mechanism of Rolling Friction, *Philosophical Magazine*, (7)43:1055-1059 (1952).
31. Sabey, B. E., Pressure Distribution beneath Spherical and Conical Shapes Pressed into a Rubber Plane, and Their Bearing on Coefficients of Friction under Wet Conditions, *Proceedings Physical Society, London*, 71B:979-988 (1958).

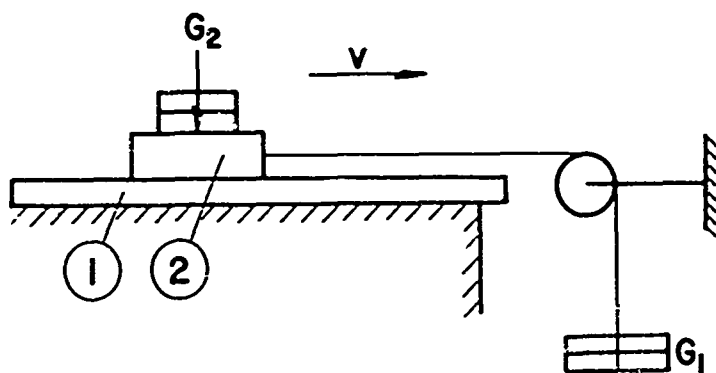
32. Giles, C. G., and Sabey, B. E., A Note on the Problem of Seasonal Variations in Skidding Resistance, Proceedings First International Skid Prevention Conference, Virginia Council of Highway Investigation and Research, University of Virginia, 1958, Part II, pp. 563-568.
33. Giles, C. G., and Sabey, B. E., Recent Investigation on the Role of Rubber Hysteresis in Skidding Resistance Measurements, Proceedings First International Skid Prevention Conference, Virginia Council of Highway Investigation and Research, University of Virginia, 1958, Part I, p. 219.
34. Stegemann, W., Rutschsicherheit, Bulletin Phoenix Gummiwerke, Harburg, W. Germany, 1953.
35. French, T., and Gough, V. E., The Role of Tires in Automobile Design and Performance, paper presented at Fifth International Technical Congress of the Motor Industry, Munich, 1954.
36. Mills, J. P. and Shelton, W. B., Virginia Accident Information Relating to Skidding, Proceedings First International Skid Prevention Conference, Virginia Council of Highway Investigation and Research, University of Virginia, 1958, Part I, p. 12.
37. Kamm, W., Selbsttaetige Richtungshaltung des Fahrzeugs, Automobiltechnische Zeitschrift, 56(5):117-121 (1954).
38. Hadekel, R., The Mechanical Characteristics of Pneumatic Tires, ASTIA, ATI No. 92172, 1952, p. 35.
39. Segel, L., Lateral Mechanical Characteristics of Non-stationary Pneumatic Tires, Cornell Aeronautical Laboratory, Report YD-1059-F-1, 1956.
40. Dillard, J. H., and Allen, T. M., Correlation Study, Proceedings First International Skid Prevention Conference, Virginia Council of Highway Investigation and Research, University of Virginia, 1958, Part II, p. 381.
41. Hershey, M. P., Tires for High Speed Operations, SAE Journal, 65:85-86 (1957).
42. Giles, C. G., and Sabey, B. E., Effects of Pressure and Friction on Photographic Emulsions, British Journal of Applied Physics, 2:174 (1951).
43. See Ref. 31, p. 979.
44. Weber, G., Theory des Reifens mit ihren Auswirkungen auf die Praxis bei hohen Beanspruchungen, Automobiltechnische Zeitschrift, 56(12): 325-330 (1954).

45. Hofelt, C., Effect of Speed, Load Distribution, and Inflation Pressure, Proceedings First International Skid Prevention Conference, Virginia Council of Highway Investigation and Research, University of Virginia, 1958, Part I, p. 181.
46. Mercer, S., Locked Wheel Skid Performance of Various Tires on Clean, Dry Road Surfaces, National Research Council, Highway Research Board, Bulletin 186, 1958, pp. 8-25.
47. Deflection of Moving Tires, U.S. Army Engineer Waterway Experiment Station, Corps of Engineers, Vicksburg, Mississippi, Technical Report 3-516, Report 1, 1959.
48. Gough, V. E., and French, T., Tires and Skidding from an European Standpoint, Proceedings First International Skid Prevention Conference, Virginia Council of Highway Investigation and Research, University of Virginia, 1958, Part I, p. 189.
49. Tabor, D., and Eldredge, K. R., Mechanism of Rolling Friction, Proceedings Royal Society, London, A229:181-219 (1955).
50. Carter, F. W., On the Action of a Locomotive Driving Wheel, Proceedings Royal Society, London, A112:151 (1926).
51. Gough, M. N., Sawyer, R. H., and Grant, J. P., Tire Runway Braking Friction Coefficient, North Atlantic Treaty Organization, Advisory Group for Aeronautical Research and Development, Report No. 51, 1956.
52. Giles, C. G., Some European Methods for the Measurement of Skid Resistance, Proceedings First International Skid Prevention Conference, Virginia Council of Highway Investigation and Research, University of Virginia, 1958, Part I, p. 267.
53. Gough, V. E., Friction of Rubber, Dunlop Development Division, Report T.D. 162, 1958.
54. Gough, V. E., Distribution of Side Force and Side Slip in the Contact Patch of the Pneumatic Tire, Dunlop Development Division, Report T.D. 154, 1958.
55. White, A. J., Tire Dynamics, Motor Vehicle Research, Inc., South Lee, New Hampshire, 1956.
56. Oleson, C. C., discussion in Proceedings First International Skid Prevention Conference, Virginia Council of Highway Investigation and Research, University of Virginia, 1958, Part I, p. 184.
57. Giles, C. G., and Lander, F. T. W., The Skid Resisting Properties of Wet Surfaces at High Speeds, Journal of the Royal Aeronautical Society, 60:83-94 (1956).
58. Reinhardt, M. A., Effect of Tread Composition, Proceedings First International Skid Prevention Conference, Virginia Council of Highway Investigation and Research, University of Virginia, 1958, Part I, p. 167.

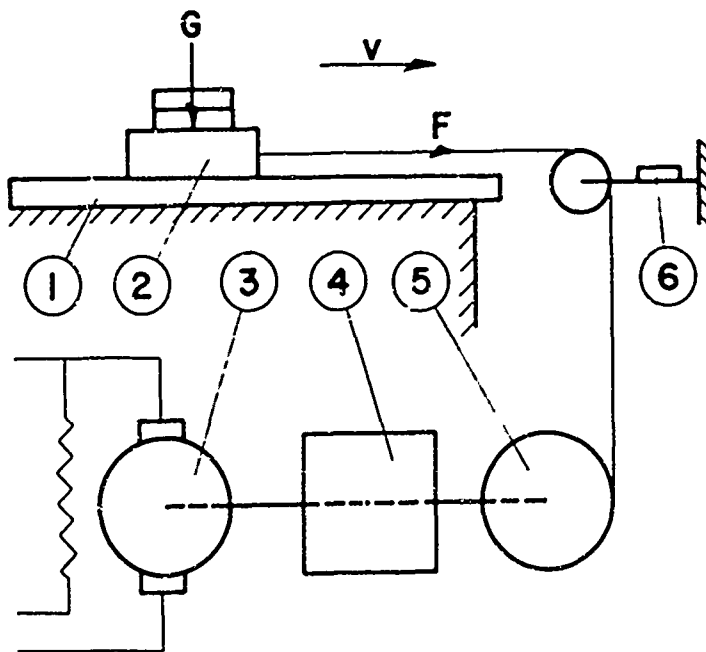
59. Trant, J. P., NACA Research on Friction Measurements, Proceedings First International Skid Prevention Conference, Virginia Council of Highway Investigation and Research, University of Virginia, 1958, Part I, p. 297.
60. Ariano, R., Road Slipperiness, Proceedings First International Skid Prevention Conference, Virginia Council of Highway Investigation and Research, University of Virginia, 1958, Part II, p. 569.
61. Giles, C. G., and Sabey, B. E., Skidding as a Factor in Accidents on the Roads of Great Britain, Proceedings First International Skid Prevention Conference, Virginia Council of Highway Investigation and Research, University of Virginia, 1958, Part I, p. 27.
62. MacLean, D. J., and Shergold, F. A., The Polishing of Road Stones in Relation to Their Selection for Use in Road Surfacing, Proceedings First International Skid Prevention Conference, Virginia Council of Highway Investigation and Research, University of Virginia, 1958, Part II, p. 497.
63. Grime, H., and Giles, C. G., The Skid-Resisting Properties of Roads and Tires, Proceedings Institution of Mechanical Engineers, Automobile Division, 1954-1955(1):19-30.
64. Book, R., Tire Drainage Experimental Investigation, M.S. thesis, Department of Mechanical Engineering, The Pennsylvania State University, 1960.
65. Moyer, R. A., Effect of Pavement Type and Composition on Slipperiness, Proceedings First International Skid Prevention Conference, Virginia Council of Highway Investigation and Research, University of Virginia, 1958, Part II, p. 469.



$$f = \frac{G \sin \alpha}{G \cos \alpha} = \tan \alpha$$



$$f = \frac{G_1}{G_2}$$



$$f = \frac{F}{G}$$

FIG. 51. Laboratory techniques to determine the coefficient of friction. Top and center, constant-pull method; bottom, constant-velocity method. 1, track; 2, rubber block; 3, constant-speed motor; 4, reduction gear; 5, drum; 6, strain gage transducer.



## APPENDIX

### LABORATORY TECHNIQUES

The objective of nearly all friction experiments with rubber is to determine the coefficient of friction as a function of sliding velocity, temperature, vertical load, rubber composition, surface type and texture, contamination, and so forth. The laboratory techniques most commonly used for such studies are (1) the constant-pull method, (2) the constant-velocity method, and (3) the pendulum method.

In the constant-pull method gravity forces overcome the frictional resistance of a rubber block slider. A special case of this method employs an inclined plane, with a single weight providing normal load and pull force (Fig. 51, top). Because the tangent of the inclination is identical with the coefficient of friction, the inclined plane permits direct reading:

$$f = F/L = G \sin \alpha / G \cos \alpha = \tan \alpha$$

For certain investigations a horizontal track is more desirable and the arrangement shown at center in Fig. 51 is used. Two weights are required,  $G_1$  for the pull force and  $G_2$  for the normal load. The coefficient is given by

$$f = F/L = G_1/G_2$$

Both of these arrangements are inexpensive, and it is common to both that the pull forces  $G \sin \alpha$  and  $G_2$  are quasi-constant because the changes in velocity of the slider are so small that inertial forces practically do not exist. The independent variables are the pull force and consequently the coefficient of friction; the sliding velocity is the dependent variable.

The "Direct Reading Friction Meter" developed by Gough (13) combines the advantages of the inclined plane and the horizontal track, using a platform built as a balanced parallelogram.

In the constant-velocity method the pulling weight is replaced by the pull of a drum connected to a constant-speed motor, or the slider is placed on an endless belt or the periphery of a rotating disk. This method is more accurate than the constant-pull method and is preferable for investigation of larger velocity ranges and transients, but it is more expensive because of the required motor, speed control, reduction gear, and force or torque measuring device. Here the sliding velocity is the independent variable; the dependent variables are pull force and therefore the coefficient of friction.

Roth, Driscoll, and Holt (14) have used both methods. Schallamach (17) used the constant-pull method extensively.

Experiments for the present study were conducted with both methods. For the constant-pull method (Fig. 51, center) the slider was placed on a

horizontal track with various surfaces, and was connected to the pulling weight by a cotton fishline passed over an aluminum pulley mounted on two precision ball bearings. Attached to the pulley was a Teflon contact disk that transmitted to a brush recorder 32 voltage pulses per revolution (equal to one pulse per 0.30 in. travel of the slider). Given the paper speed  $v_p$  of the recorder and the distance  $\ell$  between two pulses, the sliding velocity of the rubber sample was obtained by

$$v = 0.30(v_p / \ell)$$

For the constant-velocity method (Fig. 51, bottom) the same track was used. The cotton fishline was replaced by a thin steel wire passed over the pulley and wound on a steel drum. The drum was connected to a 1/4 hp d-c motor by a double worm gear. The speed of the motor was governed by a control unit. In this case the pulley was mounted on a cantilever to which strain gages were bound, forming a temperature-compensated bridge. The input voltage to the bridge was variable to secure full deflection of the measuring instrument for the range of normal loads. The bridge output was amplified and displayed on a 16 point recorder.

The results obtained by both methods were in fair agreement in the load and velocity range investigated.

The pendulum method, based on conservation of energy, is a handy way to measure the relative slipperiness of surfaces, either in the laboratory or on the road. The difference of the initial and final heights of the pendulum head is proportional to the average friction force encountered by the rubber block when sliding over the surface. The value measured is relative because the friction does not reach steady-state conditions. It is therefore referred to as "relative skid resistance."

This method approximates the conditions encountered by a tread element of a tire running under slip, and in fact produces values more nearly representing the critical coefficient of friction than the sliding coefficient. It is inexpensive, but the design of the pendulum head requires considerable attention. The tester is portable, and rubber specimens can be changed readily.

#### ROAD FRICTION TESTING

Four very different groups conduct friction tests or experiments, each for its own purposes: the tire, automobile, and road surfacing industries, and agencies in charge of specifying or maintaining roads and highways. Some twenty diverse approaches to designing apparatus for measuring the friction between tire and road have been reported, most of which are described in the Proceedings of the First International Skid Prevention Conference.

Although the variety of the design solutions is surprising, each is intended to measure the critical coefficient or the sliding coefficient of friction. Under all practical conditions the first is higher than the latter. For reasons of safety the automobile industry bases the layout

of brake systems on the critical coefficient or a fictive higher coefficient, whereas the sliding coefficient (or an even smaller value) is used to plan transients and banking in highway design and to establish criteria for safe stopping distances.

Measurement of the Critical Coefficient. In one of the two methods generally followed, the driving or braking force between tire and road is measured with the tire running under a certain slip, the critical slip if possible, somewhere between 8% and 20%. From the text discussion of the pattern of motion prevailing in the contact area in this case, it is obvious that this method requires a forced rotation of the tire, either faster or slower than the vehicle speed. Because a constant slip control is very difficult to obtain, the tests are conducted at constant speed. Single-wheel and two-wheel trailers of various design are employed. The method is satisfactory for all speeds in the range of interest for automobiles. The wear pattern of the tire is uniform.

The second method utilizes the cornering characteristics of the pneumatic tire at low slip angles. The tire runs freely at a certain slip angle, the critical slip angle if possible, and the force normal to the wheel plane is measured. The critical slip angle corresponding to critical slip is found to be between 10 and 20 degrees. Tire wear is more severe, mainly affecting one side of the running band. This method is fairly independent of speed because the side force, like the brake force, is dependent only on slip, which changes with slip angle not with speed. Single-wheel trailers are commonly employed, but two-wheel rigs offer the advantage that both tires may run under opposite yaw, eliminating a resultant side force. In this method the towing vehicle has to overcome only a small drag component, and the horsepower requirements are smaller. A few existing trailers, such as the Penn State test trailer, are so designed that the tire may run under slip and yaw at the same time, permitting the study of superpositioned brake and cornering forces.

Measurement of the Sliding Coefficient. Whereas the methods used to determine the critical coefficient can be applied to continuous measurements at steady-state temperatures, those giving the sliding coefficient provide only interrupted measurements.

Here again two methods prevail. The first locks the tire and drags it along at constant speed. To prevent excessive tire damage, measurements are usually limited to speeds below 50 mph. Artificial wetting is required. In one instance (57) this method was used up to 100 mph. At high speeds the wear pattern is patchy and local blistering of the running band eventually occurs. Relatively inexpensive and adaptable to either single-wheel or two-wheel trailers, this method is extensively employed.

The second method uses a normal vehicle, most often a passenger car, and measures the stopping distance. From this the effective coefficient is obtained by energy considerations. Because of the skidding hazard, the method is restricted to the lower speed range and to roads carrying little traffic. Above a certain vehicle speed, it measures a higher coefficient of sliding than that actually developed between tire and road. The discrepancy between the apparent and the actual coefficient increases

with the square of the initial speed. It is the only method, however, that closely reproduces the situation of a panic stop and brings into play the combined effects of vehicle, tire, road, and operating conditions.

The pendulum method, described under "Laboratory Techniques," is used on the road to determine a relative value of road slipperiness or skid resistance.

## THE PENN STATE BRAKE TEST TRAILER

As part of The Pennsylvania State University's research activities in the field of automotive and traffic safety, a test trailer was developed for the study of vehicle skid during braking and for investigating means to prevent the locking of wheels during braking. The trailer can also be used to measure the coefficient of friction between tire and road, by either the locked wheel or the slip angle method. It can be adapted to many other purposes, such as studies of brake mechanisms and tires.

For road studies the trailer is hitched to a pickup truck, which carries the required instrumentation. It is also used in the laboratory without modification. There it is held stationary, and its wheel runs on a motor-driven drum of 30 in. diameter. Road speeds up to 75 mph can be simulated in this manner.

### DESCRIPTION

The test trailer is of the single-wheel parallelogram type (Fig. 52), incorporating a standard passenger car wheel and brake assembly. It is of welded construction, with cross members and a configuration giving sufficient stiffness to ensure accuracy of all measurements. The pitch and yaw pivots are generously dimensioned pins, each supported in two double-row ball bearings. The brake backing plate is rotatable about the wheel axis. It is mounted on a double-row ball bearing and restrained by the rod forming the lower side of the trailer parallelogram. This arrangement prevents brake torque from affecting the wheel load.

The trailer wheel is loaded by a passenger car air-suspension unit. This solution provides ease of handling and keeps mass forces small. The diaphragm area of the air cylinder remains constant within the normal range of travel, making the wheel load directly proportional to the pressure in the air cylinder.

### INSTRUMENTATION

SR-4 strain gages measure brake and side forces. Wheel load and hydraulic pressures in the braking system are measured by suitable pressure transducers. Two d-c generators indicate the speed of the test wheel and an additional control wheel. The control wheel rolls true on the road surface under all conditions; therefore, the difference in the speeds of the two wheels is a measure of the slip of the test wheel. Additional measurements on the brake system are made as required.

The signals from the various transducers are fed, as necessary, into a 14-channel oscillograph via an 8-channel bridge balance. The required 115-v a-c power is supplied by a 1500-w engine-generator set carried on the test truck. Aircraft-type plugs provide for quick connect and disconnect of the trailer and the recording instruments. For field tests, the strain gage transducer on the lower parallelogram link can be replaced by a hydraulic converter connected to a gage, which permits direct reading of the coefficient.

## BRAKING SYSTEM

At present the test wheel is equipped with a standard passenger car hydraulic braking system. The master cylinder, located on the hitch, is actuated by means of a pneumatic booster, by an operator riding on the test truck.

## SPECIFICATIONS

### Overall dimensions of trailer:

Length	70 in.
Width	38 in.
Height	30 in.

### Distances:

Wheel center line to pitch axis	40.00 in
Wheel center line to yaw axis	43.75 in.

### Travel of trailer arm:

Around pitch axis	+8 deg
Around yaw axis	-5 and +35 deg

### Ranges:

Wheel slip	up to critical and 100%
Slip angle	0 to 15 deg

### Weights:

Total trailer weight	320 lb
Dead weight on wheel	150 lb
Maximum applied load on wheel	850 lb
Total wheel load	150 to 1000 lb

### Test wheel:

Rim	passenger car
Tire	7.50 x 14

The tests referred to in this report were conducted with a tube-type passenger car tire, 4 ply, synthetic rubber. The tire was operated at a wheel load of 900 lb and 24 psi inflation pressure, unless otherwise specified.

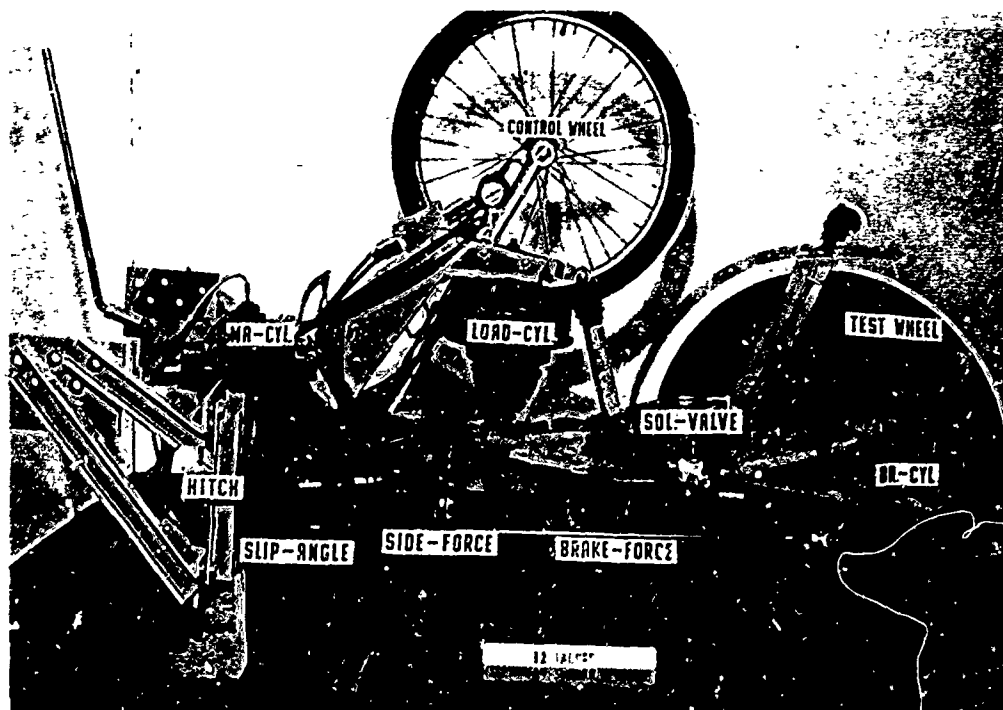
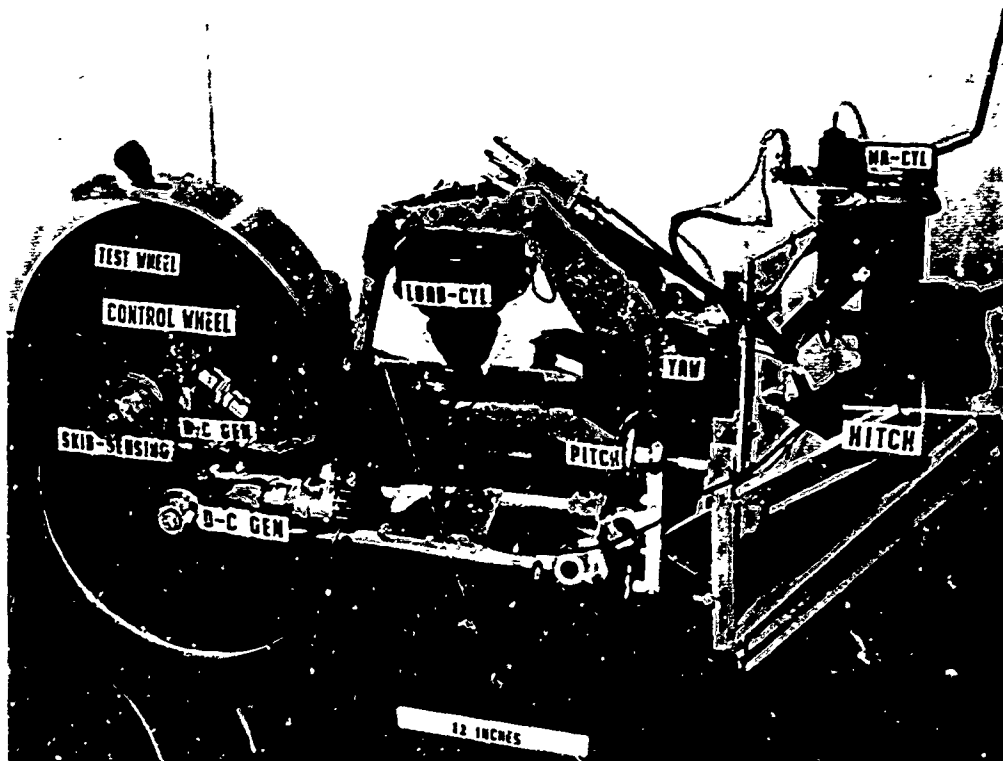


FIG. 52. Penn State brake test trailer, right and left views. Left view shows control wheel in transport position. Designed for road studies, trailer can be used in laboratory without modification.

## REMARKS ON THE STOPPING DISTANCE METHOD

Figure 29 shows the decrease of the critical coefficient and the sliding coefficient with vehicle speed under dry and wet conditions. The data obtained by the stopping distance method do not follow this trend, and in this particular instance they exhibit an increase when the initial speed exceeds about 30 mph.

An increase of the coefficient with sliding velocity cannot be explained on the basis of the friction characteristics of rubber. The following analysis takes a closer look at the results obtained from the stopping distance and demonstrates that the discrepancy in Fig. 29 is only an apparent one.

Since the wheels are locked throughout the stopping maneuver, the vehicle ground speed  $V_v$  is equal to the sliding velocity of the tires  $V_{sl}$ . The symbol  $V$  is therefore used without subscripts.

The kinetic energy  $E_k$  of a vehicle proceeding at a speed  $V$  is given by

$$E_k = LV^2/2g \quad (A)$$

where  $L$  is the weight of the vehicle and  $g$  is the gravity constant. The work done on the vehicle to brake it down to zero speed is given by

$$E_b = Fs \quad (B)$$

where  $F$  is the decelerating force and  $s$  is the stopping distance. Equating Eq. A and B produces the well-known relation

$$\bar{f}_{st} = F/L = V^2/2gs \quad (C)$$

where  $\bar{f}_{st}$  is the stopping distance coefficient.

To avoid misinterpretation of  $\bar{f}_{st}$ , the meaning of  $F$  in Eq. C must be understood. It is the sum of the decelerating forces (tire-road friction  $F_{gr}$  plus aerodynamic drag  $F_{air}$ ), taken as an average value over the interval  $s$ . Then, more properly,

$$\bar{f}_{st} = 1/s \int_0^s [(F_{gr} + F_{air}) ds] / L = V^2/2gs \quad (Ca)$$

The stopping distance method automatically integrates the sum of the two forces as a function of  $s$ . It is evident, then, that  $\bar{f}_{st}$  can give no direct information on the tire-road friction.



The coefficient experienced by a decelerating car at any velocity is given by

$$f_{st} = [F_{gr}(V) + F_{air}(V_r)] / L \quad (D)$$

where  $V_r$  is the vehicle's speed with respect to the air mass:

$$V_r = V + V_w \quad (E)$$

in which  $V_w$  is the wind velocity (head wind taken as positive).

Let the tire-road friction be approximated by

$$F_{gr} = F_0 - mV \quad (F)$$

where  $F_0$  is the maximum friction projected to zero velocity and  $m$  is the slope of the function. (That  $F_0$  actually occurs at a low sliding velocity is of no concern here.)

The aerodynamic drag is given by

$$F_{air} = c_w (A\gamma/2g) V_r^2 \quad (G)$$

or by

$$F_{air} = C(V + V_w)^2 \quad C = c_w A\gamma/2g \quad (Ga)$$

where  $c_w$  is the drag coefficient,  $A$  the effective face area of the vehicle, and  $\gamma$  the specific weight of the air.

Inserting Eq. F and Ga in Eq. D,

$$f_{st} = [(F_0 - mV) + C(V + V_w)^2] / L \quad (H)$$

$f_{st}$  is plotted in Fig. 53 and shows a minimum at  $V^*$ . The corresponding vehicle speed is found by differentiating Eq. H with respect to  $V$  and setting the derivative equal to zero:

$$df(V)/dV = [-m + 2C(V + V_w)] / L = 0$$

from which, for a head wind,

$$V^* = m/2C - V_w \quad (I)$$

As would be expected, the vehicle speed at which the coefficient reaches a minimum depends only on the ratio of the slope of the friction curve to the product of drag coefficient and effective face area, and the wind velocity.

Since the stopping distance produces an average coefficient over the interval  $s$ , the corresponding coefficient averaged over the interval  $V_1$  (the initial vehicle speed) must be determined.

$$\bar{f}_{st} = \left[ (\bar{F}_{gr}(V) + \bar{F}_{air}(V)) \right] / L \quad (J)$$

where  $\bar{F}_{gr}$  is the tire-road friction and  $\bar{F}_{air}$  is the aerodynamic drag, both averaged over the interval  $V_1$  so that

$$\bar{F}_{gr} = 1/V_1 \int_0^{V_1} F_{gr} dV \quad (K)$$

$$\bar{F}_{air} = 1/V_1 \int_0^{V_1} F_{air} dV \quad (L)$$

Inserting Eq. F and Ga in Eq. K and L respectively, performing the integration, and inserting the resulting expressions in Eq. J:

$$\bar{f}_{st} = \left\{ F_0 - (m/2)V_1 + c \left[ (V_1^2/3) \pm V_1 V_w \pm V_w^2 \right] \right\} / L \quad (M)$$

The function is plotted in Fig. 54.

A good criterion for the relative influence of the tire-road friction and aerodynamic drag is the initial vehicle speed at which  $\bar{f}_{st}$  reaches its minimum, indicating that the decay of the friction is compensated by the air resistance. Differentiating Eq. M with respect to  $V_1$  and letting the derivative be equal to zero, the initial vehicle speed at which the average coefficient reaches a minimum is given by

$$V' = 3m/4c - (3/2)V_w \quad (N)$$

Comparing Eq. I and Eq. N, it is apparent that

$$V' = (3/2)V^* \quad (O)$$

If a stop is made from an initial speed higher than that given by Eq. N, the coefficient obtained by the stopping distance method begins to rise again, as it does in the case illustrated by Fig. 29.

The following example shows that the initial vehicle speed for a given condition need not be high to bring about an increase of the coefficient  $\bar{f}_{st}$  with speed.

$$\begin{aligned} \text{Let } m &= 0.45 \text{ lb-sec/ft} \\ g &= 32.2 \text{ ft/sec}^2 \\ \gamma &= 0.075 \text{ lb/ft}^3 \\ A_v &= 20 \text{ ft}^2 \\ c_w &= 0.40 \\ V_w &= 0 \end{aligned}$$

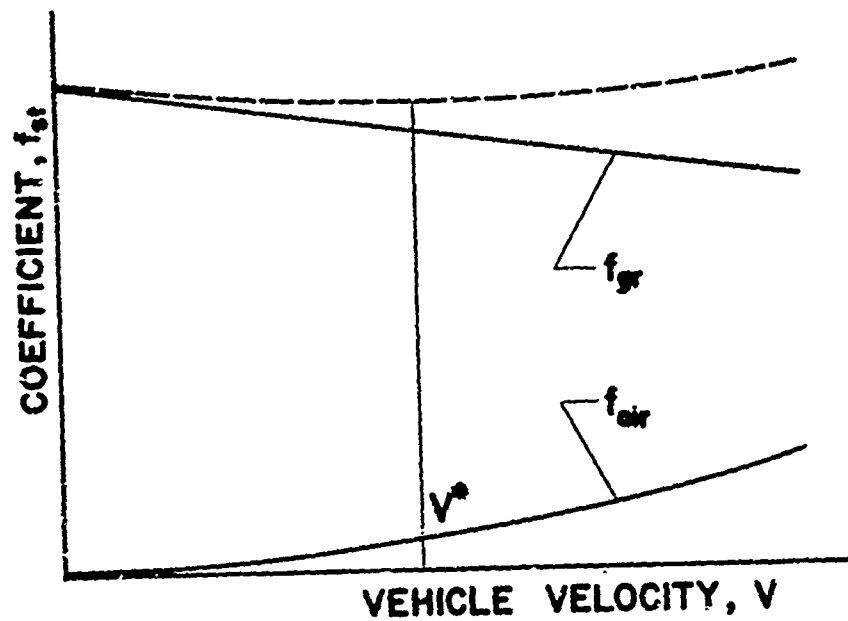


FIG. 53. Coefficient from stopping distance method (dotted line), and components due to tire-ground friction and air drag.

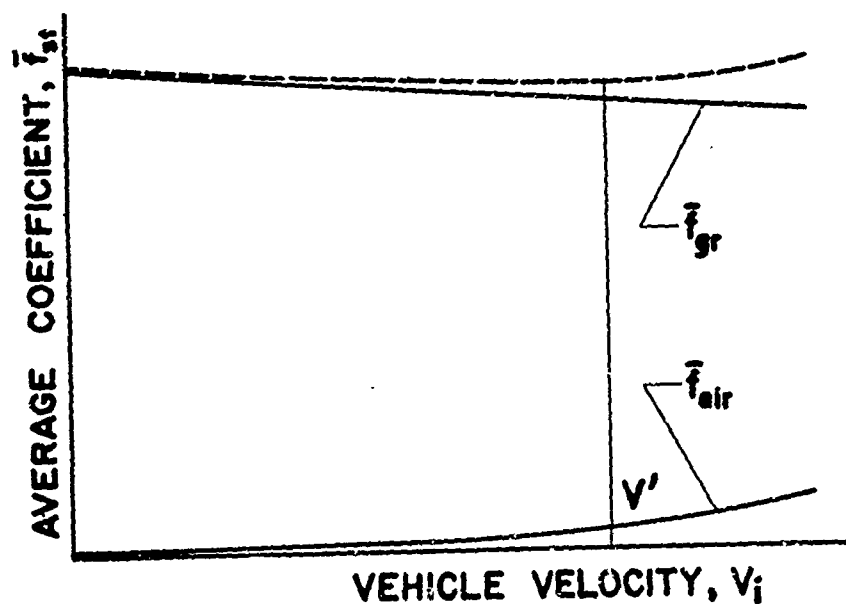


FIG. 54. Coefficient from stopping distance method and components, averaged over interval  $V_i$ .

Inserting these values in Eq. N, the initial velocity required to cause a reversal of the trend is

$$V_i = 24 \text{ mph}$$

This result is surprising, since it is believed that the aerodynamic drag component can be neglected at low vehicle speeds.

There is a reason why this reversal occurs so early. The influence of temperature on the locked wheel coefficient was discussed. Reasoning indicates that the friction curve obtained from a series of locked wheel tests conducted at constant sliding velocities must look different from the curve obtained from a test in which the velocity is steadily decreased. In the first case, a steady-state condition is reached with respect to the temperature in the contact patch. In the second case, the temperature will be higher for any velocity, except at the beginning of the stop. Consequently, for the stopping distance method the slope of the line approximating the coefficient as a function of speed will be smaller.

U.Ed. 1-270